AD_____

Award Number: W81XWH-04-1-0478

TITLE: Gamma-Secretase and Notch Signaling: Novel Therapeutic Targets in Breast Cancer

PRINCIPAL INVESTIGATOR: Lucio Miele, M.D., Ph.D.

CONTRACTING ORGANIZATION: University of Illinois
Chicago, IL 60612-7205

REPORT DATE: May 2005

TYPE OF REPORT: Annual

PREPARED FOR: U.S. Army Medical Research and Materiel Command
Fort Detrick, Maryland 21702-5012

DISTRIBUTION STATEMENT: Approved for Public Release;
Distribution Unlimited

REPORT DOCUMENTATION PAGE

Form Approved
OMB No. 0704-0188

1. REPORT DATE *(DD-MM-YYYY)*	2. REPORT TYPE	3. DATES COVERED *(From - To)*
01-05-2005	Annual	15 Apr 04 – 14 Apr 05

4. TITLE AND SUBTITLE
Gamma-Secretase and Notch Signaling: Novel Therapeutic Targets in Breast Cancer

5a. CONTRACT NUMBER

5b. GRANT NUMBER
W81XWH-04-1-0478

5c. PROGRAM ELEMENT NUMBER

6. AUTHOR(S)
Lucio Miele, M.D., Ph.D.

E-Mail: lmiele@uic.edu

5d. PROJECT NUMBER

5e. TASK NUMBER

5f. WORK UNIT NUMBER

7. PERFORMING ORGANIZATION NAME(S) AND ADDRESS(ES)
University of Illinois
Chicago, IL 60612-7205

8. PERFORMING ORGANIZATION REPORT NUMBER

9. SPONSORING / MONITORING AGENCY NAME(S) AND ADDRESS(ES)
U.S. Army Medical Research and Materiel Command
Fort Detrick, Maryland 21702-5012

10. SPONSOR/MONITOR'S ACRONYM(S)

11. SPONSOR/MONITOR'S REPORT NUMBER(S)

12. DISTRIBUTION / AVAILABILITY STATEMENT
Approved for Public Release; Distribution Unlimited

13. SUPPLEMENTARY NOTES

14. ABSTRACT

We are on track and have made significant progress in our project. We have determined that, as predicted by our hypothesis, LY411,575 is a Notch inhibitor which synergizes with paclitaxel. We have discovered an additional synergism with tamoxifen. We have made several key mechanistic observations on how Notch inhibition causes growth arrest and death in breast cancer cells regardless of ER status. We have determined the optimal conditions for in vivo administration of LY411,575 and we have obtained preliminary xenograft data which confirm significant anti-tumor activity at safe doses of this compound. We expect to complete our study and publish its results within the expected 3-year time frame. We expect our results will not only demonstrate that a GSI/paclitaxel regimen is a promising treatment for ER negative breast cancer, but also that a GSI/tamoxifen combination could be just as promising in ER positive cancers. Based on these data, we will propose 2 phase 1 clinical trials of this compound or its close derivative(s) produced by Eli Lilly in the neo-adjuvant setting at first.

In conclusion, we expect that the completion of this project will directly lead to the identification of a new broadly active class of agents for the treatment of breast cancer, the clarification of their primary mode of action and the suggestion of possible combination therapeutic regimens.

15. SUBJECT TERMS
No subject terms provided.

16. SECURITY CLASSIFICATION OF:			17. LIMITATION OF ABSTRACT	18. NUMBER OF PAGES	19a. NAME OF RESPONSIBLE PERSON
a. REPORT	b. ABSTRACT	c. THIS PAGE			USAMRMC
U	U	U	UU	81	19b. TELEPHONE NUMBER *(include area code)*

Table of Contents

Introduction:

NOTCH genes encode transmembrane receptors that participate in communication between contiguous cells (1;2). Mature Notch receptors derive from proteolytic processing of single polypeptide precursors (3) which are cleaved by a furin-like protease (4) into non-covalent heterodimers comprising an extracellular subunit (N^{EC}) and a transmembrane subunit (N^{TM}). N^{EC} contains multiple EGF-like repeats while N^{TM} includes an extracellular stump containing 3 "Lin-Notch" repeats, a single pass transmembrane domain and an intracellular domain. Notch receptors are activated by membrane associated ligands of the Delta or Jagged (Serrate) families. Ligands dissociate the N^{EC} subunit from the N^{TM} subunit, triggering a two-step proteolytic cleavage of N^{TM}. First, N^{TM} is clipped extracellularly by TACE (TNF-alpha Converting Enzyme) (5;6). This makes N^{TM} susceptible to cleavage by a γ-secretase activity (7), which cleaves it within the transmembrane sequence, releasing an intracellular domain, N^{IC}. The latter migrates to the nucleus and activates CBF-1 dependent transcription. ***Thus, γ-secretase is essential for the activation of Notch receptors***. Activation of Notch signaling induces proliferation and survival of numerous cancer cells (8). Inhibitors of this enzyme have been in development for several years as potential treatments for Alzheimer's disease, since γ-secretase also generates the beta-amyloid pathogenic peptide in that disease (9). At the time of submission of this grant proposal, γ-secretase inhibitors (henceforth, GSIs) were at the pre-clinical stage of investigation. Moreover, the only data indicating that activation of Notch signaling was observed in breast cancer were our own preliminary data, which we have now extended and confirmed (Miao et al., in preparation). Since then, 2 phase 1 clinical trials have opened with a Merck GSI in T-ALL and stage IV breast cancer respectively (J. Aster, personal communication, Patricia LoRusso, personal communication). A recent publication in Cancer Research by the Egan group shows a strong correlation between high Notch-1 and Jagged-1 mRNA and poor prognosis in breast cancer (10). This makes our investigation of LY411,575, an Eli Lilly- derived GSI in combination with paclitaxel even more relevant to the treatment of breast cancer. In fact, I have recently given a seminar at Lilly, encouraging them to develop their compound in breast cancer in collaboration with our group. During the first year of award we have made considerable progress in testing our hypothesis (see below), and made important mechanistic observations. My move to Loyola University Medical Center, as Director of Breast Cancer Preclinical Research, has further stimulated progress in this project, and we have already begun clinical collaborations to identify the patient population most likely to benefit from treatment with GSI (with Drs. Kathy Albain, medical oncology, Katharine Yao, surgical oncology, and Prabha Rajan, Pathology).

Body:

During the course of our first year of funding and since moving to Loyola on April 1, we have pursued the Tasks outlined in our approved statement of work. We have also extended our investigation (with internal funds) to include the combination of LY411,575 and tamoxifen. The results obtained so far for each Task are summarized below:

Task 1: To determine the activity profile of LY411,575 and its effects on Notch signaling

To that end, we have obtained LY411,575 from our collaborator Todd Golde. This compound has 2 chiral centers (Figure 1). Dr. Golde synthesized for us both the racemic mixture and the four individual diastereoisomers.

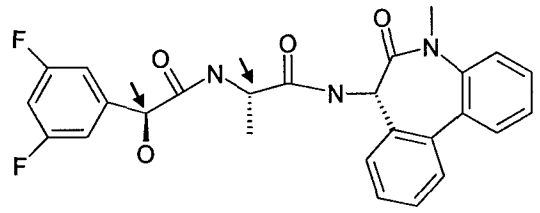

Figure 1: structure of LY411,575. Chiral centers are indicated by red arrows.

We determined that the racemic mixture has equivalent activity to isolated diastereomers, at least in vitro in reporter assays and cytotoxicity assays. Individual diastereoisomers remain available for further studies should we determine that one of them is preferable to the others.

We confirmed that LY411,575 inhibits Notch-dependent reporter activity in a dose- and time-dependent manner as determined by CBF-1-dependent luciferase assays in T47D:A18 (ER-alpha positive) and MDA-MB231 (ER-alpha negative) breast cancer cells (Figure 2).

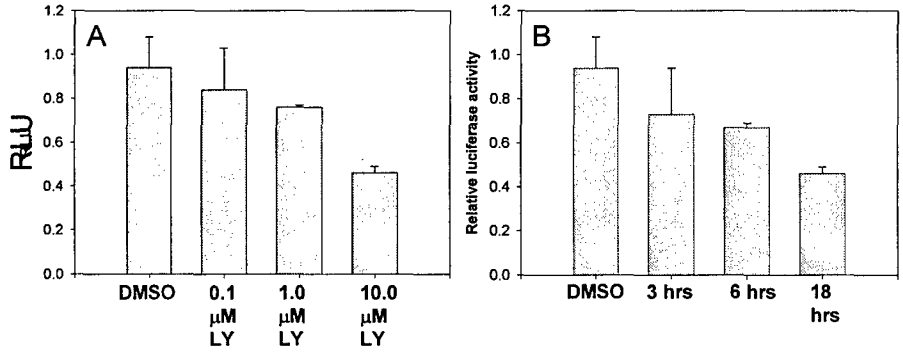

Figure 2: Dose- and time-dependent inhibition of CBF-1 luciferase activity by LY411,575 racemic mixture. MDA-MB231 cells were transfected with a CBF-1 reporter plasmid carrying 3 tandem CBF-1 responsive elements. Twenty-four hours later, cells were treated with the indicated concentrations of LY411,575. A, luciferase activity was measured 18 hours after treatment. B, a fixed concentration of 10 μM was used, for different times.

Subsequently, we determined that LY411,575, like the peptide GSI we used for preliminary experiments, has cytotoxic activity in vitro on breast cancer cells and shows synergism with paclitaxel. Because new data from our lab indicate that ER-alpha inhibits Notch signaling, we also expected to see that tamoxifen synergizes with GSIs in vitro in ER-alpha positive cells. These results are shown in Figures 3 and 4.

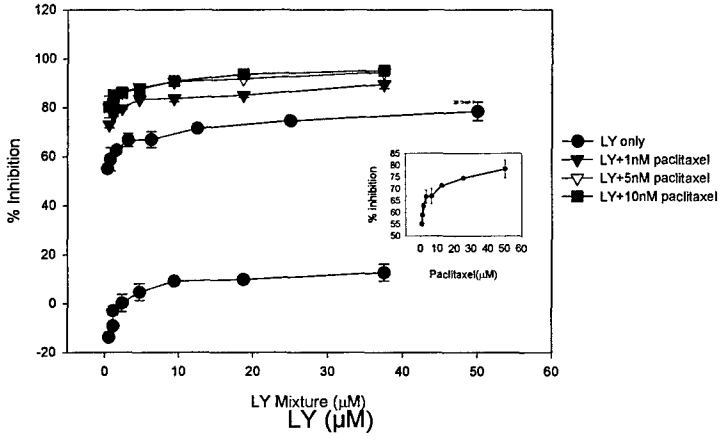

Figure 3: MTT assays showing that LY411,575 manifests remarkable synergism with paclitaxel in MDA-MB231 cells. Note that cytotoxicity of LY411,575 alone is limited. However, when as little as 1 nM paclitaxel is added, the combination shows virtually complete inhibition of cell viability. The inset shows the dose response curve of paclitaxel alone under these conditions.

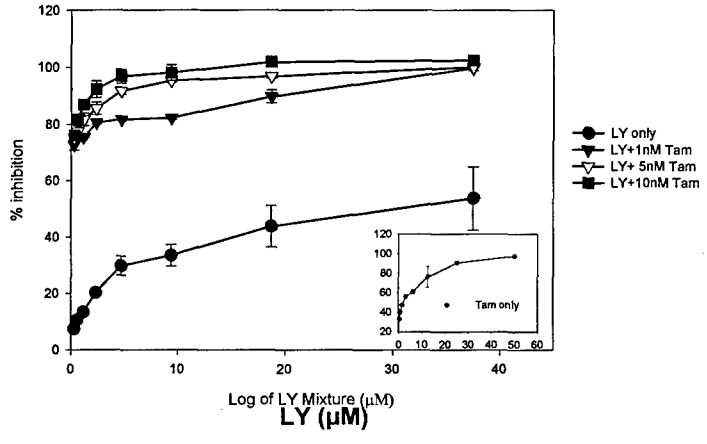

Figure 4: MTT assays showing that LY411,575 manifests remarkable synergism with tamoxifen in T47D:A18 cells (ER-alpha positive). Note that cytotoxicity of LY411,575 alone is more pronounced than in MDA-MB231 cells. In the presence of even 1 nM 4-OH-tamoxifen, the combination is strikingly cytotoxic, showing even more remarkable synergism than with paclitaxel. The dose response of 4-OH tamoxifen alone is shown in the inset.

To identify appropriate markers of efficacy for Notch inhibitors in breast cancer, we explored the mechanism of action through which Notch inhibition (by GSIs and by siRNA silencing) results in cytotoxicity in breast cancer cells. We determined that GSIs and Notch-1 siRNA cause a G2 arrest in MDA-MB231 as well as T47D: A18 cells. This is accompanied by remarkable downregulation of cyclin A and B mRNA and protein expression (Figure 5). These experiments were conducted before we had LY411,575. Thus, they were conducted with peptide GSI cbz-Leu-Leu-Nle-CHO. We are currently conducting the same experiments with LY411,575.

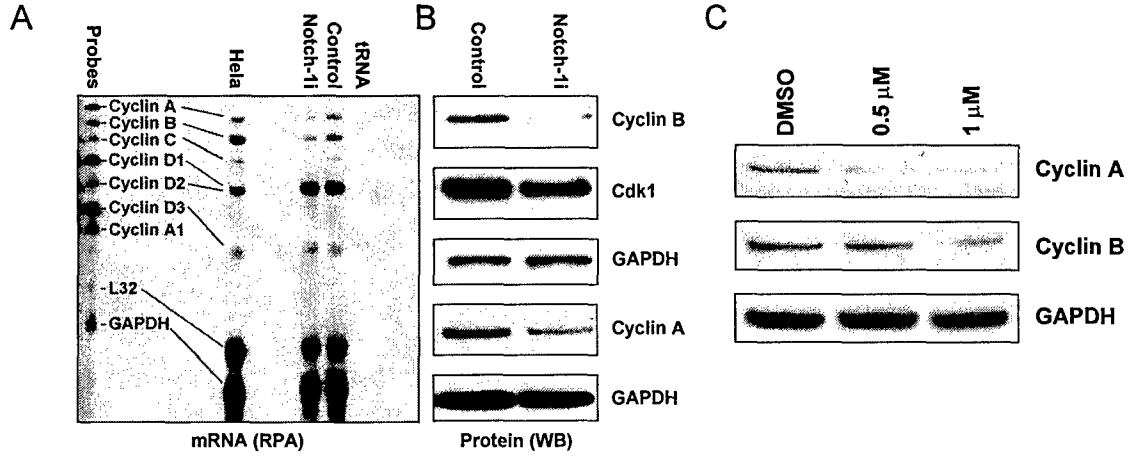

Figure 5: Inhibition of cyclin A and B1 expression by Notch-1 siRNA (A and B), and by GSI (C). A is a ribonuclease protection assay and B and C Western blots.

The G2 arrest is followed by apoptosis with induction of NOXA, a BH3-only pro-apoptotic protein (not shown). Our data show that NOXA is induced in a p53-independent manner by both Notch-1 siRNA and GSI. Therefore, our data suggest that GSIs cause a G2 arrest through inhibition of cyclins A and B expression, follwed by induction of NOXA and apoptosis. Cell death is maximal at about 48 hours in oth MDA-MB231 and T47D:A18 cells. Induction of NOXA is a particularly promising efficacy marker because NOXA is not observed in untransformed cells except during cell death, and is not induced by Notch inhibitors in normal cells. For the remainder of Task 1, we will continue with the experiments outlined in our proposal, with emphasis on determineing the role of cyclins A and B1 in cell cycle arrest induced by GSIs and the role of NOXA in apoptosis. We already know that LY411,575 induces NOXA, like Notch-1 siRNA and peptide GSI (not shown). A manuscript will be submitted for publication in the next 2-3 weeks detailing our findings on Notch as a therapeutic target in breast cancer. These findings have been summarized in an abstract at the June Era of Hope meeting (Rizzo et al., 2005).

Task 2. To determine the optimal oral dose and delivery regimen of LY411,575.

This Task is essentially complete. In collaboration with Dr. Golde, we conducted dose-ranging experiments with LY411,575 both orally (formulated in chow) and intraperitoneally. Toxicity was determined by examining animal weight, behavior and

pathology post-mortem. The maximum tolerated dose (MTD) of LY411,575 in C57/bl6 mice is 10 mg/kg. At this dose, toxicities included changes in hair color, followed by hair loss and weight loss. Additional findings included loss of thymocytes and an immunomodulatory effect on the Th1/Th2 response that may actually find therapeutic applications. In fact, we showed in a parallel project that this effect can be used advantageously in the treatment of a mouse model of multiple sclerosis (11). A similar MTD was found in nude mice. When the compound was administered orally, we observed intestinal goblet cell metaplasia, as reported by Wong et al (12). This is a possible cause of weight loss due to secretory diarrhea. However, when the compound was administered parenterally, we did not observe diarrhea or intestinal metaplasia. In nude mice, which obviously have no hair, we observed a different type of cutaneous effect. This consisted in barely visible patches of hyperkeratosis, which appeared after 3 weeks of treatment and disappeared upon treatment discontinuation. Histologically, these were areas of hyperkeratosis with parakeratosis (not shown). This is consistent with a role of Notch in controlling epidermal differentiation. Of note, all the adverse events we observed were non-lethal up to and including the MTD, required at least 2-3 weeks of treatment to appear and were completely reversible. Based on these findings, we have selected a dose of 5 mg/kg intraperitoneally for therapeutic experiments.

Task 3. To determine the anti-neoplastic activity of LY411,575 in a breast cancer model.

This Task is in progress. A new large scale synthesis of LY411,575 will be required to complete it. With the compound we had left which was used for in vitro work and pilot animal experiments, we have conducted one preliminary experiment. For this experiment we elected to investigate the apparent synergism with tamoxifen, which appeared extremely impressive in vitro. We used T47D:A18 xenografts which were maintained in ovariectomized nude mice. Estrogen support was provided via s.c. capsules releasing a post-menopausal-equivalent estradiol dose. Animals were treated orally with a daily low dose of tamoxifen (0.5 mg/kg), and received i.p. LY411,575 every other day for 3 weeks in DMSO. The results (Figure 6) were very encouraging.

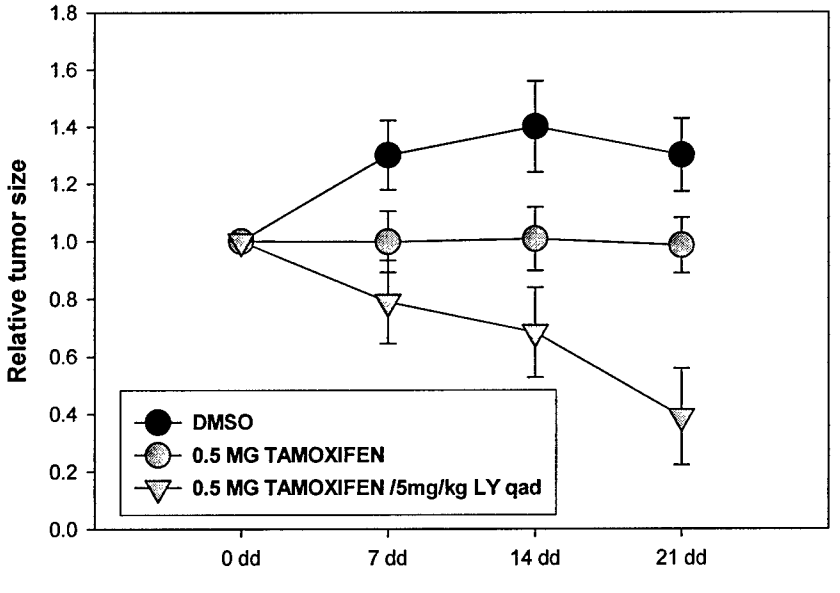

Figure 6: LY411,575 strongly potentiates the effects of tamoxifen in vivo in T47D:A18 xenografts.

Tamoxifen alone caused a stabilization of tumor volume but did not cause tumor shrinkage. However, in the presence of LY411,575 plus tamoxifen, the tumors dramatically shrank to approximately 30% of pre-treatment volume. Histologically, the tumors at the end of the treatment were characterized by massive cell death and hemorrhage. The latter may be due to an anti-angiogenic effect of Notch inhibition (13-15). A LY411,575 group alone was not done in this preliminary experiment because we did not have enough compound. Under these conditions, we did not observe toxicity except for a few skin patches of hyperkeratosis. Animal weight was not significantly affected. We are now in the process of continuing the Task as described in the original proposal, and we would like to add tamoxifen to the originally planned experiments (at no additional cost). We have obtained IACUC approval to conduct the paclitaxel experiments outlined in the original proposal. We are now seeking approval to extend these experiments to tamoxifen, and repeat the experiment shown in Figure 6 with an additional group treated with LY411,575 alone. The tumors will be examined for evidence of inhibition of Notch signlaing, as well as cyclin A and B1, NOXA, apoptosis (caspase 3 and TUNEL). Due to the possibility of an anti-angiogenic effect we will also study endothelial cell density by Von Willebrandt factor staining.

Key research accomplishments

Task 1 (in progress)

1. Synthesis of LY411,575 as racemic mixture
2. Synthesis of individual diastereoisomers of LY411,575
3. In vitro characterization of cytotoxicity and Notch-inhibitory activity of LY411,575
4. Demonstration of in vitro synergism between LY411,575 and paclitaxel
5. Discovery of in vitro synergism between LY411,575 and tamoxifen
6. Discovery of mechanism of growth arrest induced by GSIs (cyclin A and B inhibition)
7. Discoverey of novel mechanism of apoptosis induction by GSIs and Notch silencing (NOXA induction).

Task 2 (complete)

1. Determination of optimal dose and route of administration of LY411,575 in mice
2. Identification of LY411,575 adverse effects depending on administration route
3. Discovery of immunomodulatory effects of LY411,575 with potential therapeutic applications (Nature Immunology paper).

Task 3 (in progress)

1. First in vivo experiments with LY411,575 confirm remarkable synergism with tamoxifen and significant anti-tumor activity at virtually non-toxic doses of LY411,575.

Additional finding ("bonus" consequence of collaboration with Dr. Golde):

1. LY411,575 is also active in Kaposi sarcoma cells, where it induces G2 arrest just as in breast cancer cells (16).

Reportable outcomes

1. **Rizzo et al. abstract, Era of Hope Meeting 2005 (Philadelphia, PA) Appendix 1)**
2. **Miao et al., manuscript completed, to be submitted (Appendix 2)**
3. **Minter et al., Nature Immunology 2005 (Appendix 3)**
4. **Curry et al.., Oncogene 2005 (Appendix 4)**

Conclusions

We are on track and have made significant progress in our project. We have determined that, as predicted by our hypothesis, LY411,575 is a Notch inhibitor which synergizes with paclitaxel. We have discovered an additional synergism with tamoxifen. We have made several key mechanistic observations on how Notch inhibition causes growth arrest and death in breast cancer cells regardless of ER status. We have determined the optimal conditions for in vivo administration of LY411,575 and we have obtained preliminary xenograft data which confirm significant anti-tumor activity at safe doses of this compound. We expect to complete our study and publish its results within the expected 3-year time frame. We expect our results will not only demonstrate that a GSI/paclitaxel regimen is a promising treatment for ER negative breast cancer, but also that a GSI/tamoxifen combination could be just as promising in ER positive cancers. Based on these data, we will propose 2 phase 1 clinical trials of this compound or its close derivative(s) produced by Eli Lilly in the neo-adjuvant setting at first.
In conclusion, we expect that the completion of this project will directly lead to the identification of a new broadly active class of agents for the treatment of breast cancer, the clarification of their primary mode of action and the suggestion of possible combination therapeutic regimens.

References

1. Artavanis-Tsakonas,S., Rand,M.D., and Lake,R.J. 1999. Notch signaling: cell fate control and signal integration in development. *Science* 284:770-776.

2. Greenwald,I. 1998. LIN-12/Notch signaling: lessons from worms and flies. *Genes Dev.* 12:1751-1762.

3. Blaumueller,C.M., Qi,H., Zagouras,P., and Artavanis-Tsakonas,S. 1997. Intracellular cleavage of notch leads to a heterodimeric receptor on the plasma membrane. *Cell* 90:281-291.

4. Logeat,F., Bessia,C., Brou,C., LeBail,O., Jarriault,S., Seidah,N.G., and Israel,A. 1998. The Notch1 receptor is cleaved constitutively by a furin-like convertase. *Proc.Natl.Acad.Sci.U.S.A.* 95:8108-8112.

5. Mumm,J.S., Schroeter,E.H., Saxena,M.T., Griesemer,A., Tian,X., Pan,D.J., Ray,W.J., and Kopan,R. 2000. A ligand-induced extracellular cleavage regulates gamma-secretase-like proteolytic activation of Notch1. *Mol.Cell* 5:197-206.

6. Brou,C., Logeat,F., Gupta,N., Bessia,C., LeBail,O., Doedens,J.R., Cumano,A., Roux,P., Black,R.A., and Israel,A. 2000. A novel proteolytic cleavage involved in Notch signaling: the role of the disintegrin-metalloprotease TACE. *Mol.Cell 2000.Feb.;5.(2.):207.-16.* 5:207-216.

7. Saxena,M.T., Schroeter,E.H., Mumm,J.S., and Kopan,R. 2001. Murine notch homologs (N1-4) undergo presenilin dependent proteolysis. *J.Biol.Chem.* 276:40268-40273.

8. Nickoloff,B.J., Osborne,B.A., and Miele,L. 2003. Notch signaling as a therapeutic target in cancer: a new approach to the development of cell fate modifying agents. *Oncogene* 22:6598-6608.

9. Kopan,R. and Ilagan,M.X. 2004. Gamma-secretase: proteasome of the membrane? *Nat.Rev.Mol.Cell Biol.* 5:499-504.

10. Reedijk,M., Odorcic,S., Chang,L., Zhang,H., Miller,N., McCready,D.R., Lockwood,G., and Egan,S.E. 2005. High-level coexpression of JAG1 and NOTCH1 is observed in human breast cancer and is associated with poor overall survival. *Cancer Res.* 65:8530-8537.

11. Minter,L.M., Turley,D.M., Das,P., Shin,H.M., Joshi,I., Lawlor,R.G., Cho,O.H., Palaga,T., Gottipati,S., Telfer,J.C. *et al.* 2005. Inhibitors of gamma-secretase block in vivo and in vitro T helper type 1 polarization by preventing Notch upregulation of Tbx21. *Nat.Immunol.* 6:680-688.

12. Wong,G.T., Manfra,D., Poulet,F.M., Zhang,Q., Josien,H., Bara,T., Engstrom,L., Pinzon-Ortiz,M., Fine,J.S., Lee,H.J. *et al.* 2004. Chronic treatment with the gamma-secretase inhibitor LY-411,575 inhibits beta-amyloid peptide production and alters lymphopoiesis and intestinal cell differentiation. *J.Biol.Chem* 279:12876-12882.

13. Zeng,Q., Li,S., Chepeha,D.B., Giordano,T.J., Li,J., Zhang,H., Polverini,P.J., Nor,J., Kitajewski,J., and Wang,C.Y. 2005. Crosstalk between tumor and endothelial cells promotes tumor angiogenesis by MAPK activation of Notch signaling. *Cancer Cell* 8:13-23.

14. Li,J.L. and Harris,A.L. 2005. Notch signaling from tumor cells: a new mechanism of angiogenesis. *Cancer Cell* 8:1-3.

15. Soares,R., Balogh,G., Guo,S., Gartner,F., Russo,J., and Schmitt,F. 2004. Evidence for the notch signaling pathway on the role of estrogen in angiogenesis. *Mol.Endocrinol.* 18:2333-2343.

16. Curry,C.L., Reed,L.L., Golde,T.E., Miele,L., Nickoloff,B.J., and Foreman,K.E. 2005. Gamma secretase inhibitor blocks Notch activation and induces apoptosis in Kaposi sarcoma cells. *Oncogene* in press.

NOTCH SIGNALING IS ALTERED IN BREAST CANCER AND IS A POTENTIAL THERAPEUTIC TARGET

Paola Rizzo, Haixi Miao, Kalliopi Siziopikou, Lynda L. Song, Suzanne Selvaggi, Amina Bashir, Frederick Koerner, Vijaya Chaturvedi, Jian-Zhong Qin, Brian J. Nickoloff, Lucio Miele*
University of Illinois at Chicago, Loyola University Chicago, Rush University Chicago, University of Wisconsin, Brigham and Women's Hospital
*lmiele@lumc.edu

Notch signaling is deregulated in several malignancies and maintains the neoplastic phenotype in Ras-transformed human cell lines in vitro and in vivo. While Notch-1 and Notch-4 have been implicated in mammary carcinogenesis in mice, the role of Notch signaling in human breast cancer remains unclear. We studied 77 archival cases including normal breast, hyperplastic lesions, carcinomas in situ and invasive ductal and lobular breast carcinomas for Notch receptor and ligand expression. Infiltrating carcinomas co-express Notch-1 and -4, while normal breast and hyperplastic lesions do not express Notch-4, and in situ lesions do so inconsistently. All breast cancers we studied express one or more Notch ligands. Untransformed human mammary epithelial cells grown in vitro express high levels of uncleaved Notch-1 but low levels of the active, cleaved receptor. Conversely, breast cancer cell lines of diverse genetic backgrounds consistently express high levels of cleaved, active Notch-1. Notch-dependent transcriptional activity corresponds to levels of active Notch-1. H-Ras induces Notch-1 and -4. Notch-1 can induce Notch-4 in breast cancer cells. Estradiol increases Notch-1 but not Notch-4 expression in estrogen receptor α (ERα)-positive cells. RNAi silencing of Notch-1 or Notch-4 in MDA-MB231 breast cancer cells significantly inhibits matrix invasion and subsequently increases the fraction of cells in G2/M, eventually inducing death. Similarly, pharmacological interruption of Notch signaling in MDA-MB231 cells via a γ-secretase inhibitor induces G2/M accumulation and death. Both RNAi and γ-secretase inhibitor cause a striking decrease in cyclins B and A1, but not D or E. Importantly, genetic or pharmacological interruption of Notch signaling strikingly potentiated the effects of paclitaxel in both ERα-positive and ERα-negative cells, and the effects of tamoxifen in ERα-positive cells. Our data suggest that inhibition of the Notch signaling pathway is an attractive new strategy for the treatment of breast cancers irrespective of estrogen receptor status and that γ-secretase inhibitors, a class of drugs currently in clinical trial for non-oncological indications, may be used for the treatment of breast cancer in combination with taxanes or SERMS.

The U.S. Army Medical Research and Materiel Command under W81XWH-04-1-1263 supported this work.

APPENDIX 2

Ras-activated Notch signaling in breast cancer is inhibited by estrogen receptor and controls proliferation through cyclins A and B

Haixi Miao[1], Kalliopi Siziopikou[2], Paola Rizzo[1], Lynda Li Song[1], Suzanne Selvaggi[3], Amina Bashir[1], Frederick Koerner[4], Pamela Pollock[5] Vijaya Chaturvedi[6], Jian-Zhong Qin[6], Brian J. Nickoloff[6] and Lucio Miele[1¶]

[1]Breast Cancer Program, Cardinal Bernardin Cancer Center, Loyola University Chicago
[2]Department of Pathology, Rush University Chicago
[3]Department of Pathology, University of Wisconsin, Madison, WI
[4]Department of Pathology, Brigham and Women's Hospital, Boston, MA
[5]TGEN, Phoenix, Arizona
[6]Skin Cancer Program, Cardinal Bernardin Cancer Center, Loyola University Chicago

[¶]To whom correspondence should be addressed at:
Dr. Lucio Miele
Loyola University of Chicago
Cardinal Bernardin Cancer Center
2160 S. First Avenue, Room 236
Maywood, IL 60153
Tel. 708-327-3298
FAX 708-327-2245
e-mail lmiele@lumc.edu

Abstract

Notch signaling is dysregulated in various malignancies and maintains the neoplastic phenotype in Ras-transformed human cells *in-vitro* and *in-vivo*. Notch-1 and Notch-4 can cause mammary carcinogenesis in mice, but Notch signaling in human breast cancer remains unexplored. We studied 78 cases including normal breast, hyperplastic lesions, carcinomas in situ and invasive ductal and lobular breast carcinomas for Notch receptor and ligand expression. Infiltrating carcinomas consistently co-express Notch-1 and -4, while normal breast and hyperplastic lesions do not express Notch-4, and in-situ lesions do so inconsistently. Notch-1 induces Notch-4 in breast cancer cells. H-Ras induces Notch-1 and -4, while estradiol, through the estrogen receptor α (ERα), antagonizes the effects of Ras on Notch activity. Overexpression of Notch-1 in MCF-7 cells increases proliferation and extracellular matrix invasion. Notch-4 or Notch-1 silencing in breast cancer cells inhibits matrix invasion and causes loss of cyclins A and B1, G2/M accumulation and eventually death. Identical effects are observed upon pharmacological inhibition of Notch activation via γ-secretase inhibition. A γ-secretase inhibitor caused death in breast cancer cells regardless of p53 and ERα-status. Our data indicate that Notch signaling is frequently dysregulated in breast cancer and is a potential therapeutic target irrespective of ERα status.

INTRODUCTION

Notch receptors regulate cell differentiation, proliferation and apoptosis during intercellular contact, in response to membrane ligands of the Delta and Jagged/Serrate families (1;2). Notch precursor proteins are cleaved by a furin-like protease to generate mature heterodimers (3;4) comprised of a transmembrane subunit (N^{TM}) non-covalently associated with an extracellular subunit (N^{EC}) that contains EGF-like repeats. Upon ligand binding, the transmembrane subunit is cleaved by an extracellular disintegrin metalloprotease (5) and a presenilin-1 (PS-1)-dependent γ-secretase (6). This releases a cytoplasmic subunit (N^{IC}), which regulates the function of several transcription factors, modulating cell fate decisions (1;7;8).

Notch signaling participates in neoplastic transformation. Constitutively active Notch-1 mutants devoid of N^{EC} are associated with T-cell acute lymphoblastic leukemia (T-ALL) (9) and over 50% of T-ALL carry activating Notch-1 mutations (10). Intracellular forms of Notch receptors have transforming activity *in vitro* (11) and in animal models (12-14). Deregulated expression of wild-type Notch receptors, ligands and targets has been described in several solid tumors (15-21), and hematological malignancies (22;23).

In murine models, constitutive activation of Notch-1 (24;25) and Notch-4 (14) can cause mammary carcinogenesis. However, to date the possible role of Notch signaling in human breast cancer remains poorly understood. We have shown that activation of Notch-1 maintains the neoplastic phenotype in Ras-transformed human fibroblasts and kidney epithelial cells (26). In those models, Notch-1 also induces Notch-4. In that study, we detected expression of Notch-1 in seven cases of breast cancer. Expression appeared stronger in H-Ras overexpressing cases (26). Since H-Ras is frequently overexpressed in breast cancer (27;28), we studied the status of Notch signaling in breast cancer. We present a comprehensive examination of Notch-1 and -4 expression and signaling in breast cancer, including 78 new clinical cases. Notch-1 and Notch-4 are consistently co-expressed in breast cancers and breast cancer cells, while normal human breast and hyperplastic lesions express Notch-1 but not Notch-4. Ras and ERα regulate Notch levels and have opposite effects on Notch-dependent transcriptional activity. The effects of Ras on Notch levels in breast cells are mediated at least in part by PKB/AKT. Genetic or pharmacological inhibition of Notch-1 or Notch-4 signaling inhibits proliferation and extracellular matrix invasion in breast cancer cells. Anti-proliferative effects were observed regardless of p53 and ERα status. We describe a previously unrecognized effect of Notch signaling on the S and G2/M stages of the cell cycle, mediated by transcriptional regulation of cyclins A and B1. Our data indicate that Notch signaling may be a novel therapeutic target and diagnostic marker in breast cancer.

RESULTS

Notch expression is deregulated in breast cancer compared to normal and hyperplastic breast. We examined normal breast, hyperplastic, early and late neoplastic lesions (Table 1). Only one out of 4 normal breast biopsies showed weakly detectable Notch-1 in mammary ducts (Figures 1A, B). Notch-4 was undetectable in normal human breast ducts. Interestingly, areas of apocrine metaplasia (Figure 1C) were intensely positive for Notch-1. Also, apparently normal ducts near DCIS lesions were intensely positive for Notch-1 but not Notch-4, even when the nearby DCIS was Notch-1 negative (Figure 1D). DCIS lesions showed heterogeneous patterns (Table 1). Eleven/27 were intensely positive for Notch-1 alone (Figures 1E, F). Five showed only Notch-4, 7 co-expression of Notch-1 and Notch-4 (Figures 1G, H) and 4 were negative for both Notch-1 and -4. Thus, proliferative breast changes are characterized by overexpression of Notch-1 while early neoplastic lesions have diverse patterns of Notch expression, presumably reflecting genetic heterogeneity and/or different stages of tumor progression. DCIS of histological grades I, II or III all showed Notch receptor expression. In grade I non-comedo DCIS 4/7 tumors were Notch-1 positive, 2 were Notch-4 positive and 1 was double-positive for Notch-1 and -4. In grade II, 8/15 non-comedo DCIS expressed Notch-4, either alone (2) or with Notch-1 (6). Three grade II DCIS were Notch-1 positive without Notch-4. Conversely, comedocarcinomas (grade III) did not include samples co-expressing Notch-1 and -4. The most common pattern (4/6) was strong Notch-1 expression, with one tumor showing Notch-4 without Notch-1. Whether this reflects a biological difference between comedocarcinomas and other forms of DCIS cannot be established from this small sample. Notch-4 expression in DCIS was more common in patients older than 50 (11/21 versus 1/5 in patients younger than 50). There was no statistically significant correlation between Notch expression and immunostaining for either ER or p53. However, 5/6 p53 positive tumors were positive for Notch-1 and 2 were also positive for Notch-4. We then studied 41 cases of infiltrating breast carcinoma (27 ductal and 14 lobular) for Notch receptors and ligands. ER, PR and Her2/Neu status were obtained (Table 1). Unlike DCIS, infiltrating breast cancers showed a more consistent pattern. All tumors were positive to some degree for Notch-1 and Notch-4. For Notch-1, two distinct patterns were observed. The first pattern, "variable expression" showed different levels of Notch-1 staining in different cells within the same lesion (Figure 2B), with strongly stained cells appearing on a background of more weakly staining cells. The second pattern, "uniform expression", showed similar staining intensity throughout individual lesions (Figure 2C). Notch-4 staining was consistently uniform. Notch-1 and -4 staining was primarily cytoplasmic but individual cells showed punctate nuclear signal. We grouped cases in which staining intensity was scored as 1-2+ as "low expression" and cases in which staining intensity was scored as 3+ as "high expression". Notch ligands Jagged-1 and Delta-1 showed uniform cytoplasmic staining patterns and were classified as "high" or "low" expression as for Notch-4. All 27 ductal infiltrating carcinomas were Notch-1 positive, 17 with the "variable" pattern and 10 with the "uniform" pattern. Twenty-two/27 were Notch-4 "high", 5 were Notch-4 "low". Twenty-one were Jagged-1 "high". Delta-1 expression generally tracked that of Jagged-1, but with overall lower staining intensity, resulting in 21 Delta-1 "low" and 6 "high". Eleven/14 lobular infiltrating carcinomas showed the Notch-1 "variable" pattern and 3 the "uniform"

pattern. Thirteen/14 tumors in this group were Notch-4 "high". Nine tumors were Jagged-1 "high" and 5 "low" while for Delta-1 the proportions were reversed. Thus, most if not all the infiltrating breast carcinomas studied co-expressed Notch-1 and Notch-4, as well as one or two Notch ligands.

Notch-1 induces Notch-4 in breast cancer cells and enhances proliferation and extracellular matrix invasion. Consistent with these clinical data, human mammary epithelial cells (HMEC) proliferating in culture showed strong Notch-1 expression but near-undetectable Notch-4 (Figure 3A). Breast cancer cell lines MCF-7, MDA-MB231, T47D subclone C42 (29), and T47D subclone A18 (29) expressed variable levels of Notch-1 and Notch-4 proteins, but consistently showed Notch-4 expression. Mature Notch-1 appeared as a cluster of bands, including a ~110 kDa band, often but not always accompanied by one or two faster bands (~100 and ~97 kDa), most likely representing N^{TM}, the TACE cleavage intermediate form (5) and N^{IC} respectively (26). The relative abundance of these bands was different in different cell lines. This suggests that Notch-1 protein processing kinetics may vary between different cell lines and thus, a simple quantitation of total Notch-1 expression based on either mRNA or protein levels would not necessarily reflect the activation status of Notch-1 signaling in any individual cell line. Notch-4 appeared as a ~75 kDa band, consistent with the calculated molecular mass of intracellular Notch-4. A ~110 kDa band was also consistenly seen with Notch-4 antibodies, which followed the same pattern as the ~75 kDa band. This may represent a maturation intermediate, the product of alternate splicing (30) or the result of post-translational modifications. The specificity of these bands was verified by transfecting authentic intracellular Notch-1 and Notch-4 into primary keratinocytes and staining Western blots with the same antibodies used for breast cell lines (Figure 1D). Aggressive, estrogen-independent lines MDA-MB231 and T47D subclone C42 expressed higher Notch-1 and especially Notch-4 levels than estrogen-dependent, non-metastatic lines MCF-7 and T47D subclone A18. Enforced expression of constitutively active Notch-1 in MCF-7 cells induced Notch-4 (Figure 3B). Conversely, silencing of endogenous Notch-1 by siRNA in MDA-MB231 cells downregulated Notch-4 (Figure 3C), indicating that active Notch-1 is upstream of Notch-4 in breast cancer cells. Interestingly, overexpression of constitutively active Notch-1 in MCF-7 cells could not be maintained for more than a few passages (Figure 3B) and was consistently lost in numerous independently transfected sub-lines. This is similar to what we observed in immortalized fibroblasts (26). While it was expressed in MCF-7 cells, intracellular Notch-1 significantly stimulated proliferation as well as invasion through extracellular matrix (Figure 3D, E) suggesting that Notch-1 induces aggressive biological behavior in breast cancer cells, either directly or through Notch-4.

H-Ras and estrogens regulate Notch expression and activity in breast cancer cells. H-Ras is frequently overexpressed in breast cancer (28) and upregulates Notch-1 maturation and activation and Notch-4 expression in human fibroblasts and kidney epithelial cells (26). Additionally, Ras signaling is activated by various growth factor receptors in breast cancer cells. Therefore, we investigated whether H-Ras controlled Notch protein expression in breast cancer cells. Expression of H-Ras in MCF-7 cells strongly increased Notch-1 (particularly the two highest molecular mass bands) and Notch-4 expression, while Jagged-1 expression was constitutively high and only modestly increased by Ras (Figure 4A). The reverse experiment was performed in

T47D:C42 cells, which express constitutively high levels of Notch-1 and -4 and, unlike MDA-MB231, do not carry a K-Ras mutation. Expression of N-17 dominant negative Ras in these cells (Figure 4B) clearly downregulated all Notch-1 bands. Notch-4 was not directly affected by dominant negative Ras in transient transfection experiments, suggesting that effects of Ras on Notch-4, if any, are indirect and mediated by Notch-1. Transient transfection experiments may not cover the time frame required to see such an indirect effect, which requires expression of the dominant negative protein, inhibition of Notch-1 and subsequent inhibition of Notch-4. It should be noted that Notch-1 RNAi causes Notch-4 downregulation only after 48 hours of Notch-1 silencing. Since overall protein levels do not necessarily reflect transcriptional activity, we determined whether enforced expression of either wt H-Ras or H-RasV12 in MCF-7 cells increased CBF-1-dependent transcription, as determined by a reporter assay (26). Although the basal levels of CBF-1 dependent transcription were high in MCF-7 cells, expression of either wild-type or constitutively active H-Ras significantly increased them (Figures 4C, D) (for wt H-Ras $p = 0.001$, for H-RasV12, $p = 0.0008$). Furthermore, expression of dominant negative Ras in T47D:C42 cells significantly decreased CBF-1 dependent transcriptional activity (Figure 4E, $p= 0.002$). This is consistent with the hypothesis that Ras activates Notch signaling in breast cancer cells. The possible downstream mechanisms of this effect were explored using pharmacological inhibitors of the main Ras pathways. In fibroblasts and kidney epithelial cells, the p38 pathway is responsible for Notch signaling activation (26). Conversely, in T47D:C42 breast cancer cells, P38 inhibitor SB203580 did not affect the overall levels of Notch-1 protein for up to 48 hours (not shown). Instead, the PI3-kinase inhibitor wortmannin at nanomolar concentrations caused a dose-dependent decrease in both Notch-1 precursor and Notch-1 mature protein bands within 24 hours (Figure 4F). The MEK1 inhibitor UO126 (10 μM) but not its inactive control UO124, caused a time-dependent accumulation of Notch-1 precursor, with correspondent decrease in mature Notch-1 bands (Figure 4G, H). This data suggests that in T47D:C42 cells, a PI3-kinase-dependent pathway regulates the total amount of Notch-1, while the MEK-ERK pathway stimulates the maturation of the Notch-1 precursor. Protein kinase C inhibitors or the overexpression of PKCα did not affect Notch-1 protein levels in our hands (not shown). All inhibitors were used at concentrations that were determined to be non-cytotoxic in pilot dose-ranging experiments. Wortmannin at 25 nM causes almost complete disappearance of phospho-AKT for at least 8 hours (Figure 4I). We further probed the role of the PI3-kinase pathway in regulating Notch-1 levels using a genetic strategy. Since AKT kinases are key downstream mediators of PI3-kinase, we transiently transfected dominant negative and constitutively active AKT1 into T47D:C42 cells (Figure 4J). Expression of dominant negative AKT caused a virtual disappearance of Notch-1 precursor and a decrease in mature (transmembrane) protein, while expression of constitutively active AKT increased both Notch-1 precursor and mature protein. Finally, we examined the effects of wortmannin and AKT on CBF-1-dependent reporter transcription (Figure 4K, L). Consistent with Western blot data, wortmannin caused a dose-dependent inhibition of CBF-1 luciferase expression ($p= 0.0004$ at 50 nM, $p= 0.0006$ at 100 nM, $p= 0.0001$ at 200 nM) in 48 hour assays, as did expression of dominant negative AKT ($p = 0.0003$) negative, while expression of AKT increased CBF-1 dependent transcription ($p=0.00003$ for wild type AKT, $p= 0.006$ for constitutively active AKT). Taken together, these observations firmly place Notch-1 signaling

downstream of PI3-kinase-AKT in these cells. Interestingly, both the PI3-kinase pathway and the ERK pathway cooperate with Notch-4 in *in-vitro* transformation experiments (31). Our data indicate that they may do so by controlling the level and maturation of Notch-1, which in turn cooperates with Notch-4. We are currently investigating MEK-ERK pathways affect the maturation of Notch-1 precursor protein.

Because of the pivotal role of estrogens in breast cancer biology, we studied whether Notch expression and activity are hormonally regulated. Pure estrogen antagonist ICI 182,780 decreased Notch-1 expression in ERα-positive T47D:A18 cells (29) grown in complete medium containing fetal bovine serum and phenol red, and therefore exposed to estrogen. (Figure 5A) This indicates that estrogen may maintain Notch-1 protein levels in these cells. ICI182,780 did not affect Notch-1 expression in ERα-negative T47D:C42 cells (29). When cells were grown in steroid-free medium without phenol red and with charcoal-stripped serum, treatment with 10^{-9} M estradiol strongly upregulated Notch-1 protein in ERα-positive A18 cells but barely affected it in ERα-negative C42 cells (Figure 5B), possibly through ERβ. The slowest mature Notch-1 band, putatively inactive N^{TM}, appeared especially increased by estradiol. Estradiol consistently failed to upregulate Notch-4 in ERα-positive cells (not shown), despite the increase in Notch-1. This suggests that in ERα-positive cells Notch-1 is prevented from upregulating Notch-4, and could explain the higher levels of Notch-4 in hormone-independent cells. Real-time quantitative PCR experiments indicated that these effects of estrogen are not directly mediated by transcriptional regulation of Notch-1 expression (not shown), suggesting an estrogen effect on one or more of the many post-transcriptional mechanisms that control Notch-1 levels. Because of the consistent failure of estradiol to upregulate Notch-4, we suspected that increased Notch-1 protein levels in estradiol-treated, ERα-positive cells may not correspond to increased Notch signaling activity. Reporter experiments confirmed our hypothesis. Basal levels of CBF-1-dependent transcription were significantly higher in ERα-negative T47D:C42 cells than in ERα-positive T47D:C42 cells ($p < 0.001$, Figure 5C). Moreover, treatment of T47D:A18 cells with anti-estrogen ICI182,780 significantly and reproducibly increased CBF-1 dependent transcription ($p = 0.004$, Figure 5D). This indicates that the effect of estrogen in ERα-positive cells is to suppress Notch-1-dependent transcription, even as it increases the amount of Notch-1 protein. This was confirmed in further reporter experiments in which we demonstrated that estradiol antagonizes the effect of both wt H-Ras and H-RasV12 on CBF-1-dependent transcription, while ICI182,780 potentiates it ($p < 0.05$ for all pairwise comparisons by ANOVA, Figures 5E, F). All in all, these experiments indicate that ERα and Ras have opposite effects on Notch signaling, and that estrogen-independent breast cancer cells may have increased Notch signaling activity, especially in the presence of activated Ras signaling due to overexpression, mutation or activation by growth factor receptors.

Genetic or pharmacological inhibition of Notch signaling inhibit proliferation and extracellular matrix invasion in breast cancer cells. We investigated whether inhibition of Notch activation or expression affects the biological behavior of breast cancer cells. For these experiments, we used MDA-MB231, an invasive, estrogen-independent cell line that spontaneously expresses high levels of Notch-1 and -4. We silenced Notch expression via highly specific RNAi. The Notch-1 targeted siRNA strongly inhibited the expression of both Notch-1 and -4 (see Figure 3C). Notch-1

silencing inhibited proliferation without affecting survival in "normal" HMEC (Figure 6A) and had a similar effect in MDA-MB231 cells (Figure 6B). Notch-4 silencing (Figure 6C) caused an even stronger anti-proliferative effect in MDA-MB231 cells (Figure 6B). Additionally, Notch-1 or Notch-4 silencing significantly inhibited extracellular matrix invasion, with similar potencies (Figure 6D). Since pharmacological agents may represent a more practical way of inhibiting Notch signaling in vivo for therapeutic purposes, we investigated whether these effects of genetic Notch silencing can be replicated by non-selective, pharmacological inhibition of Notch activation with two different γ-secretase inhibitors. These were IL-X (26) (cbz-IL-CHO), which we have previously shown to have Notch-1-dependent anti-neoplastic activity in Ras-transformed fibroblasts (26), and a structurally related but more potent, commercially available compound, cbz-LLNle-CHO (GSI, Calbiochem). In MDA-MB231 cells, 25 μM IL-X (26) caused an apparent reduction in all molecular forms of Notch-1 that was clearly evident after 48 hours of treatment (Figure 7A). Notch-1 is known to induce its own expression (32), which may explain the overall decrease after prolonged treatment, as opposed to accumulation of unprocessed protein. IL-X was cytotoxic for MDA-MB231 cells only above 100 μM (Figure 7B). However, at 25 μM it significantly reduced in vitro matrix invasion of MDA-MB231 cells (Figure 7C). The more potent compound, GSI, caused a clear, dose-dependent decrease in N^{IC} and relative accumulation of the slowest, N^{TM} band, which was already evident at 24h, and virtually complete at 2 μM (Figure 7D). Consistent with this observation, GSI caused dose- and time-dependent cytotoxicity in MDA-MB231 cells that was statistically significant above 1 μM (Figure 7E). Importantly, the effects of GSI on MDA-MB231 cells were significantly rescued by concomitant transient transfection of constitutively active Notch-1 (Figure 7F). This is similar to what we observed in BJ fibroblasts (26). Together with RNAi data, these findings strongly support the hypothesis that: 1) genetic or pharmacological inhibition of Notch signaling have similar effects on MDA-MB231 cells; 2) Notch-4 mediates some, though not necessarily all, the biological effects of Notch-1 in these cells and 3) Notch inhibition is a major mechanism of action of GSI in these cells. Figure 7G-I show that GSI treatment for 48 h caused dose-dependent growth arrest not only in p53-mutant, ERα-negative MDA-MB231 cells, but also in T47D:C42 cells (p53 wild-type, ERα-negative) as well as T47D:A18 cells (p53 wild-type, ERα-positive). Thus, γ-secretase inhibition appears to be effective irrespective of p53 and ERα status.

Pharmacological or genetic inhibition of Notch signaling causes growth arrest in G2/M with decreased cyclin A and B1 levels in breast cancer cells, followed by cell death. We investigated the mechanism of the putative antiproliferative effect shown by Notch inhibitors in cell cycle experiments. Both GSI (Figure 8A) and RNAi silencing of Notch-1 (Figure 8B) or Notch-4 (Figure 8C) caused accumulation of cells in the G2/M stage of the cell cycle and a corresponding decrease in the number of cells in G1 and S.. An increase in the subG1 fraction was also seen, especially at 48 hours, indicative of cell death. With both Notch-1 and Notch-4 RNAi, the accumulation of cells in G2/M was maximal at 24 hours (Figure 8D). At 48 hours the effect disappeared and was replaced by an increased fraction of cells in the "subG1" region. These observations indicate a previously unknown effect of Notch signaling on the G2/M stages of the cell cycle in breast cancer cells. We therefore explored the effects on Notch-1 siRNA on the expression of cyclins, the main regulators of cell cycle progression. Our data (Figure 8E)

indicate that downregulation of Notch-1 decreases the expression of mRNAs for cyclins B1 and A, but not C, D, or A1. Western blot data confirmed these findings. Figure 8F shows that siRNA silencing of Notch-1 causes a striking decrease in the steady state levels of cyclin B1 at 48 hours. Cyclin A was also decreased, with a maximal effect at 24 hours. CDK1 levels were only modestly affected. Cyclin A/cdk2 phosphorylates E2F-1/DP complexes at the end of S-phase, inactivating them. This prevents a re-initiation of DNA replication and assures that the genome is replicated only once at each S phase. Failure of cyclin A/cdk2 to inactivate E2F results in inappropriately persistent E2F activity, which may lead to apoptosis (33;34). E2F-1 is known to upregulate its own transcription (35). Consistent with this notion, Notch-1 siRNA caused a delayed (48 hours) accumulation of E2F-1 (Figure 8G). A known Notch-1 target, p21 (36;37), was downregulated at 24 hours (Figure 8G). Additional experiments indicated that the ratio between nuclear and cytoplasmic levels of cyclin B1 is not affected by Notch silencing (not shown). GSI treatment had identical effects as Notch-1 siRNA on cyclin A and B1 levels (Fig. 8H).

DISCUSSION

We present evidence that Notch signaling is deregulated in breast cancer and affects both proliferation and extracellular matrix invasion in breast cancer cells, thus offering a potential therapeutic target. Co-expression of Notch-1 and Notch-4 appears to be common in breast malignancies, while expression of Notch-1 alone is observed in normal and hyperplastic breast ducts. Consistent with what we described in artificially transformed fibroblasts and kidney epithelial cells (26), Ras is upstream of Notch signaling in breast cancer cells as well. However, the pathway responsible for this effect is different than in fibroblasts and kidney epithelial cells. The p38 pathway does not appear to play a role in Notch regulation in breast cancer cells. Conversely, the PI3-kinase-AKT pathway regulates the total amount of all forms of Notch-1, and the MEK-ERK pathway appears to control the maturation of Notch-1 precursor protein. Both PI3-kinase and MEK pathways are activated by multiple growth receptors in breast epithelial cells. These data suggest that Notch-1 may be a proliferation and/or survival signal in normal, hyperplastic and neoplastic human mammary cells, downstream of PI3-kinase and MEK. The effects of Ras on Notch activity are antagonized by an ERα-dependent effect of estradiol, which selectively induces accumulation of Notch-1 but not Notch-4 and inhibits CBF-1 transcriptional activity. In ERα-negative T47D:C42 cells, otherwise virtually isogenic to the T47D:A18 in which estradiol inhibits CBF-1 activity, H-Ras induces Notch-1 and indirectly, Notch-4. Consistent with this observation, enforced expression of Notch-1 in MCF-7 cells induces Notch-4 and stimulates invasion and proliferation. This is consistent with what we observed in BJ fibroblasts (26) and with the presence of multiple CBF-1 responsive elements in the Notch-4 promoter (30). In MDA-MB231 cells, which spontaneously express Notch-1 and -4, Notch-4 appears to mediate some, though not necessarily all, of the effects of Notch-1. These data suggest a model in which in normal estrogen-responsive cells Notch-1 is a hormone-modulated differentiation/survival signal. In neoplastic cells, uncontrolled Ras- or growth-factor-driven Notch-1 expression and activation stimulates proliferation and induces Notch-4, which in turn stimulates invasion. This effect is enhanced by loss of the ERα-dependent modulation of Notch-1 signaling, which contributes to activate Notch-dependent transcriptional activity. It should be noted that increased expression of Notch-4 and Jagged-1 was observed in MCF-7 cells rendered metastatic by overexpression of HMGI transcription factors (38). The model of growth factor-mediated Notch activation as a key step in tumor progression is consistent with recently published findings in pancreatic cancer, where TGFα-induced Notch activation has been shown to play a key pathogenetic role (21).

Our observations suggest that, consistent with previously described murine models, Notch-1 and -4 may cooperate in human breast cancer progression and may be valuable therapeutic targets in this disease. The molecular targets of Notch-4 remain unknown. However, Notch-1 targets include NF-κB (39;40) and cyclin D1 (41), which are frequently increased in breast cancer. Whether these effects are direct or mediated by Notch-4 remains to be established. We did not observe a downregulation of cyclin D1 expression upon Notch-1 silencing in our cells, nor did we observe accumulation of cells in G1. This does not necessarily mean that Notch-1 does not affect the cyclin D1

promoter. The cyclin D1 promoter is under the control of multiple redundant pathways (42;43), and it is possible that any effects of Notch-1 silencing may be masked by other mediators that regulate cyclin D1 expression. Our study reveals a novel effect of Notch signaling on cyclins A and B1. This observation indicates that Notch signaling plays a previously unrecognized role in cell cycle progression in S and G2/M phases. This novel function of Notch signaling is consistent with two pharmacological observations, namely, that γ-secretase inhibition in mesothelioma cells causes G2/M arrest (20) and that antisense inhibition of Notch-1 in murine erythroleukemia cells potentiates the effects of nocodazole, a microtubule poison (37) and hydroxyurea, an S-phase poison, but not those of serum starvation or farnesyltransferase inhibitors, which cause G1 accumulation. Decreased expression of cyclin A would cause slower progression through S-phase, and potentially, failure to inactivate E2F-1 at the end of S-phase. This in turn could result in multiple DNA replication initiation events and apoptosis (33;34). Decreased levels of cyclin B resulting from inhibited Notch signaling could cause delayed entry into and/or premature exit from mitosis (44-46), triggering cell death as a secondary event. The cell cycle profiles we observe (decreased number of cells in S-phase and increased number of cells with G2/M DNA content, followed at 48 hours by sub-G1 accumulation) are consistent with this model. Pharmacological inhibition of γ-secretase caused virtually complete growth arrest in three different breast cancer cell lines having different p53 and ERα status, with very similar dose-response curves. Taken together, our data indicate that inhibition of Notch signaling through genetic or pharmacological means is a potentially attractive strategy for the treatment of breast carcinomas, irrespective of histological type or hormone receptor status. Notch inhibition appears to function through a novel, unique mechanism involving decreased expression of S- and G2/M phase cyclins A and B1.

MATERIALS AND METHODS

Clinical specimens and immunohistochemistry: Archival routine formalin-fixed, paraffin-embedded blocks from the Breast Pathology Divisions, Department of Pathology, Loyola University Chicago and Brigham and Women's Hospital were studied. No patient identifiers were used. Five μm sections were cut, deparaffinized and stained with appropriate antibodies and controls. Estrogen receptor (clone 6F11, Ventana), progesterone receptor (clone PGP-1A6, Ventana), p53 (clone Bp53-11, Ventana) and Her2/Neu (monoclonal TAB250, Zymed) immunostaining was conducted using standard operating procedures for diagnostic pathology. Her2/neu was evaluated in a semiquatitatively fashion and was assigned a 0, 1+, 2+,and 3+ score (negative, weak, moderate or strong) according to surgical pathology criteria. Notch receptors and ligands were stained using commercial goat polyclonal antibodies from Santa Cruz Biotechnology (Notch-1 C-20, Cat# sc-6014 S), Notch-4 C-19, Cat# sc-8644, Delta-1 C-20, Cat# sc-8155 and Jagged-1, C-20, Cat# sc-6011). An automated Leica Histostainer Ig was used. Serial sections were simultaneously stained with goat non-specific IgG as negative controls. Incubation with primary antibody was performed for 3 hours at room temperature. Detection was performed using a commercially available kit (Vectastain, Vector Laboratories, Burlingame, CA) according to the manufacturer's protocol. Detection of antigen-antibody complexes was performed using a commercially available kit (Mouse ABC staining kit, Santa Cruz). Counterstaining was avoided in most cases to prevent hiding possible nuclear Notch signal. Slides were dehydrated and permanently mounted in non aqueous mounting medium. Staining intensity compared to simultaneously run negative controls was determined by two independent observers based on an arbitrary scale from 0 to 3+. Observers concurred in most cases. Rare discrepancies were resolved by jointly re-examining sections.

Cell lines and constructs: MCF-7 and MDA-MB231 cells were obtained from ATCC. "Normal" human mammary epithelial cells (HMEC) were obtained from Clonetics. T47D:C42 and T47D:A18 cells were a kind gift of Debra Tonetti (UIC). Human Mammary Epithelial Cells (HMEC) were purchased from Clonetics and cultured in mammary epithelial cell basal medium (MEBM) supplemented with 52 μg/ml Bovine Pituitary Extract (BPE), 10 μg/ml human recombinant Epidermal Growth Factor (hEGF), 5 μg/ml insulin, 0.5 μg/ml Hydrocortisone, 50 μg/ml Gentamicin and 50 μg/ml Amphotericin-B. MCF-7 were cultured in MEM medium with 10% FBS, 100 μM non-essential amino acid, 1 mM sodium pyruvate and 10 μg/ml insulin. MDA-MB231 were cultured in DMEM medium with 10% FBS. T47D:C42, T47D:A18 and SKBR3 were propagated in RPMI 1640 with 10% FBS, 100 μM non-essential amino acid and 6 ng /ml insulin. For estradiol treatment experiments, T47D:A18 and C42 cells were cultured in phenol red-free RPMI 1640 with 10% charcoal-stripped serum, 100 μM non-essential amino acid and 6 ng/ml insulin. For experiments in presence of estradiol and/or ICI182,780, cells were treated for 72 hours with 10^{-9} M β estradiol or 10^{-7} M ICI182,780. AKT constructs including empty vector (pUSE Cat# 21-147), constitutively active AKT (Cat#21-151), dominant negative AKT (Cat# 21-251), wild type AKT (Cat#21-153).were purchased from Upstate Biotechnology (Lake Placid, N.Y.). Notch constructs and CBF-1 luciferase reporter assays have been previously described (26).

Drugs and chemicals: Gamma secretase inhibitor IL-X (cbz-IL-CHO) (47) was a kind gift from T. Golde (Mayo Clinic Jacksonville). IL-X was dissolved in DMSO and aliquoted and stored at -80° C. Aliquots were thawed before use and not re-used. Gamma-secretase inhibitor cbz-Leu-Leu-Nle-CHO (Calbiochem 565750) was dissolved in DMSO, aliquoted and stored at -80° C. β estradiol (Sigma, St. Louis MO) was dissolved in ethanol at a concentration of 10^{-6} M and stored in aliquots at –80° C. ICI182,780 at a concentration of 10^{-4} M in ethanol was a kind gift of Dr. Debra Tonetti (UIC).

RNA interference: Double-stranded synthetic 21-mer RNA oligonucleotides (siRNAs) were purchased from Dharmacon (Lafayette, CO). The most effective sequences were selected in pilot experiments and were as follows: Notch-1 5'AAG TGT CTG AGG CCA GCA AGA3'; Notch-4 5'AAC CCT GTG CCA ATG GAG GCA3'. A control siRNA which does not match any known mammalian GENBANK sequences (Dharmacon) was used in all experiments: 5'AAC AGT CGC GTT TGC GAC TGG3'. Sequence specificity was determined by BLAST searches which determined the uniqueness of our sequences. Transfection of siRNAs was performed using Oligofectamine (Invitrogen) as recommended by the siRNA manufacturer (Dharmacon). Transfection efficiency was optimized and followed on parallel wells using DNA double stranded oligos of identical sequence to the siRNAs, labeled with biotin on one strand. Transfected cells were identified by Streptavidin-horse radish peroxidase staining (Vectastain) and counted. We routinely obtained transfection efficiencies around 80%.

Western blotting: Total cell lysates were prepared as follows: Cells grown on 6 cm dishes were scraped in lysis buffer containing 1 x PBS, 1% Nonidet P40, 0.5% deoxycholate, 0.1% SDS, freshly added aprotinin (45 μg/ml), phenylmethylsulfonyl fluoride (10μg/ml), and sodium orthovanadate (10 μM). Lysates were sonicated 4 times for 5 seconds each, followed by 30 minutes incubation on ice. Lysates were centrifuged at 10,000 *g* for 20 minutes at 4° C. Supernatant were used as total cell lysates. Nuclear extracts were prepared as follows: 10,000,000 cells were pelleted, washed, and quickly frozen in a dry ice bath. Pellets were thawed by adding 100 μl of buffer 1 (10 mM HEPES, pH 7.9, 10 mM KCl, 1.5 mM $MgCl_2$, 1 mM DTT). Nuclei were pelleted and lysed in 15 μl Buffer 2 (20 mM HEPES, pH7.9, 0.4 M NaCl, 1.5 mM $MgCl_2$, 25% glycerol, 0.2 mM EDTA, 1 mM DTT, and 0.5 mM PMSF). Lysates were diluted in 50-70 μl Buffer 3 (20 mM HEPES, pH 7.9, 50 mM KCl, 20% glycerol, 0.2 mM EDTA, 1 mM DTT, 0.5 mM PMSF). Protein concentrations were estimated using the BCA protein assay (Pierce). Supernatants were boiled in reducing SDS sample buffer (Novex). Twenty μg protein per lane were run on a 3-8% Tris acetate gel (Invitrogen) in Tris Acetate Reducing Running Buffer (Novex). Protein bands were transferred onto PVDF membranes (BioRad) using transfer buffer (Novex). Membranes were then blocked overnight at 4° C in 2% blocking solution in TBS (Roche). Primary antibodies (same as used for immunohistochemistry) were diluted in 2% Boehringer blocking solution (total volume 5 ml). Membranes were incubated for one hour at room temperature with shaking, then washed 6 times for 10 minutes each in TBS wash buffer. Membranes were incubated in secondary antibody in 2% of blocking solution for 30 minutes, then washed 6 times for 10 minutes each at RT in wash buffer. Bands were detected with chemiluminescent reagent (Roche). Membrane were stripped in 62.5 mM Tris-HCl (pH 6.7) containing 2% SDS and 0.7% β–mercaptoethanol for 30 minutes at 55°C, blocked, and then reprobed as described above.

Cytotoxicity, growth and chemoinvasion assays: Cytotoxicity and growth of attached cells were estimated by a standard assay used for cancer drug screening, through the total amount of TCA-precipitated cell proteins after drug treatment (48): 200 µl of cell suspension (100,000 cells/ml) were added to each well in a 96-well plate. After incubation at 37°C, in 5% CO_2 (30 minutes to 72 hours depending on the time course chosen), 50 µl 50% trichloroacetic acid was added to each well. After incubation at 4° C for 1 hour, precipitates were washed with water 4-5 times and air dried overnight. One hundred µl of SRB solution (0.4% sulforhodamine B in 1% acetic acid, filtered before use) was added to each well for 30 minutes. Wells were washed with 1% acetic acid 4-5 times and air dried. Two hundred µl 10 mM Tris base was added to each well. Plates were shaken for 5-10 minutes and OD at 490 nm (OD_{490}) was recorded via ELISA reader. To assay matrix invasion, 300 µl of cell suspension (1,000,000 cells/mL in serum-free medium) were added to invasion inserts (BioCoat Matrigel Invasion Chambers, Becton Dickinson, Bedford, MA) and incubated for 22 hours at 37°C, 5% CO_2. Cells were stained with 0.9% crystal violet in 10% ethanol for 20 minutes. Inserts were dipped in water several times and air dried. After removal of the non-invading cells from the interior of the inserts, stained invading cells were lysed in 10% acetic acid and OD_{595} was determined. Pilot experiments determined that this method was more reproducible than counting individual cells by light microscopy and gave comparable results. Isobolograms were constructed using TableCurve (SPSS).

Cell cycle analysis by flow cytometry. 10^6 cells were pelleted and washed twice in PBS. Cells were then fixed in 80% methanol and stored at -20°C until use. Fixed cells were pelleted and washed twice in PBS, and resuspended in 50 µl PI:PBS solution (50µg/ml PI). After RNase A (100 µg/ml) treatment at 37 °C for an hour, cells were analyzed by flow cytometry using a FACScalibur instrument.

Real-time PCR. RNA was extracted from T47D:A18 cell line after estradiol treatment using a commercially available kit (Qiagen, Valencia CA). 1 µg of RNA was reverse transcribed in 20 µl reaction using 15 units of AMV reverse transcriptase (Invitrogen, Carlsbad, CA) and 500 ng of oligo$(dT)_{20}$. Reaction conditions were as suggested by manufacturer. 2.5 µl of the cDNA mixture were used for REAL TIME PCR experiments to measure the amount of Notch 1 transcript. GAPDH mRNA was used for normalization of RNA amount. REAL TIME PCR reactions were conducted on a ABI PRISM 7700 Sequence Detector using Platinum Quantitative PCR SuperMix-UDG (Invitrogen, Carlsbad CA) with 5.5 mM $MgCl_2$ in a final volume of 25 µl. The following primers and probes were used for Notch-1: forward 5'CGG GTC CAC CAG TTT GAA TG3', reverse GTT GTA TTG GTT CGG CAC CAT, probe 6 FAM-CCG CTC TGC AGC CGG GAC AG-TAMRA. Primers and probe for GAPDH mRNA (Applied Biosystem, Foster City CA) were used for normalization of RNA amount.

Ribonuclease Protection Assays. Total RNA was prepared using the RNeasy Mini Kit (QIAGEN Cat# 74104) according to manufacturer's protocol. The multi-probe template set hCYC-1 (containing DNA templates for, Cyclin A, Cyclin B, Cyclin C, Cyclin D1, Cyclin D2, Cyclin D3, Cyclin A1, L32, and GAPDH) was purchased from BD Bioscience (Cat# 556189). The DNA template was used to synthesize a [^{32}P]UTP (10 mCi/ml, Amersham Bioscience) labelled probe in the presence of a GACU pool using a T7 RNA-polymerase (BD Bioscience RiboQuant RPA starter Package, Cat# 556144). Hybridization with 20µg of each target RNA was performed at 56 °C overnight, followed

by digestion with RNAse A and T1 according to the BD Bioscience standard protocol. After proteinase K treatment, samples were precipitated, loaded on a 4.75% acrylamide–urea gel, and run at 55W with 0.5× TBE. Gels were dried in the gel dryer undervacum for 2 hour at 90 °C. Then gels were exposed on Kodak film (Eastman Kodak, Rochester, NY) with intensifying screens and developed at -70 °C.

Statistical analysis. For pairwise comparisons, two-tailed unpaired Student's t-tests were used with $\alpha = 0.05$. When more than two samples were compared, one-way ANOVA was used (Student-Newman-Keuls method for multiple comparisons), with $\alpha = 0.05$. SigmaStat software (Jandel Scientific) was used for statistical analysis.

References

1. Artavanis-Tsakonas,S., Rand,M.D., and Lake,R.J. 1999. Notch signaling: cell fate control and signal integration in development. *Science* 284:770-776.

2. Miele,L. and Osborne,B.A. 1999. Arbiter of differentiation and death: Notch signaling meets apoptosis. *J.Cell Physiol.* 181:393-409.

3. Logeat,F., Bessia,C., Brou,C., LeBail,O., Jarriault,S., Seidah,N.G., and Israel,A. 1998. The Notch1 receptor is cleaved constitutively by a furin-like convertase. *Proc.Natl.Acad.Sci.U.S.A.* 95:8108-8112.

4. Blaumueller,C.M., Qi,H., Zagouras,P., and Artavanis-Tsakonas,S. 1997. Intracellular cleavage of notch leads to a heterodimeric receptor on the plasma membrane. *Cell* 90:281-291.

5. Mumm,J.S., Schroeter,E.H., Saxena,M.T., Griesemer,A., Tian,X., Pan,D.J., Ray,W.J., and Kopan,R. 2000. A ligand-induced extracellular cleavage regulates gamma-secretase-like proteolytic activation of Notch1. *Mol.Cell* 5:197-206.

6. Struhl,G. and Greenwald,I. 1999. Presenilin is required for activity and nuclear access of Notch in Drosophila [In Process Citation]. *Nature* 398:522-525.

7. Weinmaster,G. 1997. The ins and outs of notch signaling. *Mol.Cell Neurosci.* 9:91-102.

8. Zlobin,A., Jang,M.-S., and Miele,L. 2000. Toward the rational design of cell fate modifiers: Notch signaling as a target for novel biopharmaceuticals. *Curr.Pharm.Biotechnol.* 1:83-106.

9. Ellisen,L.W., Bird,J., West,D.C., Soreng,A.L., Reynolds,T.C., Smith,S.D., and Sklar,J. 1991. TAN-1, the human homolog of the Drosophila notch gene, is broken by chromosomal translocations in T lymphoblastic neoplasms. *Cell* 66:649-661.

10. Weng,A.P., Ferrando,A.A., Lee,W., Morris,J.P., Silverman,L.B., Sanchez-Irizarry,C., Blacklow,S.C., Look,A.T., and Aster,J.C. 2004. Activating mutations of NOTCH1 in human T cell acute lymphoblastic leukemia. *Science* 306:269-271.

11. Capobianco,A.J., Zagouras,P., Blaumueller,C.M., Artavanis-Tsakonas,S., and Bishop,J.M. 1997. Neoplastic transformation by truncated alleles of human NOTCH1/TAN1 and NOTCH2. *Mol.Cell Biol.* 17:6265-6273.

12. Pear,W.S., Aster,J.C., Scott,M.L., Hasserjian,R.P., Soffer,B., Sklar,J., and Baltimore,D. 1996. Exclusive development of T cell neoplasms in mice transplanted with bone marrow expressing activated Notch alleles. *J.Exp.Med.* 183:2283-2291.

13. Bellavia,D., Campese,A.F., Alesse,E., Vacca,A., Felli,M.P., Balestri,A., Stoppacciaro,A., Tiveron,C., Tatangelo,L., Giovarelli,M. *et al.* 2000. Constitutive activation of NF-kappaB and T-cell leukemia/lymphoma in Notch3 transgenic mice. *EMBO J.* 19:3337-3348.

14. Callahan,R. and Raafat,A. 2001. Notch signaling in mammary gland tumorigenesis. *J.Mammary.Gland.Biol.Neoplasia* 6:23-36.

15. Zagouras,P., Stifani,S., Blaumueller,C.M., Carcangiu,M.L., and Artavanis-Tsakonas,S. 1995. Alterations in Notch signaling in neoplastic lesions of the human cervix. *Proc.Natl.Acad.Sci.U.S.A.* 92:6414-6418.

16. Daniel,B., Rangarajan,A., Mukherjee,G., Vallikad,E., and Krishna,S. 1997. The link between integration and expression of human papillomavirus type 16 genomes and cellular changes in the evolution of cervical intraepithelial neoplastic lesions. *J.Gen.Virol.* 78:1095-1101.

17. Leethanakul,C., Patel,V., Gillespie,J., Pallente,M., Ensley,J.F., Koontongkaew,S., Liotta,L.A., Emmert-Buck,M., and Gutkind,J.S. 2000. Distinct pattern of expression of differentiation and growth-related genes in squamous cell carcinomas of the head and neck revealed by the use of laser capture microdissection and cDNA arrays. *Oncogene* 19:3220-3224.

18. Rae,F.K., Stephenson,S.A., Nicol,D.L., and Clements,J.A. 2000. Novel association of a diverse range of genes with renal cell carcinoma as identified by differential display. *Int.J.Cancer* 88:726-732.

19. Suzuki,T., Aoki,D., Susumu,N., Udagawa,Y., and Nozawa,S. 2000. Imbalanced expression of TAN-1 and human notch4 in endometrial cancers. *Int.J.Oncol.* 17:1131-1139.

20. Bocchetta,M., Miele,L., Pass,H.I., and Carbone,M. 2003. Notch-1 induction, a novel activity of SV40 required for growth of SV40-transformed human mesothelial cells. *Oncogene* 22:81-89.

21. Miyamoto,Y., Maitra,A., Ghosh,B., Zechner,U., Argani,P., Iacobuzio-Donahue,C.A., Sriuranpong,V., Iso,T., Meszoely,I.M., Wolfe,M.S. *et al.* 2003. Notch mediates TGFalpha-induced changes in epithelial differentiation during pancreatic tumorigenesis. *Cancer Cell* 3:565-576.

22. Tohda,S. and Nara,N. 2001. Expression of Notch1 and Jagged1 proteins in acute myeloid leukemia cells. *Leuk.Lymphoma* 42:467-472.

23. Jundt,F., Anagnostopoulos,I., Forster,R., Mathas,S., Stein,H., and Dorken,B. 2002. Activated Notch1 signaling promotes tumor cell proliferation and survival in Hodgkin and anaplastic large cell lymphoma. *Blood* 99:3398-3403.

24. Dievart,A., Beaulieu,N., and Jolicoeur,P. 1999. Involvement of Notch1 in the development of mouse mammary tumors. *Oncogene* 18:5973-5981.

25. Kiaris,H., Politi,K., Grimm,L.M., Szabolcs,M., Fisher,P., Efstratiadis,A., and Artavanis-Tsakonas,S. 2004. Modulation of notch signaling elicits signature tumors and inhibits hras1-induced oncogenesis in the mouse mammary epithelium. *Am.J.Pathol.* 165:695-705.

26. Weijzen,S., Rizzo,P., Braid,M., Vaishnav,R., Jonkheer,S.M., Zlobin,A., Osborne,B.A., Gottipati,S., Aster,J.C., Hahn,W.C. *et al.* 2002. Activation of Notch-1 signaling maintains the neoplastic phenotype in human Ras-transformed cells. *Nat.Med.* 8:979-986.

27. Clark,G.J. and Der,C.J. 1995. Aberrant function of the Ras signal transduction pathway in human breast cancer. *Breast Cancer Res.Treat.* 35:133-144.

28. Malaney,S. and Daly,R.J. 2001. The ras signaling pathway in mammary tumorigenesis and metastasis. *J.Mammary.Gland.Biol.Neoplasia* 6:101-113.

29. Pink,J.J., Bilimoria,M.M., Assikis,J., and Jordan,V.C. 1996. Irreversible loss of the oestrogen receptor in T47D breast cancer cells following prolonged oestrogen deprivation. *Br.J.Cancer* 74:1227-1236.

30. Li,L., Huang,G.M., Banta,A.B., Deng,Y., Smith,T., Dong,P., Friedman,C., Chen,L., Trask,B.J., Spies,T. *et al.* 1998. Cloning, characterization, and the complete 56.8-kilobase DNA sequence of the human NOTCH4 gene. *Genomics* 51:45-58.

31. Fitzgerald,K., Harrington,A., and Leder,P. 2000. Ras pathway signals are required for notch-mediated oncogenesis. *Oncogene* 19:4191-4198.

32. Deftos,M.L., He,Y.-W., Ojata,E.W., and Bevan,M.J. 1998. Correlating Notch signaling with thymocyte maturation. *Immunity* 9:777-786.

33. Nevins,J.R., Chellappan,S.P., Mudryj,M., Hiebert,S., Devoto,S., Horowitz,J., Hunter,T., and Pines,J. 1991. E2F transcription factor is a target for the RB protein and the cyclin A protein. *Cold Spring Harb.Symp.Quant.Biol.* 56:157-162.

34. Yam,C.H., Fung,T.K., and Poon,R.Y. 2002. Cyclin A in cell cycle control and cancer. *Cell Mol.Life Sci.* 59:1317-1326.

35. Lavia,P. and Jansen-Durr,P. 1999. E2F target genes and cell-cycle checkpoint control. *Bioessays* 21:221-230.

36. Rangarajan,A., Talora,C., Okuyama,R., Nicolas,M., Mammucari,C., Oh,H., Aster,J.C., Krishna,S., Metzger,D., Chambon,P. *et al.* 2001. Notch signaling is a direct determinant of keratinocyte growth arrest and entry into differentiation. *EMBO J.* 20:3427-3436.

37. Jang,M.-S., Miao,H., Carlesso,N., Shelly,L.L., Zlobin,A., Darack,N., Qin,J.-Z., Nickoloff,B.J., and Miele,L. 2003. Notch-1 regulates cell death independently of differentiation in murine erythroleukemia cells through multiple apoptosis and cell cycle pathways. *J.Cell Physiol.* in press.

38. Reeves,R., Edberg,D.D., and Li,Y. 2001. Architectural transcription factor HMGI(Y) promotes tumor progression and mesenchymal transition of human epithelial cells. *Mol.Cell Biol.* 21:575-594.

39. Cheng,P., Zlobin,A., Volgina,V., Gottipati,S., Osborne,B., Simel,E.J., Miele,L., and Gabrilovich,D.I. 2001. Notch-1 Regulates NF-kappaB Activity in Hemopoietic Progenitor Cells. *J.Immunol.* 167:4458-4467.

40. Nickoloff,B.J., Qin,J.Z., Chaturvedi,V., Denning,M.F., Bonish,B., and Miele,L. 2002. Jagged-1 mediated activation of notch signaling induces complete maturation of human keratinocytes through NF-kappaB and PPARgamma. *Cell Death Differ.* 9:842-855.

41. Ronchini,C. and Capobianco,A.J. 2001. Induction of cyclin D1 transcription and CDK2 activity by Notch(ic): implication for cell cycle disruption in transformation by Notch(ic). *Mol.Cell Biol.* 21:5925-5934.

42. Sherr,C.J. 1995. D-type cyclins. *Trends Biochem.Sci.* 20:187-190.

43. Coqueret,O. 2002. Linking cyclins to transcriptional control. *Gene* 299:35-55.

44. Nigg,E.A. 2001. Mitotic kinases as regulators of cell division and its checkpoints. *Nat.Rev.Mol.Cell Biol.* 2:21-32.

45. O'Farrell,P.H. 2001. Triggering the all-or-nothing switch into mitosis. *Trends Cell Biol.* 11:512-519.

46. Shapiro,G.I. and Harper,J.W. 1999. Anticancer drug targets: cell cycle and checkpoint control. *J.Clin.Invest* 104:1645-1653.

47. McLendon,C., Xin,T., Ziani-Cherif,C., Murphy,M.P., Findlay,K.A., Lewis,P.A., Pinnix,I., Sambamurti,K., Wang,R., Fauq,A. *et al.* 2000. Cell-free assays for gamma-secretase activity. *FASEB J.* 14:2383-2386.

48. Likhitwitayawuid,K., Angerhofer,C.K., Cordell,G.A., Pezzuto,J.M., and Ruangrungsi,N. 1993. Cytotoxic and antimalarial bisbenzylisoquinoline alkaloids from Stephania erecta. *J.Nat.Prod.* 56:30-38.

Table 1: Expression of Notch receptors and ligands in human normal, pre-neoplastic and neoplastic breast.

	Normal (n=4)	HUT (n=5)	DCIS (n=27)	IDC (n=27)	ILC (n=14)
Notch-1 N	3 (75)	1 (20)	9 (33)	0	0
Notch-1 V	0	0	0	17 (63)	11 (79)
Notch-1 U	1 (25)	4 (80)	18 (67)	10 (37)	3 (21)
Notch-4 N	4 (100)	5 (100)	15 (56)	0	0
Notch-4 H	0	0	0	22 (81)	13 (93)
Notch-4 L	0	0	12 (44)	5 (19)	1 (7)
Jagged-1 H	ND	ND	ND	21 (78)	9 (64)
Jagged-1 L	ND	ND	ND	6 (22)	5 (36)
Delta-1 H	ND	ND	ND	6 (22)	5 (36)
Delta-1 L	ND	ND	ND	21 (78)	9 (64)
p53	ND	ND	6 (22)	ND	ND
ER	ND	ND	21	23 (86)	13 (93)
PR	ND	ND	ND	21 (78)	9 (64)
Her2/Neu	ND	ND	ND	7 (26)	2 (14)

Percent values are in parentheses. Abbreviations: N = negative; V = Variable intensity; U = uniform intensity; H = high intensity (3+); L = low intensity (1-2+); ER = estrogen receptor; PR = progesterone receptor; HUT = hyperplasia of usual type; DCIS = ductal carcinoma in situ; IDC = infiltrating ductal carcinoma; ILC = infiltrating lobular carcinoma.

FIGURE LEGENDS:

Figure 1: Immunohistochemistry detection of Notch receptors in normal and hyperplastic breast and DCIS. A, normal human breast negative for Notch-1. The only staining is background within ductal lumina; B, normal human breast positive for Notch-1 (1+); C, a DCIS lesion intensely positive for Notch-1 (3+); D, the same DCIS lesion, negative for Notch-4; E, apocrine metaplasia, positive for Notch-1 (2+), F, a DCIS lesion, negative for Notch-1, next to normal ducts which appear intensely positive for Notch-1 (3+); G, DCIS, positive for Notch-1 (2+); H, the same DCIS, positive for Notch-4 (2+)

Figure 2: Immunohistochemistry detection of Notch receptors and ligands in a representative case of infiltrating ductal carcinoma. A, hematoxylin-eosin; B, variable intensity positive staining for Notch-1 (2+); C, uniform intensity positive staining for Notch-4 (2-3+); D; Jagged-1 staining (2+); E. Delta-1 staining (2+) F, negative control run in parallel (non-immune goat IgG as primary antibody).

Figure 3: Notch-1 is upstream of Notch-4 in breast cancer cell lines and induces proliferation and extracellular matrix invasion. Western blots showing Notch expression. A, Breast cancer cell lines consistently express Notch-1, and 4/5 co-express Notch-1 and 4. HMEC proliferating in culture expressed high levels of Notch-1 and nearly undetectable Notch-4. B, enforced expression of constitutively active Notch-1 induced Notch-4 but was unstable in MCF-7 cells: two independently transfected non-clonal sub-lines of MCF-7 cells expressing intracellular Notch-1 (Notch-1A and -1B) expressed high levels of Notch-1 and -4. After 6 passages (p6) Notch-1 expression had returned to control levels. This phenomenon was observed in at least 4 independent experiments; C, Silencing of Notch-1 in MDA-MB231 cells by RNA interference (RNAi) also silenced Notch-4. The siRNA sequence used had no counterpart in Notch-4 nor any other known genes. Control was a siRNA with no homology to known mammalian genes (Dharmacon); D, controls for antibody specificity. Primary human keratinocytes were transfected with pLZRS constructs encoding Notch-1 or Notch-4 N^{IC} respectively, and extracts were analyzed by Western blotting as was done for breast cell lines; E MCF-7 cells expressing Notch-1 invaded through Matrigel-coated filters significantly more effectively than cells transfected with empty vector ($p=0.00197$, $n = 3$); F, MCF-7 cells expressing Notch-1 grew significantly faster than cells transfected with empty vector ($n = 3$). Error bars are standard deviations. Each experiment was repeated at least 3 times.

Figure 4: Ras is upstream of Notch -1 and -4 in breast cancer cells and controls Notch-1 levels via a PI3-kinase-AKT pathway. A, B, Western blots showing expression of Notch receptors and ligand Jagged-1. A, Enforced expression of wild-type H-Ras induced Notch-1 and -4 in MCF-7 cells. Notch-1 transmembrane and intracellular forms were increased by Ras, as we have previously shown in fibroblasts and kidney epithelial cells. Jagged-1 expression was constitutively high in these cells; B, enforced expression of dominant-negative H-Ras (N-17) in spontaneously "Notch-high" T47D:C42 cells (ER-negative), downregulated Notch-1 but did not simultaneously affect Notch-4, suggesting that any effects of Ras on Notch-4 in these cells are indirect; C, D, E, transfection of wild-type H-Ras (C) or H-RasV12 (D) in MCF-7 cells significantly

increased CBF-1 transcriptional activity as measured by a reporter plasmid, ($p = 0.001$ for wild type H-Ras and $p = 0.0008$ for H-RasV12), while transfection of dominant-negative H-Ras (E) significantly decreased CBF-1 activity in "Notch-high" T47D:C42 cells ($p= 0.002$). Error bars are standard deviations. Each experiment was repeated at least 3 times; F, Wortmannin (25 and 50 nM) reduced the levels of both full-length (FL) and mature Notch-1 (N^{TM}, N^{IC}) detected by Western blotting; G, H, MEK inhibitor UO126, but not its inactive control UO124, did not reduce overall levels of Notch-1 but caused relative accumulation of the full-length precursor protein and decrease in the mature forms, most evident at 48 hours; I, Wortmannin at 50 nM caused virtually complete loss of phospho-AKT up to at least 8 hours. The effect was reversed after 24 h (not shown); J, transient transfection of dominant-negative, MYC-tagged AKT (DN) decreased overall Notch-1 levels in T47D:C42 cells as detected by Western blotting and caused virtual disappearance of the full-length precursor band, while transfection of MYC-tagged constitutively active (CA) AKT increased levels of both precursor and mature forms of Notch-1; K, Wortmannin (50, 100 and 200 nM) significantly decreased CBF-1 transcriptional activity as measured by a luciferase reporter ($p= 0.0004$ at 50 nM, $p= 0.0006$ at 100 nM, $p= 0.0001$ at 200 nM) in 48 hour assays; L, transient transfection of dominant-negative (DN) AKT in T47D:C42 cells significantly decreased CBF-1 transcriptional activity while either wild-type (WT) or constitutively active (CA) AKT increase it ($p = 0.0003$ for dominant negative AKT, $p=0.00003$ for wild type AKT, $p= 0.006$ for constitutively active AKT). Error bars are standard deviations. Each experiment was repeated at least 3 times.

Figure 5: ERα regulates Notch -1 in breast cancer cells and antagonizes the effects of Ras. Western blots showing Notch-1 expression. A, ER antagonist ICI182,780 downregulated Notch-1 in T47D subclone A18 (ERα-positive) but not in T47D subclone C42 (ERα-negative) grown in regular medium; B, estradiol added to steroid-free medium upregulated Notch-1 expression in T47D:A18 cells but not in C42 cells. Results are representative of 5 independent experiments; C, basal CBF-1 activity determined by a luciferase reporter was strikingly higher in ERα-negative T47D:C42 cells than in ERα-positive T47D:C42 cells ($p <0.001$); D, treatment of T47D:A18 cells with anti-estrogen ICI182,780 significantly increased CBF-1 dependent transcription ($p = 0.004$); E, F, estradiol antagonized the effect of both wt H-Ras and H-RasV12 on CBF-1-dependent transcription, while ICI182,780 potentiated it ($p <0.05$ for all pairwise comparisons by ANOVA). Error bars are standard deviations. Each experiment was repeated at least 3 times.

Figure 6: Genetic silencing of Notch receptors inhibits proliferation in HMEC and has anti-neoplastic effects on MDA-MB231 cells. A, Silencing of Notch-1 by RNAi inhibited the proliferation of "normal" HMEC cells. See Figure 3C for effects on Notch-1 and -4 expression. Error bars are standard deviations ($n = 3$). Representative data of 3 experiments. B, RNAi silencing of Notch-1 (which also affects Notch-4) or silencing of Notch-4 alone inhibited the proliferation of MDA-MB231 cells; C, Western blots showing nearly quantitative inhibition of Notch-4 expression by RNAi; D, silencing of Notch-1 and -4 (Notch-1i) or Notch-4 (Notch4i) significantly inhibited migration of MDA-MB231 cells through matrigel-coated filters ($p = 0.0003$ and 0.0004 for Notch-1

and -4 respectively). Control was a siRNA with no homology with known mammalian genes (Dharmacon).

Figure 7: Inhibition of γ-secretase has anti-neoplastic effects on breast cancer cells irrespective of p53 and ERα status. A-C: Exposure to non-cytotoxic concentrations of γ-secretase inhibitor IL-X inhibits extracellular matrix invasion in MDA-MB231 cells. A, Western blots showing reduced levels of Notch-1 protein, both N^{IC} and N^{TM}, after 48 hours treatment with IL-X. At 24h only modest relative accumulation of N^{TM} was observed (not shown); B, time and concentration-dependent cytotoxicity tests, showing that at 48 hours IL-X did not affect the growth of MDA-MB231 cells at concentrations up to 50 μM; C, treatment with 25 or 50 μM IL-X significantly inhibited migration of MDA-MB231 cells through matrigel-coated filters (p =0.01 at 25 μM and 0.006 at 50 μM). D, Western blots showing dose-dependent reduction of N^{IC} levels in the presence of more potent inhibitor γ-secretase inhibitor cbz-LLNle-CHO (GSI) for 24 h; E, time and concentration-dependent cytotoxicyty tests, showing that GSI had significant toxicity above 2 μM at 24 h and above 1 μM at 48 hours; F, transient transfection of intracellular Notch-1 (N^{IC}) strikingly rescued cell killing by GSI compared to empty vector at all concentrations tested. Since transfection efficiency in these experiments is never 100%, and 100% of the cells are exposed to GSI, the extent of rescue, though remarkable, is underestimated by these experiments; G, H, I, dose response curves of growth inhibition by GSI in three different breast cancer cell lines: MDA-MB231 (p53 mutant, ERα negative), T47D:C42 (p53 wild type, ERα negative) and T47D:A18 (p53 wild type, ERα positive).

Figure 8: Pharmacological or genetic inhibition of Notch signaling causes G2/M arrest in MBA-MD231 cells. A, dose-dependent growth arrest of MDA-MB231 cells treated overnight with GSI. Cell cycle distribution was determined by flow cytometry. Data are representative of 3 independent experiments. B, RNAi silencing of Notch-1 caused comparable G2 accumulation as cytotoxic doses of GSI; C, Notch-4 silencing gave virtually identical results. Data representative of 3 independent experiments each performed in triplicate (p = 0.000026 for Notch-4 and 0.01 for Notch-1 respectively); D, representative raw data from flow cytometry experiments, showing the effects of RNAi silencing of Notch-1 and -4 on cell cycle distribution of MDA-MB231 cells. Notice the relative accumulation of cells in G2/M at 24 hours followed by appearance of prominent "sub-G1" peaks at 48 h, indicative of cell death. Numbers above the graphs indicate percentages of cells in subG1, G1, S, and G2/M respectively. Sub-G1 induction was statistically significant (p = 0.01) compared to controls transfected with an inactive siRNA; E, ribonuclease protection assay showing that mRNA levels for cyclins A and B1 were reduced in cells transfected with Notch-1 siRNA. L32 (rRNA) and GAPDH were internal controls. Additional controls were untreated cells and tRNA (non-specific protection control); F, Western blots showing that cells transfected with Notch-1 siRNA had dramatically reduced levels of cyclin B1 and cyclin A proteins, with a somewhat more modest effect on cdk1(cdc2); G, Western blots showing that Notch-1 siRNA silencing causes accumulation of E2F-1 at 48 h and downregulation of p21 at 24 h; H, GSI treatment for 24 h decreases cyclin A and B1. Cyclin A was strikingly decreased at 0.5 μM, while cyclin B was decreased at 1 μM.

ACKNOWLEDGMENTS

The authors are grateful to Dr. Debra Tonetti for helpful discussions and for the gift of ICI182,780, to Dr. Barbara Osborne for helpful discussions and to Dr. Todd Golde for the gift of IL-X. This work was supported by NIH grant R01 CA 84065/01/CA/NCI.

Figure 1

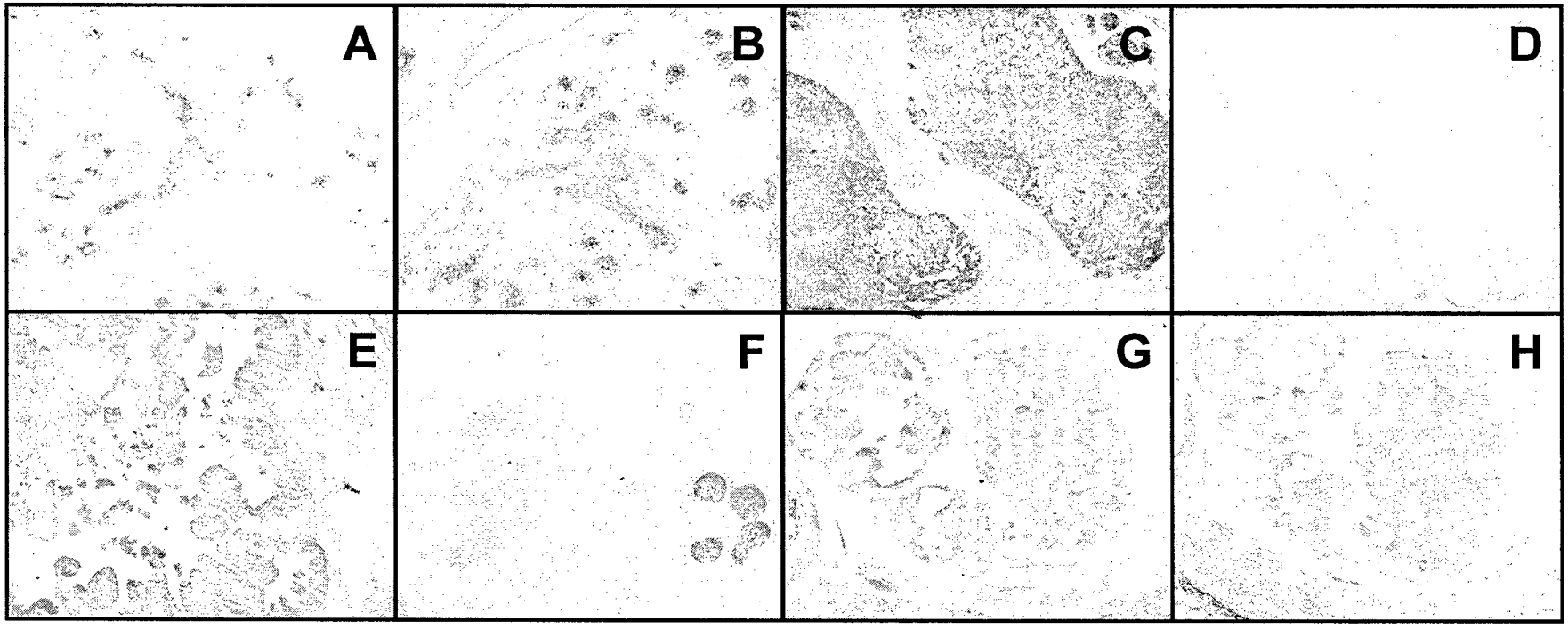

Figure 2

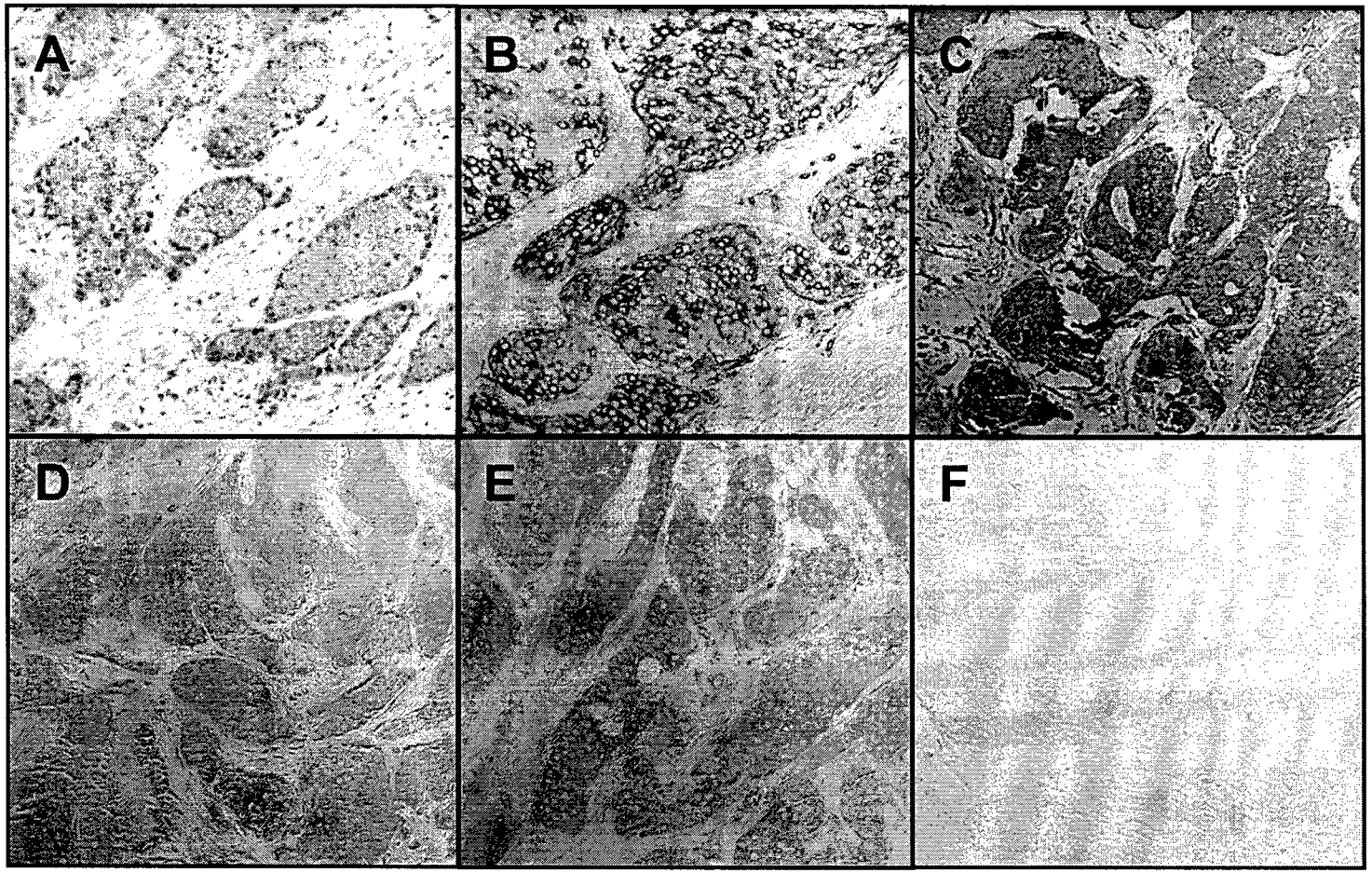

Figure 3

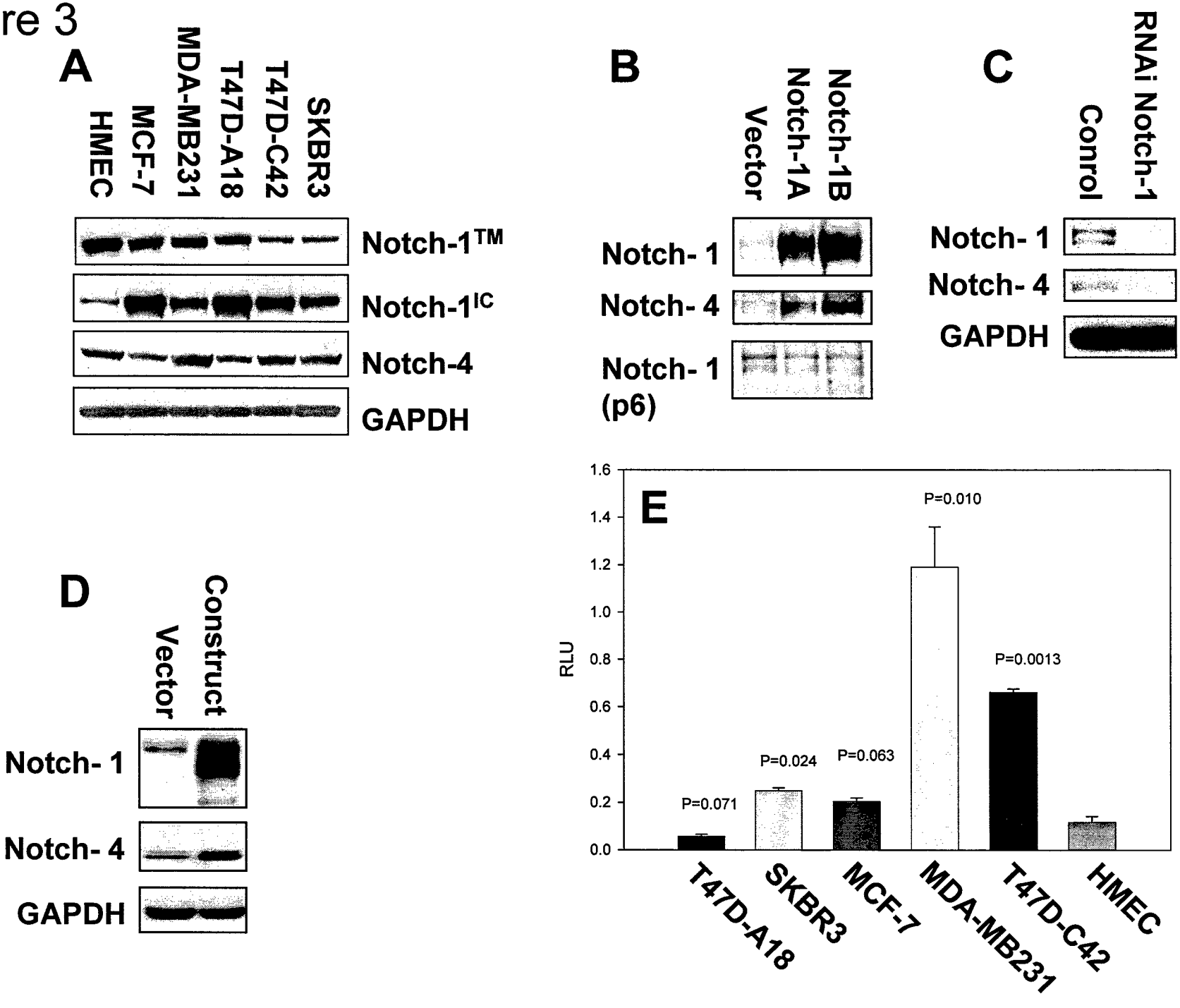
A
HMEC
MCF-7
MDA-MB231
T47D-A18
T47D-C42
SKBR3
Notch-1TM
Notch-1IC
Notch-4
GAPDH
B
Vector
Notch-1A
Notch-1B
Notch- 1
Notch- 4
Notch- 1 (p6)
C
Conrol
RNAi Notch-1
Notch- 1
Notch- 4
GAPDH
D
Vector
Construct
Notch- 1
Notch- 4
GAPDH
E
RLU
1.6
1.4
1.2
1.0
0.8
0.6
0.4
0.2
0.0
P=0.071
P=0.024
P=0.063
P=0.010
P=0.0013
T47D-A18
SKBR3
MCF-7
MDA-MB231
T47D-C42
HMEC

Figure 3

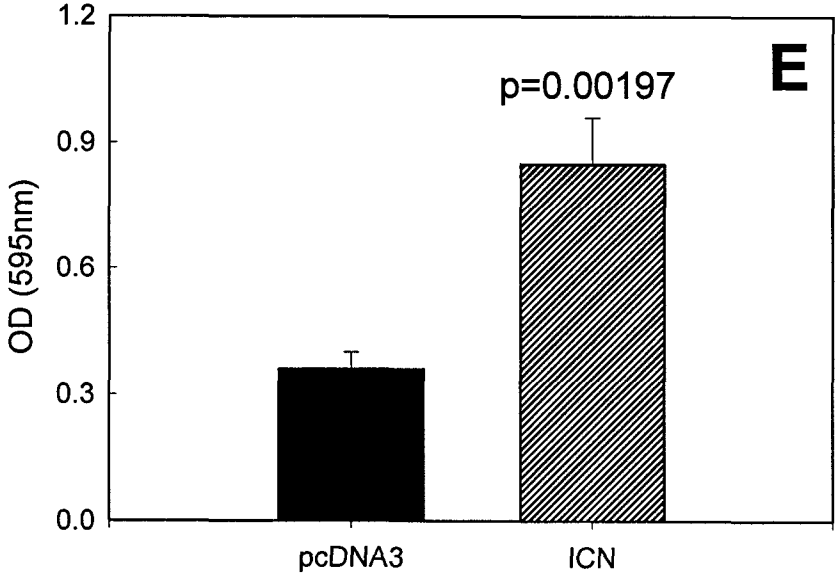
E
p=0.00197
OD (595nm)
1.2
0.9
0.6
0.3
0.0
pcDNA3
ICN

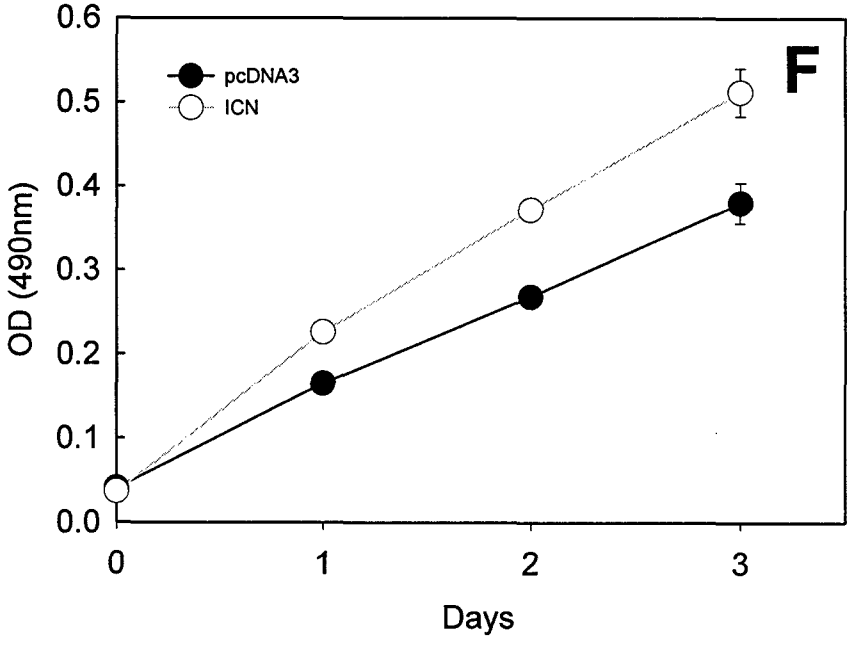
F
pcDNA3
ICN
OD (490nm)
0.6
0.5
0.4
0.3
0.2
0.1
0.0
0
1
2
3
Days

Figure 4

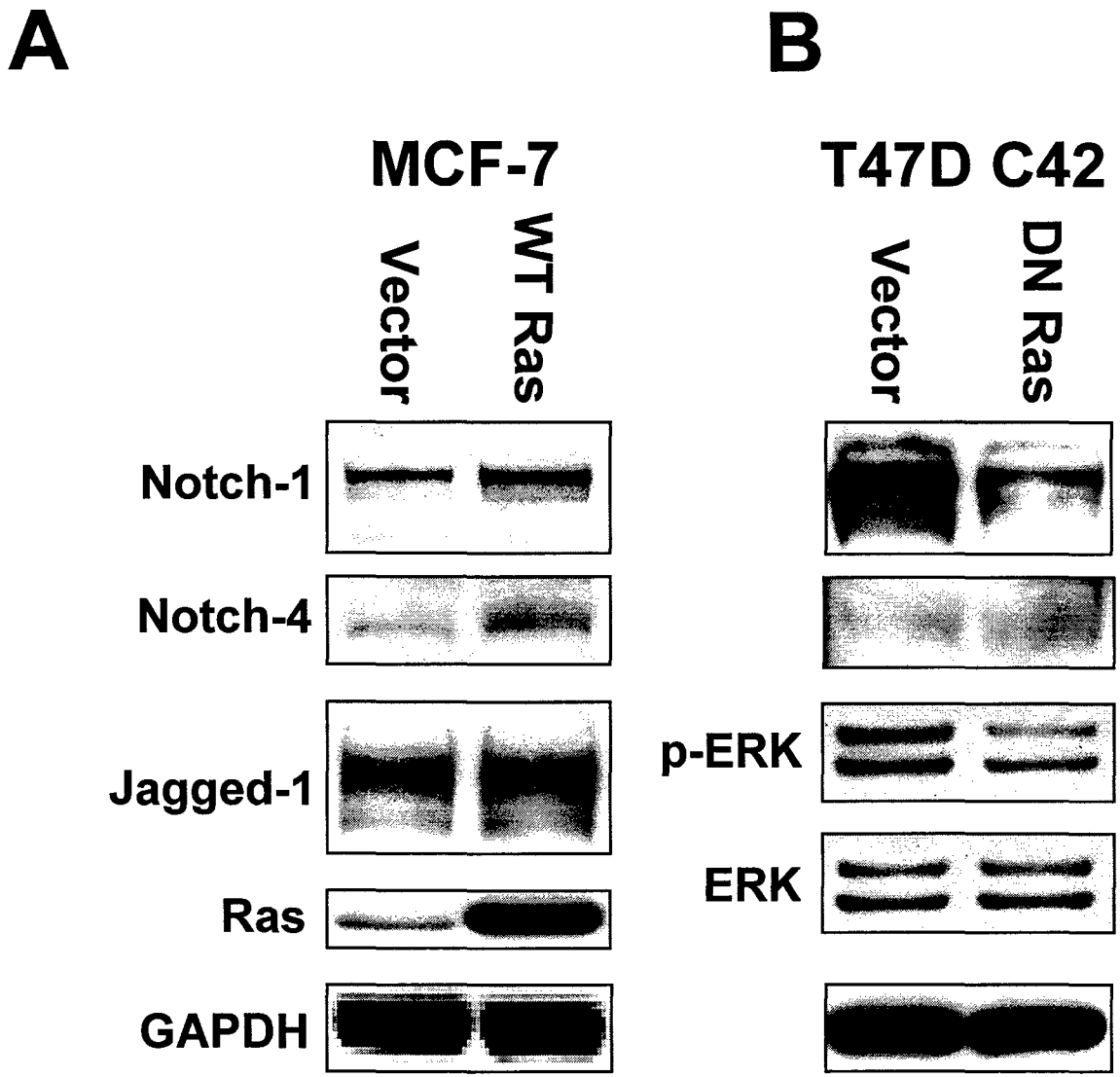
A
B
MCF-7
T47D C42
Vector
WT Ras
Vector
DN Ras
Notch-1
Notch-4
Jagged-1
Ras
GAPDH
p-ERK
ERK

Figure 4

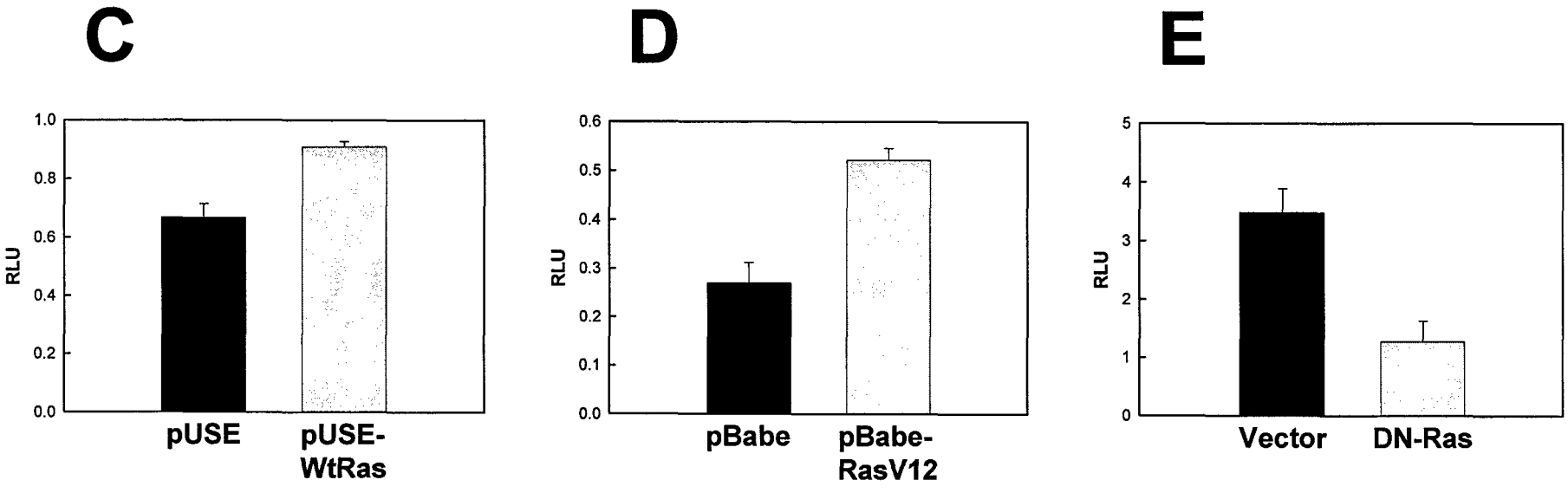
C
D
E
RLU
1.0
0.8
0.6
0.4
0.2
0.0
pUSE
pUSE-WtRas
0.6
0.5
0.4
0.3
0.2
0.1
0.0
pBabe
pBabe-RasV12
5
4
3
2
1
0
Vector
DN-Ras

Figure 4

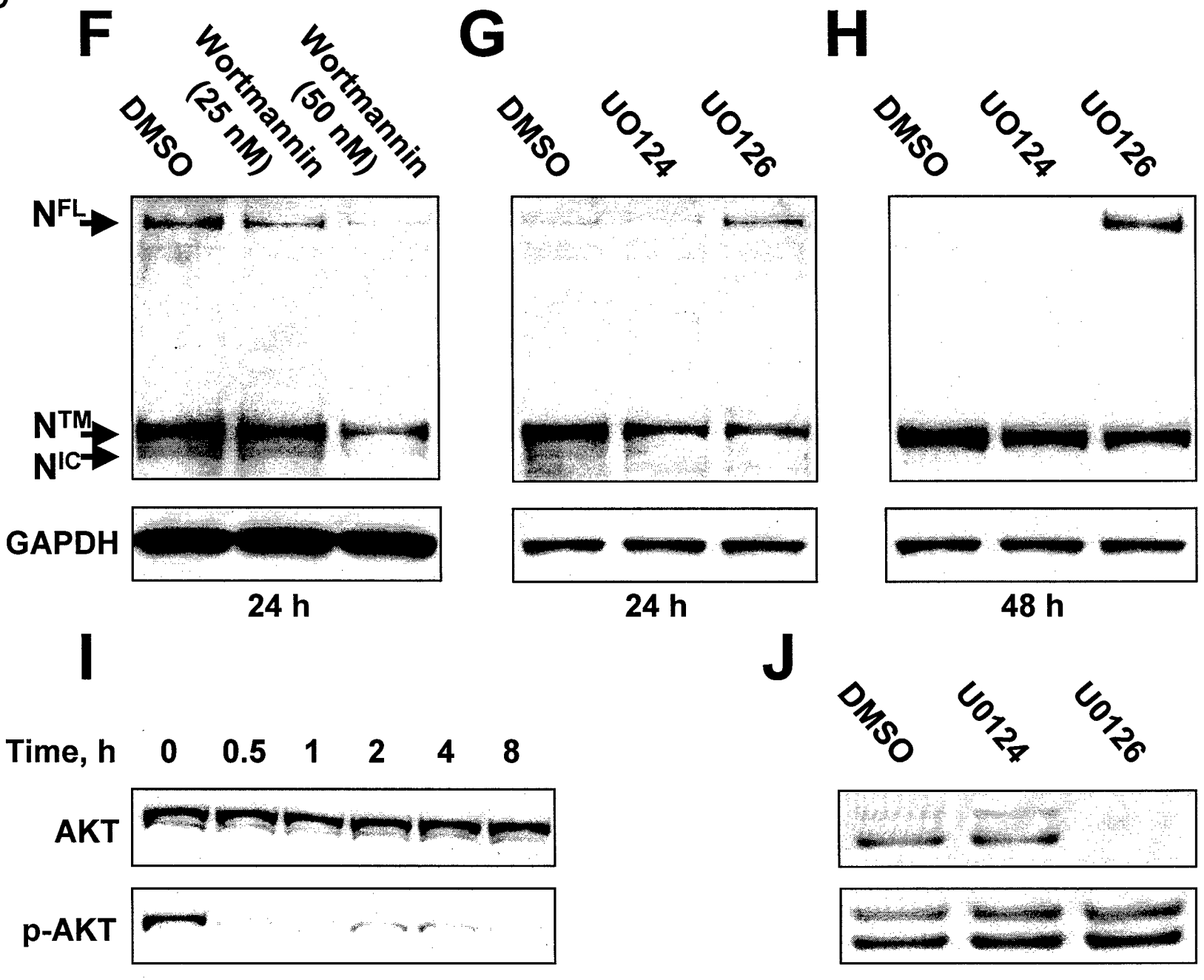
F
DMSO
Wortmannin (25 nM)
Wortmannin (50 nM)
N^FL
N^TM
N^IC
GAPDH
24 h
G
DMSO
UO124
UO126
24 h
H
DMSO
UO124
UO126
48 h
I
Time, h 0 0.5 1 2 4 8
AKT
p-AKT
J
DMSO
UO124
UO126

Figure 4

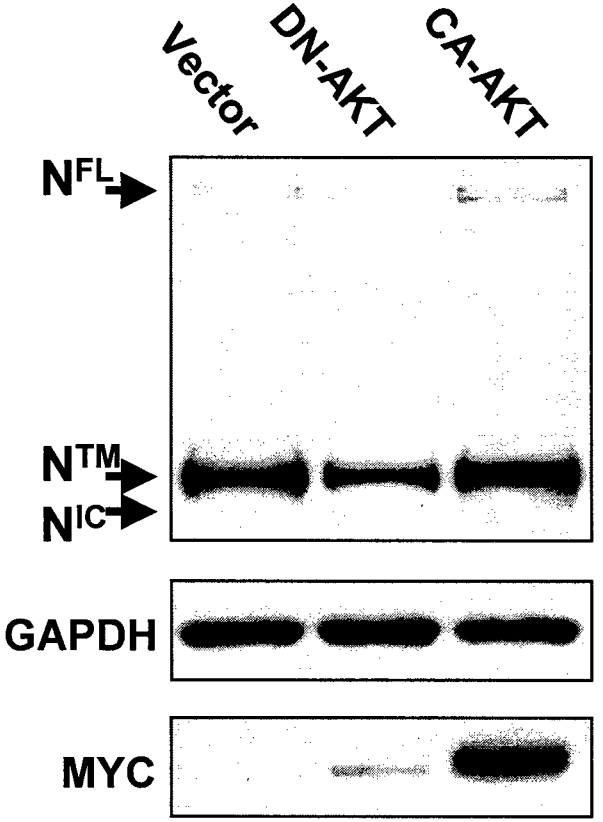
I
Vector
DN-AKT
CA-AKT
N^FL
N^TM
N^IC
GAPDH
MYC

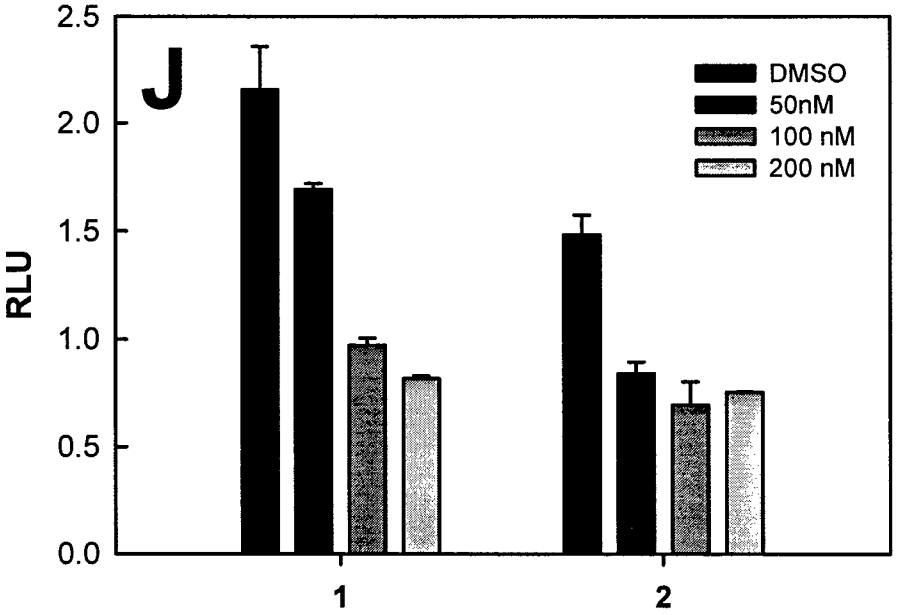
J
DMSO
50nM
100 nM
200 nM
RLU
2.5
2.0
1.5
1.0
0.5
0.0
1
2

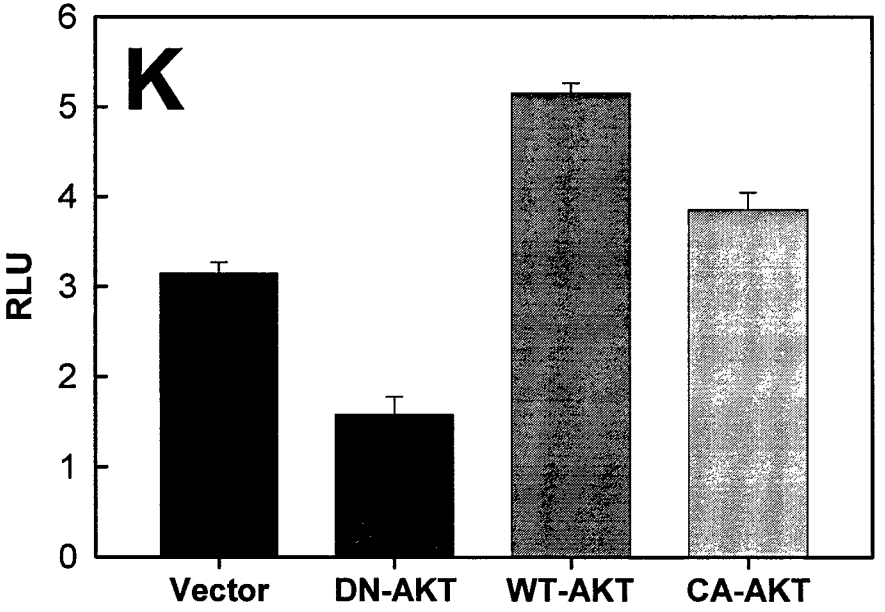
K
RLU
6
5
4
3
2
1
0
Vector
DN-AKT
WT-AKT
CA-AKT

Figure 5

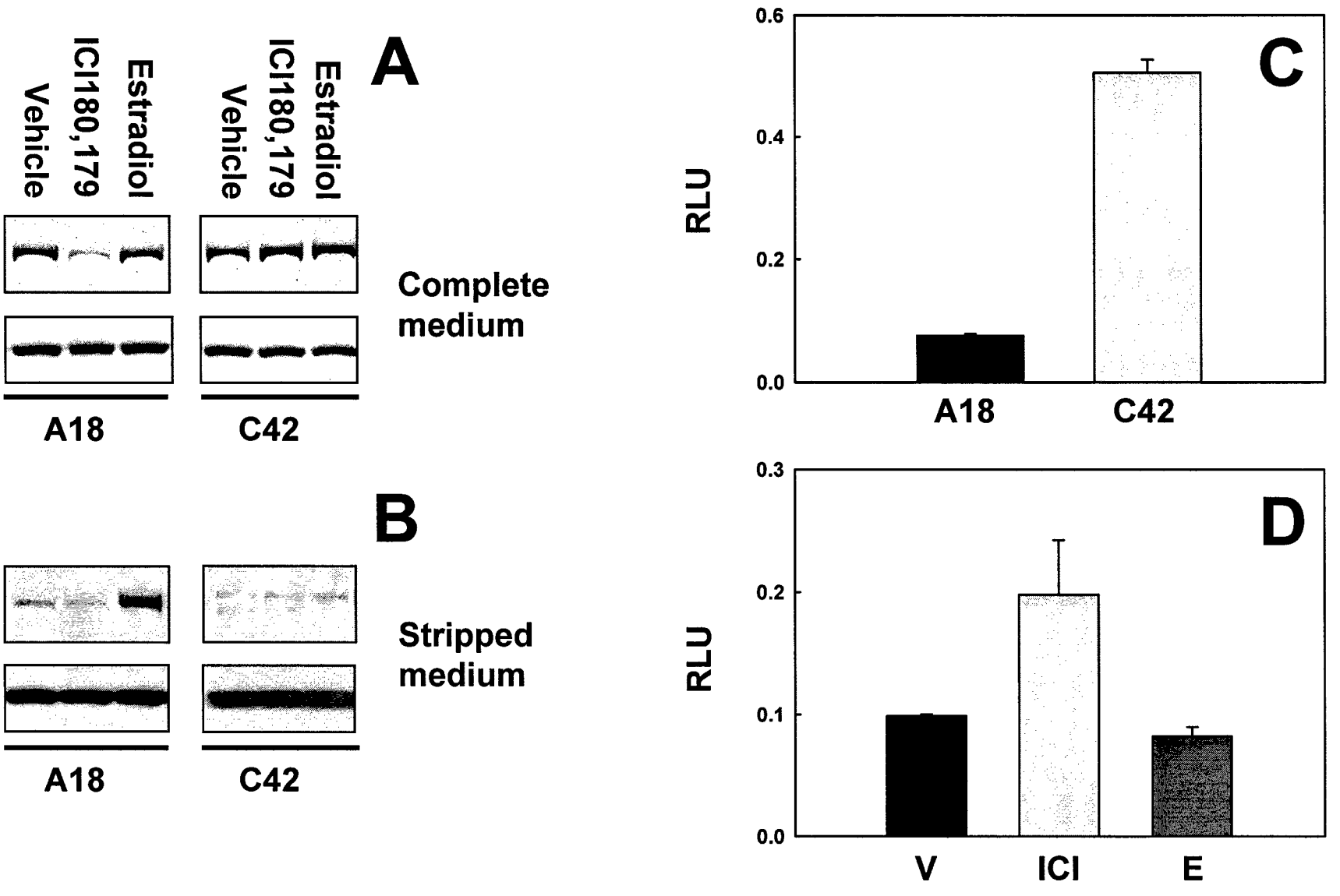
A
Vehicle
ICI180,179
Estradiol
Vehicle
ICI180,179
Estradiol
Complete medium
A18
C42
B
Stripped medium
A18
C42
C
RLU
0.6
0.4
0.2
0.0
A18
C42
D
RLU
0.3
0.2
0.1
0.0
V
ICI
E

Figure 5

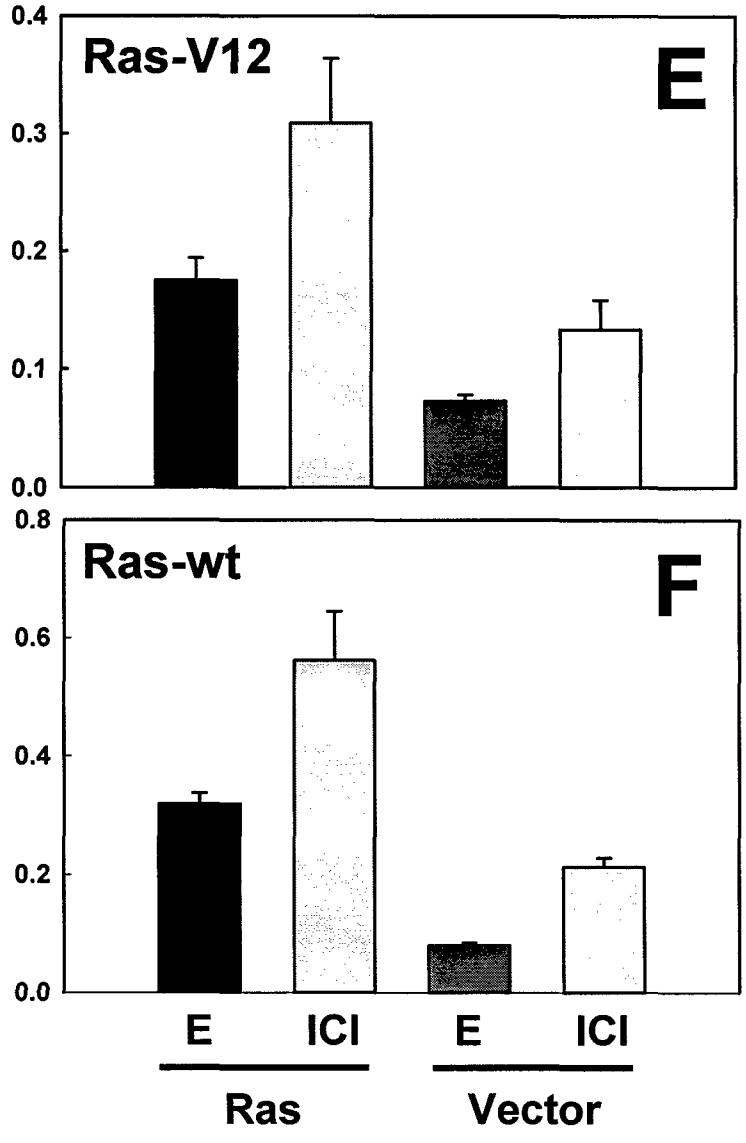
Ras-V12
E
0.4
0.3
0.2
0.1
0.0
Ras-wt
F
0.8
0.6
0.4
0.2
0.0
E
ICI
E
ICI
Ras
Vector

Figure 6

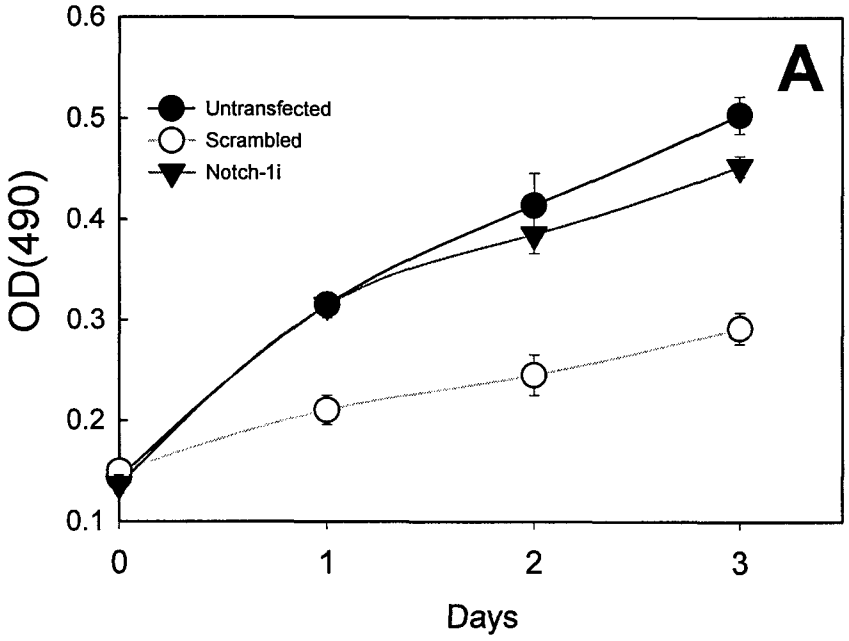
A
Untransfected
Scrambled
Notch-1i
OD(490)
Days
0.6
0.5
0.4
0.3
0.2
0.1
0
1
2
3

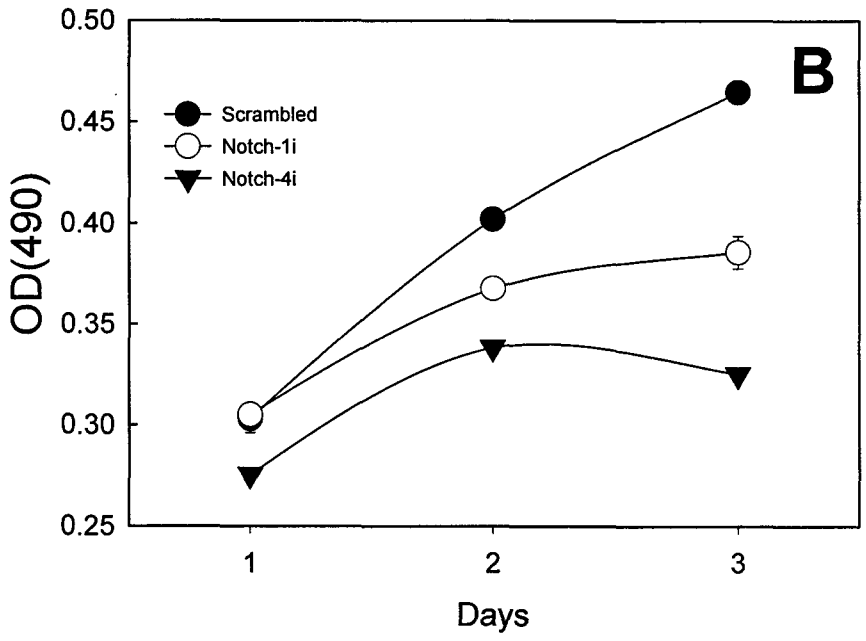
B
Scrambled
Notch-1i
Notch-4i
OD(490)
Days
0.50
0.45
0.40
0.35
0.30
0.25
1
2
3

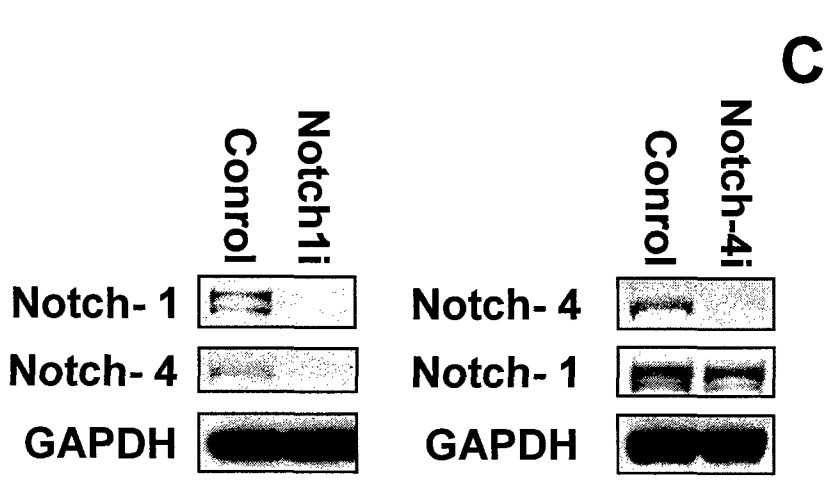
C
Conrol
Notch1i
Notch- 1
Notch- 4
GAPDH
Conrol
Notch-4i
Notch- 4
Notch- 1
GAPDH

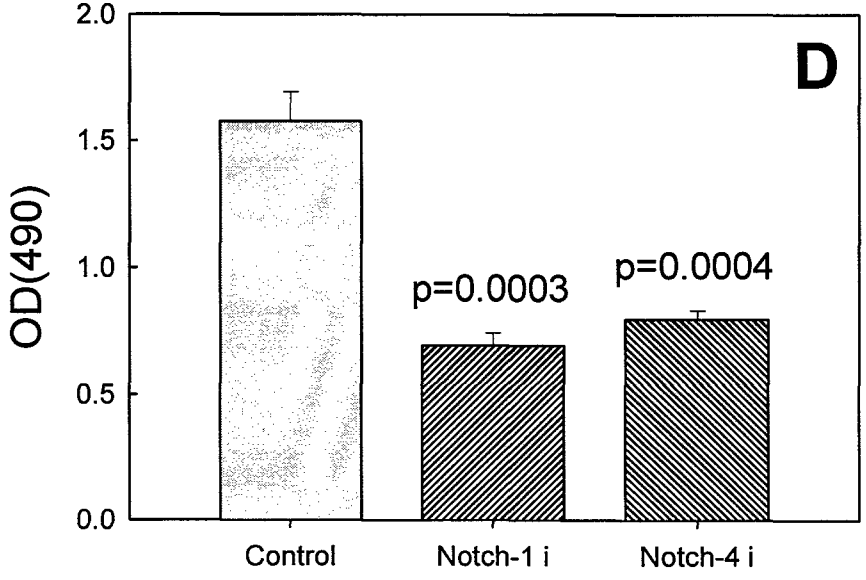
D
OD(490)
2.0
1.5
1.0
0.5
0.0
p=0.0003
p=0.0004
Control
Notch-1 i
Notch-4 i

Figure 7

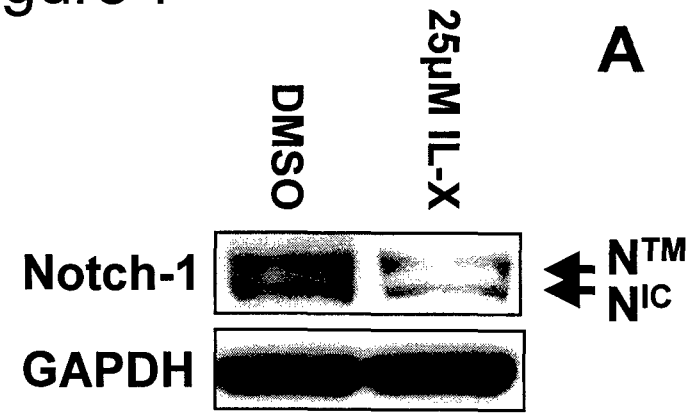
A
DMSO
25μM IL-X
Notch-1
GAPDH
N^TM
N^IC

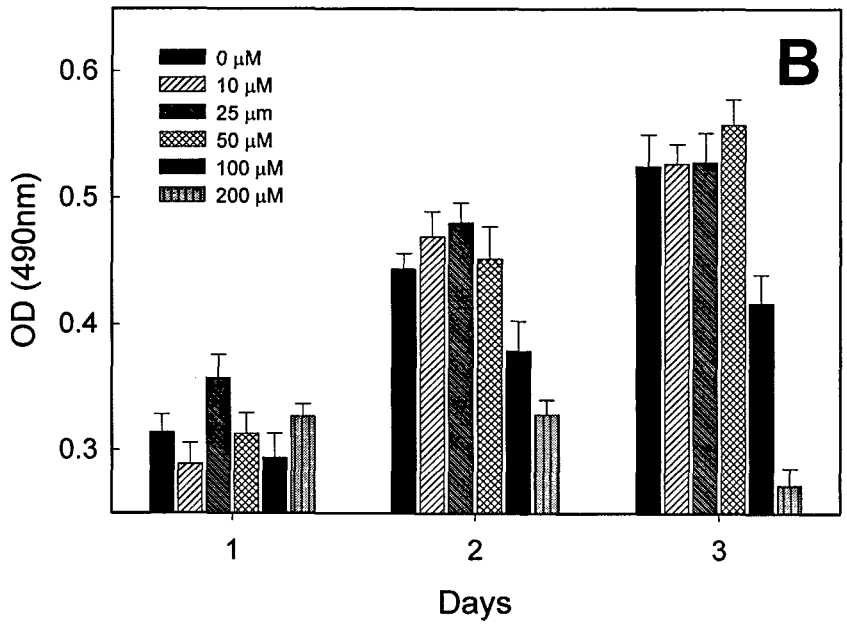
B
0 μM
10 μM
25 μm
50 μM
100 μM
200 μM
OD (490nm)
0.6
0.5
0.4
0.3
1
2
3
Days

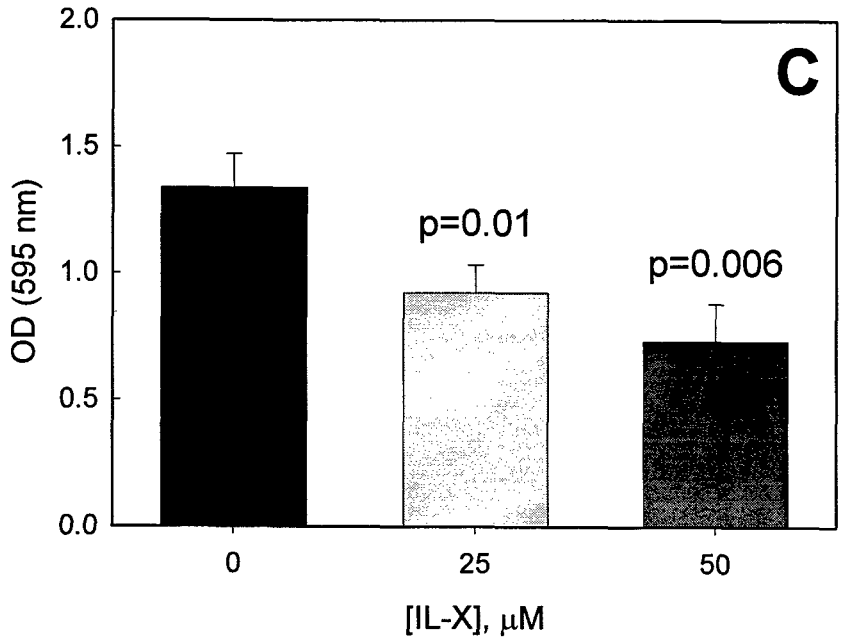
C
OD (595 nm)
2.0
1.5
1.0
0.5
0.0
p=0.01
p=0.006
0
25
50
[IL-X], μM

Figure 7

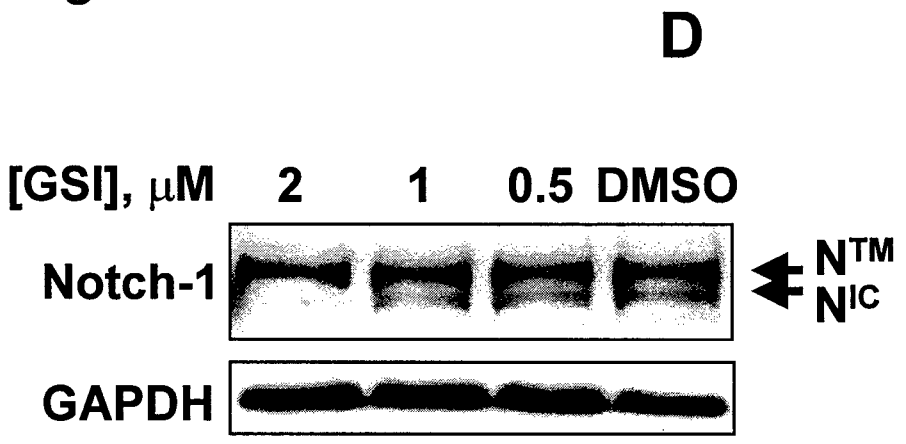
D
[GSI], μM 2 1 0.5 DMSO
Notch-1
GAPDH
NTM
NIC

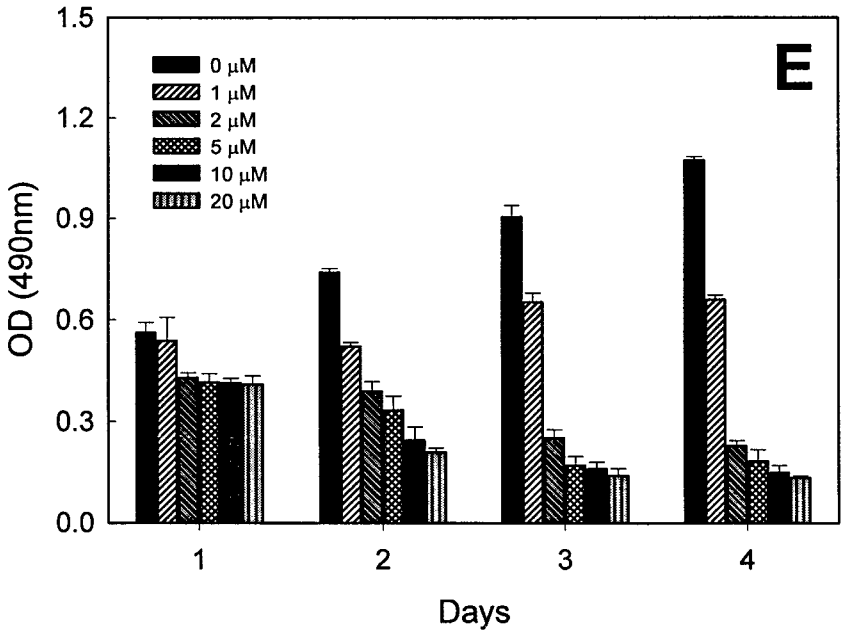
E
0 μM
1 μM
2 μM
5 μM
10 μM
20 μM
OD (490nm)
1.5
1.2
0.9
0.6
0.3
0.0
1
2
3
4
Days

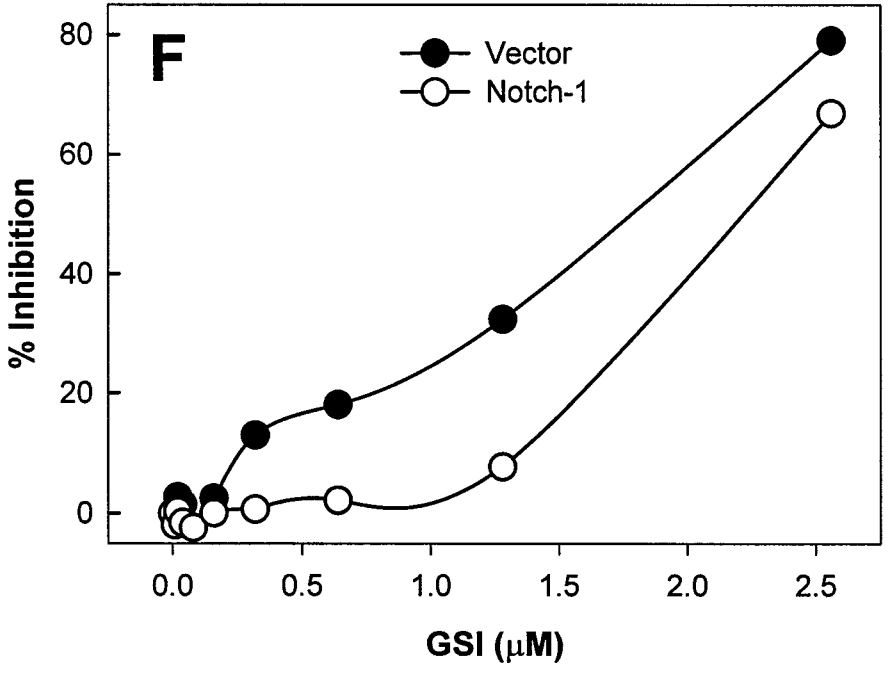
F
Vector
Notch-1
% Inhibition
80
60
40
20
0
0.0
0.5
1.0
1.5
2.0
2.5
GSI (μM)

G

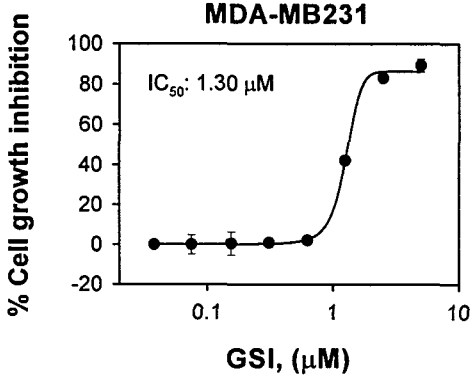
MDA-MB231
% Cell growth inhibition
100
80
60
40
20
0
-20
IC50: 1.30 μM
0.1
1
10
GSI, (μM)

H

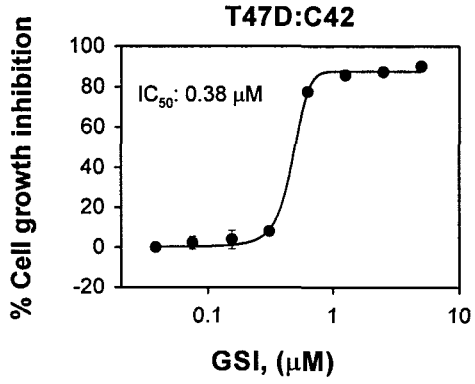
T47D:C42
% Cell growth inhibition
100
80
60
40
20
0
-20
IC50: 0.38 μM
0.1
1
10
GSI, (μM)

I

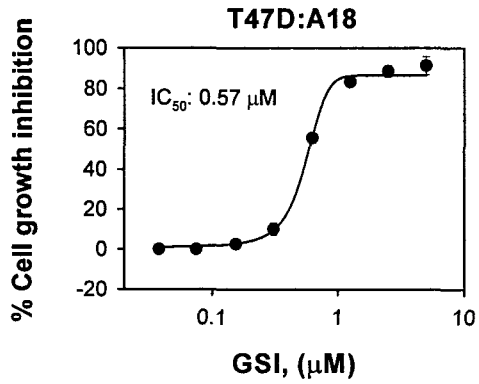
T47D:A18
% Cell growth inhibition
100
80
60
40
20
0
-20
IC50: 0.57 μM
0.1
1
10
GSI, (μM)

Figure 8

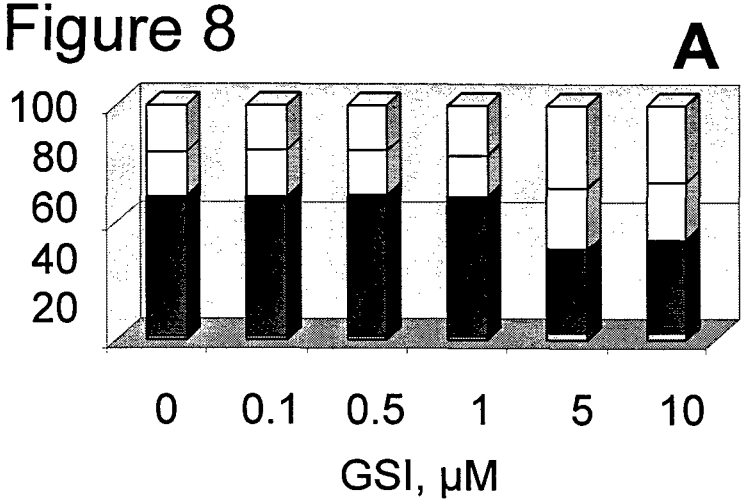
A
100
80
60
40
20
0
0.1
0.5
1
5
10
GSI, μM

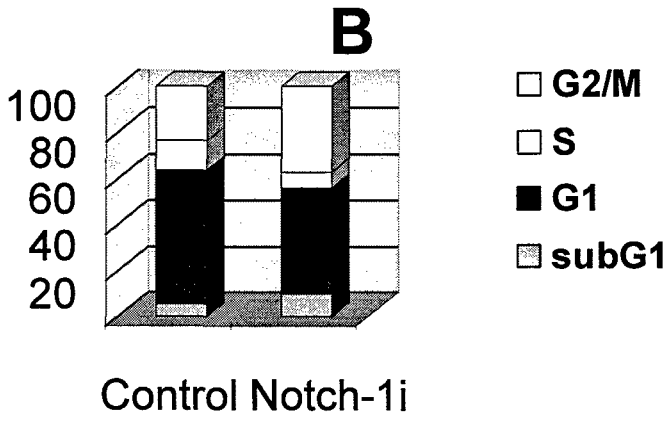
B
100
80
60
40
20
Control
Notch-1i
G2/M
S
G1
subG1

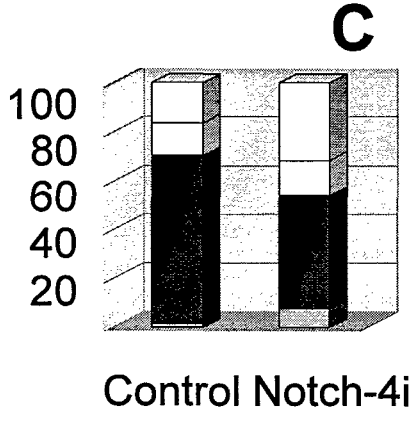
C
100
80
60
40
20
Control
Notch-4i

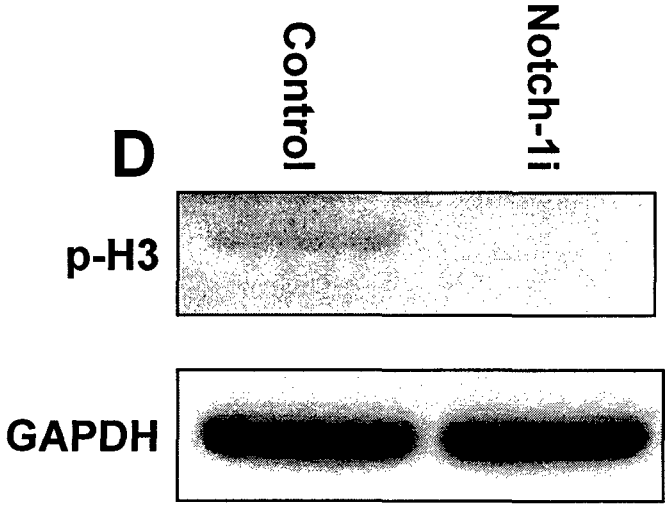
D
Control
Notch-1i
p-H3
GAPDH

Figure 8

D

Control	Notch-1 i	Notch-4 i	
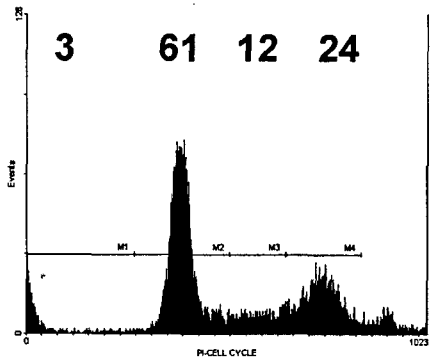	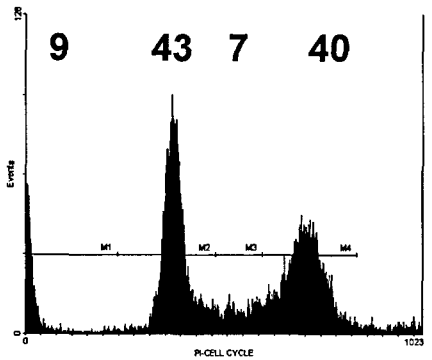	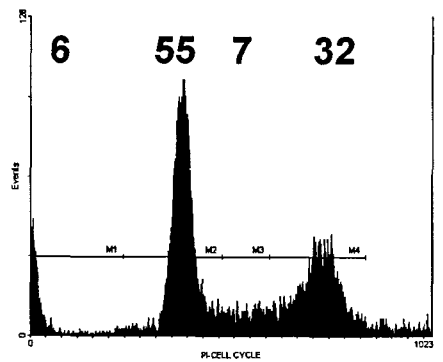	24 h
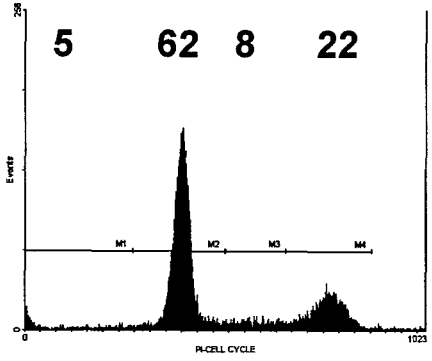	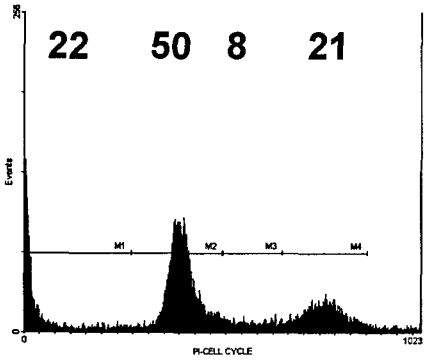	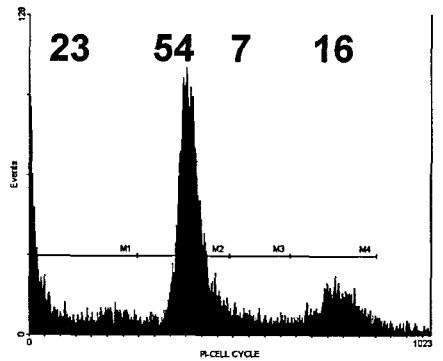	48 h

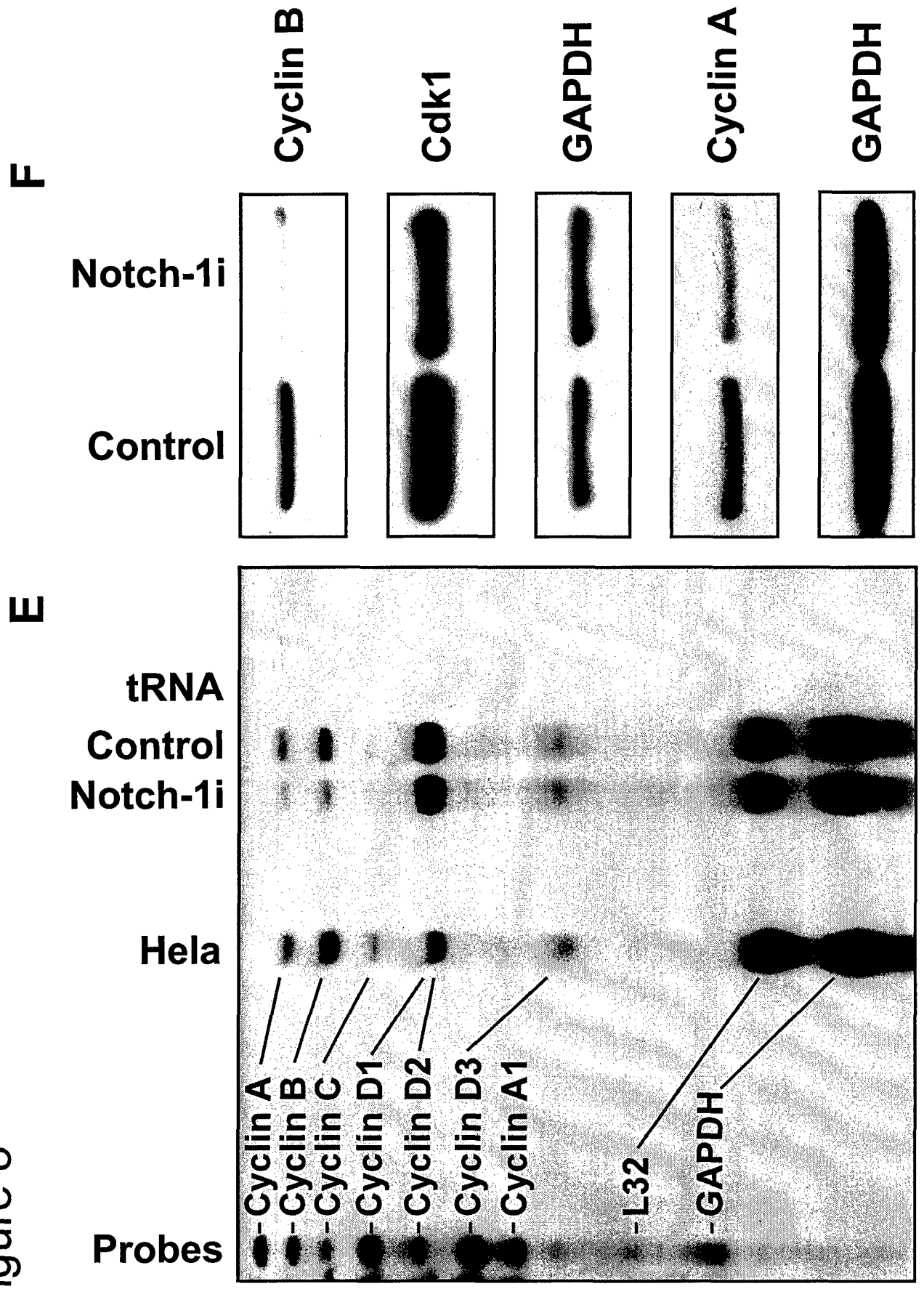
F
Cyclin B
Cdk1
GAPDH
Cyclin A
GAPDH
Notch-1i
Control
E
tRNA
Control
Notch-1i
Hela
Cyclin A
Cyclin B
Cyclin C
Cyclin D1
Cyclin D2
Cyclin D3
Cyclin A1
L32
GAPDH
Probes

Figure 8

Figure 8

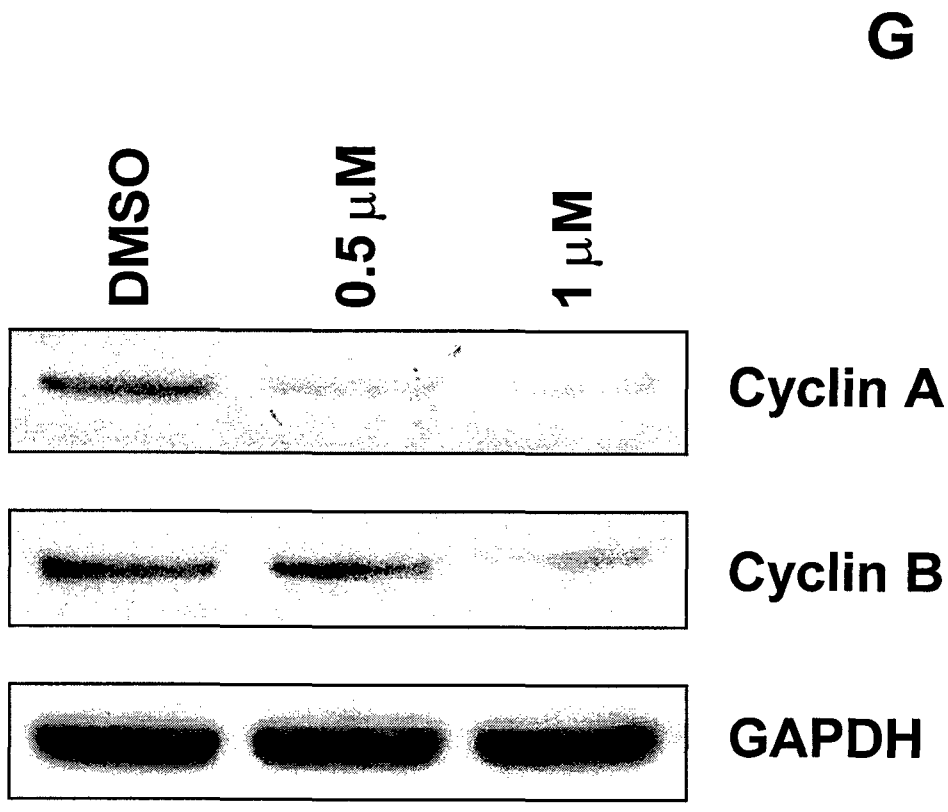

Figure 8

H

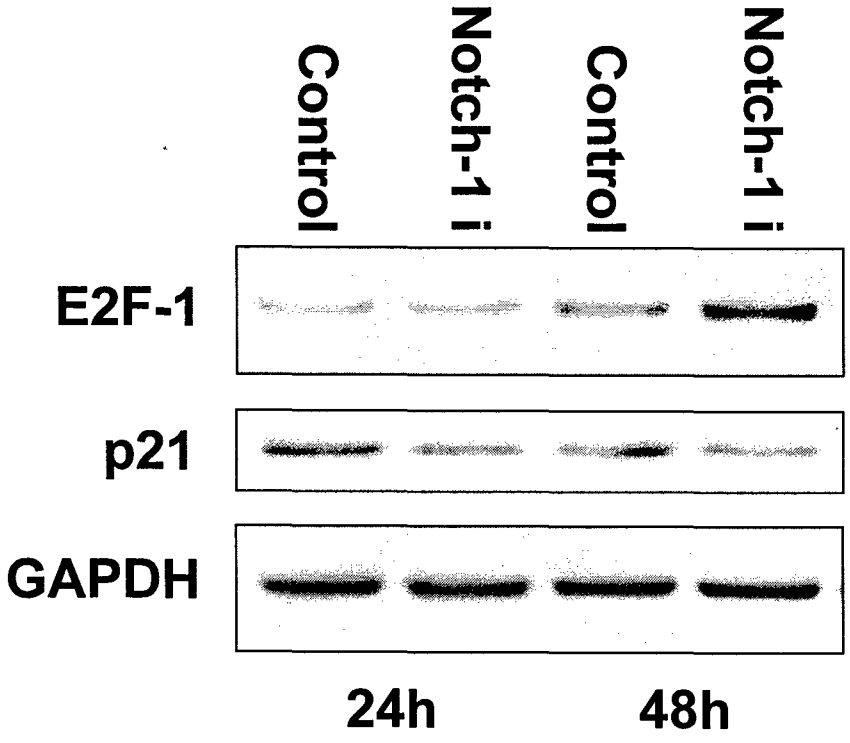

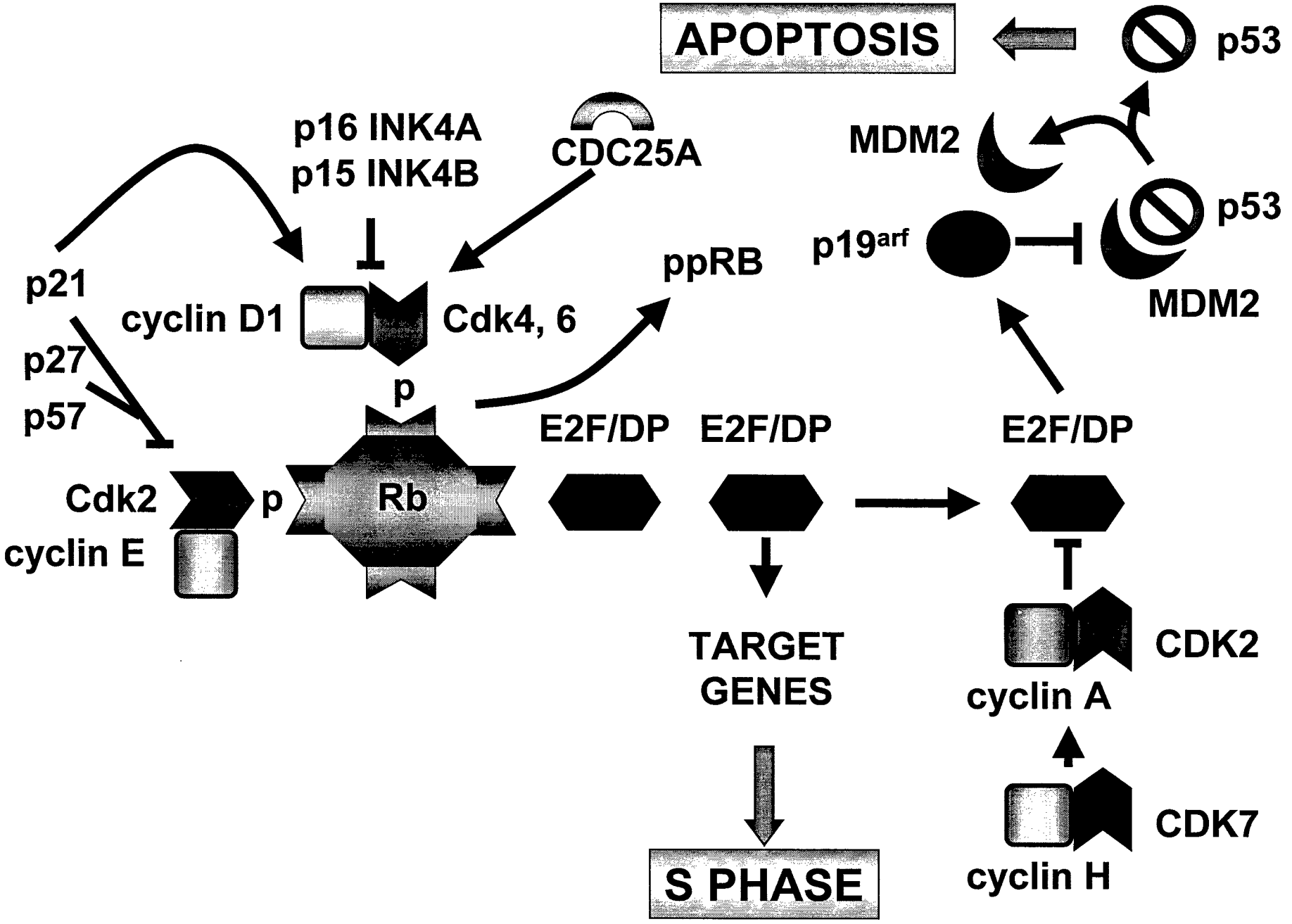
APOPTOSIS
p53
p16 INK4A
p15 INK4B
CDC25A
MDM2
p53
p19arf
MDM2
p21
ppRB
cyclin D1
Cdk4, 6
p27
p57
p
E2F/DP
E2F/DP
E2F/DP
Cdk2
p
Rb
cyclin E
TARGET
GENES
CDK2
cyclin A
CDK7
cyclin H
S PHASE

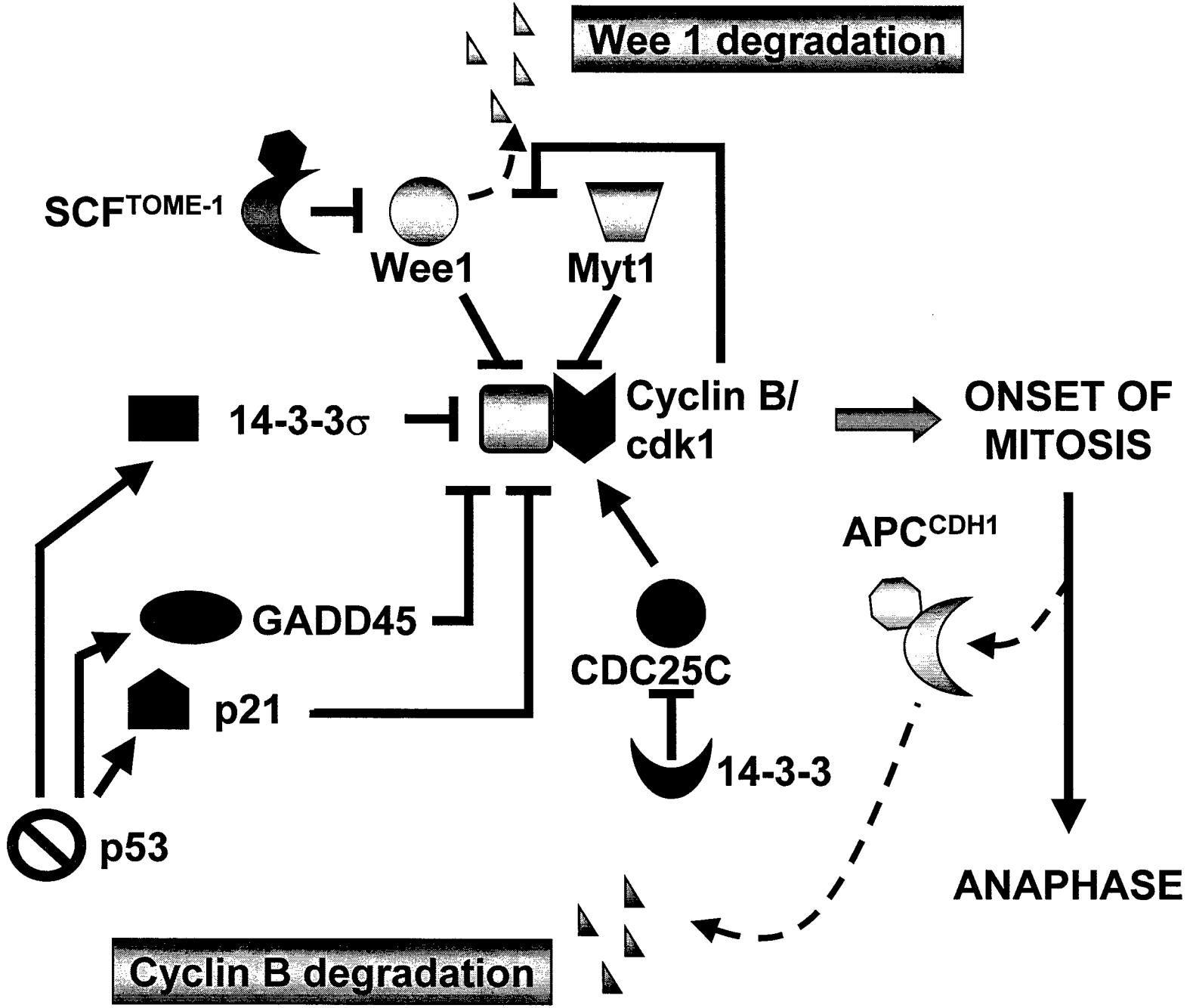
Wee 1 degradation
SCF TOME-1
Wee1
Myt1
14-3-3σ
Cyclin B/
cdk1
ONSET OF
MITOSIS
APC CDH1
GADD45
p21
CDC25C
14-3-3
p53
ANAPHASE
Cyclin B degradation

Figure 8

H

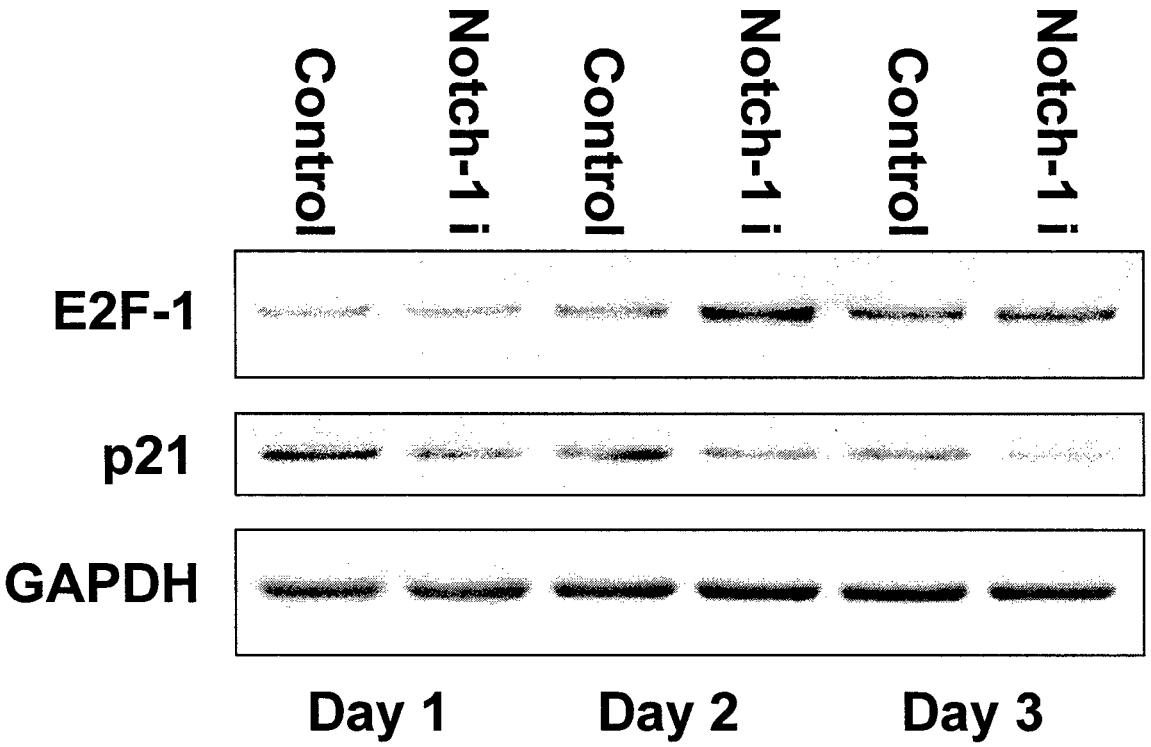
Control
Notch-1 i
Control
Notch-1 i
Control
Notch-1 i
E2F-1
p21
GAPDH
Day 1
Day 2
Day 3

nature immunology

APPENDIX 3

Inhibitors of γ-secretase block *in vivo* and *in vitro* T helper type 1 polarization by preventing Notch upregulation of *Tbx21*

Lisa M Minter[1,6], Danielle M Turley[2,6], Pritam Das[3], Hyun Mu Shin[1], Ila Joshi[1], Rebecca G Lawlor[1], Ok Hyun Cho[1], Tanapat Palaga[4], Sridevi Gottipati[1], Janice C Telfer[1], Lisa Kostura[3], Abdul H Fauq[3], Katherine Simpson[3], Kimberly A Such[1], Lucio Miele[5], Todd E Golde[3], Stephen D Miller[2] & Barbara A Osborne[1]

Notch receptors are processed by γ-secretase acting in synergy with T cell receptor signaling to sustain peripheral T cell activation. Activated CD4+ T cells differentiate into T helper type 1 (T_H1) or T_H2 subsets. Molecular cues directing T_H1 differentiation include expression of the T_H1-specific transcription factor T-bet, encoded by *Tbx21*. However, the regulation of *Tbx21* remains incompletely defined. Here we report that Notch1 can directly regulate *Tbx21* through complexes formed on the *Tbx21* promoter. *In vitro*, γ-secretase inhibitors extinguished expression of Notch, interferon-γ and *Tbx21* in T_H1-polarized CD4+ cells, whereas ectopic expression of activated Notch1 restored *Tbx21* transcription. *In vivo*, administration of γ-secretase inhibitors substantially impeded T_H1-mediated disease progression in the mouse experimental autoimmune encephalomyelitis model of multiple sclerosis. Thus, using γ-secretase inhibitors to modulate Notch signaling may prove beneficial in treating T_H1-mediated autoimmunity.

Notch proteins are transcriptional activators expressed first as transmembrane heterodimeric surface receptors. Four mammalian Notch proteins, Notch1–Notch4, and five Notch ligands, Jagged 1 and 2 and Delta-like 1, 3 and 4, have been identified[1]. After ligand binding, Notch undergoes proteolytic processing, including a final cleavage by γ-secretase to release its intracellular signaling peptide, which translocates to the nucleus and activates transcription of target genes[2,3]. Pharmacological γ-secretase inhibitors (GSIs) effectively prevent activation of all Notch receptors by inhibiting this final enzymatic cleavage[4]. Although the function of Notch in hematopoiesis and thymocyte development has been well documented[5], Notch also acts in synergy with T cell receptor signaling to sustain T cell activation and interferon-γ (IFN-γ) production[6,7], providing evidence Notch is also important in regulating peripheral T cell responses.

Activated CD4+ T cells can further differentiate into T helper type 1 (T_H1) or T_H2 cells[8]. Studies have suggested Notch may influence both T_H1 and T_H2 polarization[9,10]. During terminal maturation, T_H1 and T_H2 subsets acquire the ability to express and respond to a 'signature' cytokine profile. IFN-γ, tumor necrosis factor and interleukin 12 (IL-12) are cytokines associated with T_H1 responses, whereas T_H2 responses are characterized mainly by IL-4, IL-5 and IL-13. Although its regulation remains poorly defined, expression of the canonical T_H1 transcription factor T-bet, encoded by *Tbx21*, is both necessary and sufficient to drive CD4+ T_H1 differentiation and secretion of the primary T_H1 effector cytokine IFN-γ[11,12]. IFN-γ in turn positively regulates *Tbx21* expression 'downstream' of the IFN-γ receptor through a pathway mediated by the transcription factor STAT1 (ref. 13). Whether IFN-γ acts to initiate or to sustain *Tbx21* expression has not been fully resolved. Reports have argued for the existence of an IFN-γ receptor–STAT1–independent means of inducing *Tbx21* (refs. 9,14,15), and abrogation of T-bet signaling but not of STAT1 provides protection from experimental autoimmune encephalomyelitis (EAE)[16,17], a T_H1-mediated model of multiple sclerosis[18]. Those observations led us to ask whether Notch facilitates T_H1 differentiation by directly regulating *Tbx21* and whether blocking of Notch signaling using GSIs can effectively abrogate T_H1 polarization and alter the disease progression of EAE.

RESULTS

Blocking Notch activation prevents T_H1 polarization

In vivo, T helper cell differentiation is orchestrated by multiple cell types in a complex cytokine milieu; however, we used an *in vitro* T helper cell polarization assay to focus on CD4+ T cell–intrinsic effects of GSIs[19] (**Fig. 1**). We first examined the polarization of CD4+

[1]Department of Veterinary and Animal Sciences, University of Massachusetts Amherst, Amherst, Massachusetts 01003, USA. [2]Department of Microbiology-Immunology and Interdepartmental Immunobiology Center, Feinberg School of Medicine, Northwestern University, Chicago, Illinois 60611, USA. [3]Department of Neuroscience, Mayo Clinic, Mayo Clinic College of Medicine, Jacksonville, Florida 32224, USA. [4]Department of Microbiology, Faculty of Science, Chulalongkorn University, Bangkok 10330, Thailand. [5]Department of Biopharmaceutical Sciences, University of Illinois at Chicago, Chicago, Illinois 60612, USA. [6]These authors contributed equally to this work. Correspondence should be addressed to B.A.O. (osborne@vasci.umass.edu).

Published online 29 May 2005; doi:10.1038/ni1209

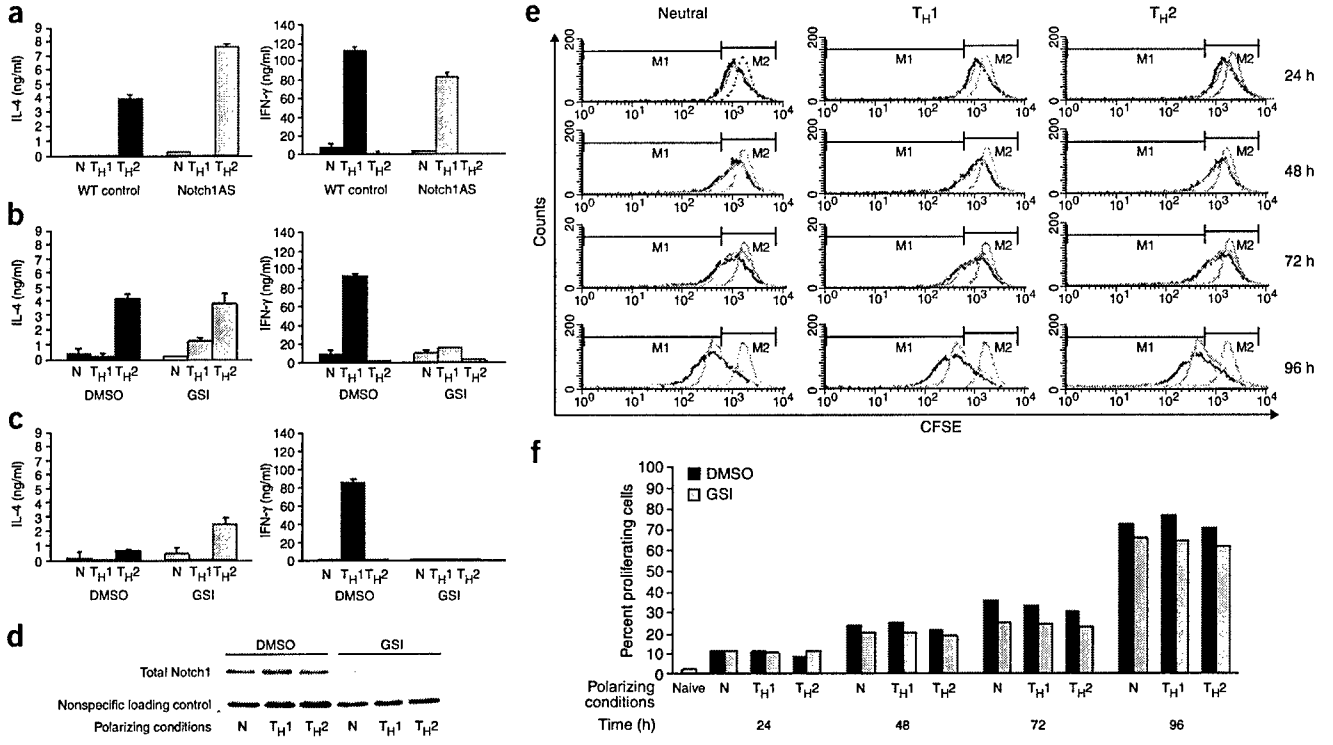

Figure 1 Blocking Notch signaling decreases the capacity of CD4+ T cells to adopt a T_H1 cell fate without affecting proliferation. (**a–c**) *In vitro* polarization assays with CD4+ T cells from Notch1AS mice (**a**), C57BL/6 mice pretreated for 3 d with orally administered GSI (**b**) or C57BL/6 mice pretreated *ex vivo* with GSI (**c**). IL-4 and IFN-γ were measured by ELISA. Results are the mean of triplicate wells + s.d. Results are representative of two (**a,b**) or four (**c**) independent polarization assays. N, neutral. (**d**) Immunoblot analysis of Notch1 expression in whole-cell lysates of CD4+ T cells from C57BL/6 mice treated as described in **b**. Results are representative of two independent treatments. (**e,f**) Flow cytometry of polarized CD4+ cells. Naive CD4+ T cells from C57BL/6 mice were labeled with CFSE, pretreated with GSI or DMSO and cultured for 96 h in polarizing conditions. (**e**) Flow cytometry. M1, proliferating populations; M2, nonproliferating cell populations. Light gray dotted lines, naive T cells; dark gray solid lines, GSI-treated cells; black solid lines, DMSO-treated cells. (**f**) Percentage of DMSO- or GSI-pretreated cells proliferating over a 96-hour period. Results (**e,f**) are representative of two independent replicates.

cells isolated from mice with transgenic expression of a Notch1 antisense construct (Notch1AS mice)[20]. Notch1AS mice express 30–40% less Notch1 protein than do wild-type mice[20]. We cultured Notch1AS CD4+ cells for 3 weeks in neutral or T_H1- or T_H2-inducing conditions and, after restimulating the cells, analyzed the supernatants by enzyme-linked immunosorbant assay (ELISA) for secreted IFN-γ and IL-4. Notch1AS CD4+ cells produced less IFN-γ than did wild-type controls when cultured in T_H1-polarizing conditions, but retained their ability to adopt a T_H2 phenotype (**Fig. 1a**). These data agree with earlier work showing no overt defects in T_H2 profiles for CD4+ cells from transgenic mice with conditional deletion of *Notch1* in CD4+ cells[21]. Those mice with conditional deletion of *Notch1* in CD4+ cells also mount effective T_H1 responses *in vivo* to clear infection with *Leishmania major*[21], consistent with our data from Notch1AS mice demonstrating decreased but not abrogated IFN-γ (**Fig. 1a**). These data suggest that functional redundancy of other Notch family members may compensate for diminished Notch1 signaling in T_H1 conditions.

Next we treated C57BL/6 mice for 3 d *in vivo* with orally administered GSI, or with dimethyl sulfoxide (DMSO) as control, before isolating CD4+ cells. After culturing the cells for 24 h in polarizing conditions, we assayed total Notch1 protein as an indicator of GSI efficacy. We detected total Notch1 protein in whole-cell lysates of CD4+ cells from DMSO-treated mice regardless of polarization, with slightly more expression in T_H1-polarized cultures. By comparison, total Notch1 protein was nearly undetectable in CD4+ cells from GSI-treated mice (**Fig. 1d**). We did parallel *in vitro* polarization assays of CD4+ cells and analyzed supernatants for IFN-γ and IL-4. Compared with controls, CD4+ cells from GSI-treated mice produced much less IFN-γ in T_H1-inducing conditions but retained their ability to secrete IL-4 (**Fig. 1b**), in agreement with our results using Notch1AS CD4+ cells. Finally, we pretreated CD4+ cells from C57BL/6 mice *in vitro* with GSI before T helper cell polarization. Consistent with results using Notch1AS mice and mice treated with GSI *in vivo*, *in vitro* treatment of CD4+ cells abrogated IFN-γ but not IL-4 production (**Fig. 1c**). Collectively these data show that blockade of Notch signaling using GSI either *in vivo* or *in vitro* prevents T_H1 differentiation and IFN-γ secretion. However, in the absence of Notch signaling, T_H2 polarization seems able to proceed through Notch-independent mechanisms.

Lineage commitment in developing T helper cells requires multiple cell divisions for the implementation of genetic programming that confers a T_H1 or T_H2 cell fate[22,23]. With increasing numbers of cell divisions, the ability to successfully 'reprogram' a T_H1 cell toward a T_H2 fate, and vice versa, diminishes[24,25]. GSI remained biologically active for approximately 24 h (data not shown), after which Notch-inhibitory properties were lost. This short-lived activity suggested to us that using GSI to block early activation of Notch in CD4+ cells during *in vitro* polarization produced profound and long-lasting effects on their ability to adopt a T_H1 but not a T_H2 fate. Therefore,

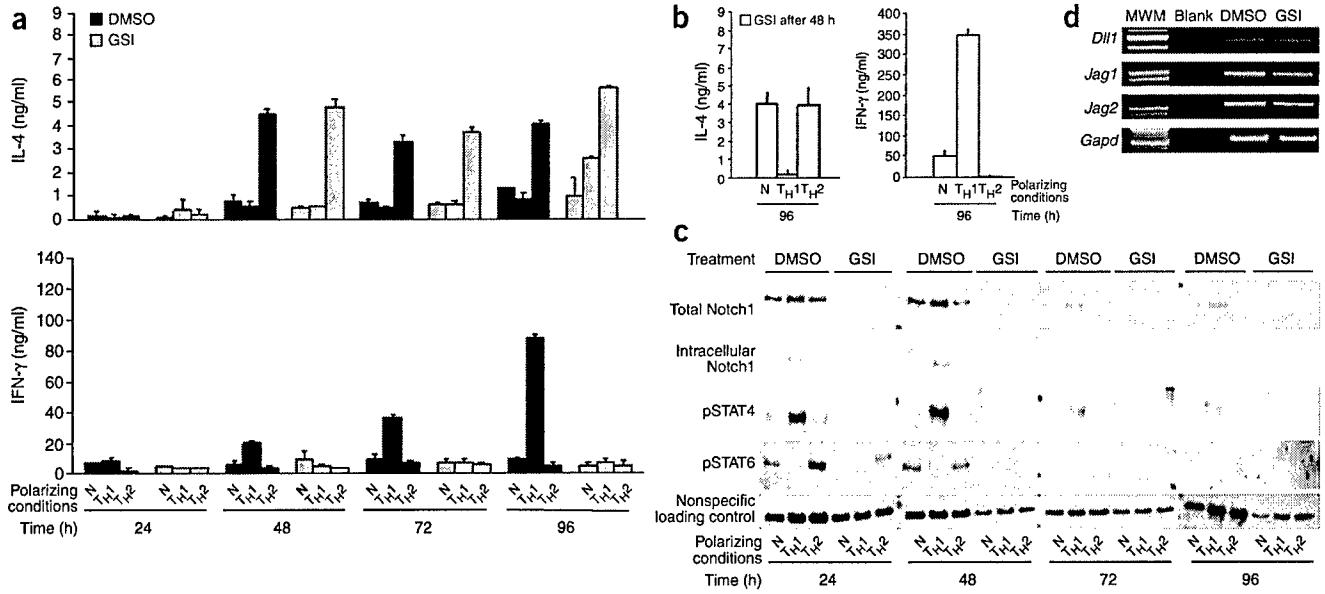

Figure 2 Preventing Notch activation early during polarization abrogates IFN-γ production and expression of Notch1 and phospho-STAT4. **(a,b)** ELISA of IL-4 and IFN-γ in supernatants of naive CD4$^+$ T cells from C57BL/6 mice. Cells were pretreated *in vitro* with GSI or with DMSO (as a control) before **(a)** or were treated with GSI or DMSO after **(b** and data not shown, respectively) 48 h of culture in neutral (N) or T_H1- or T_H2-polarizing conditions. Results are the mean of triplicate wells ± s.d. and are representative of four independent polarizations. **(c)** Immunoblot of whole-cell lysates generated from pretreated cultures described in **a**, analyzing expression of (from top to bottom) total Notch1, intracellular Notch1, phospho-STAT4 (pSTAT4) and phospho-STAT6 (pSTAT6). Nonspecific band (bottom blots), loading control. Results are representative of two independent replicates for each time point. **(d)** Expression of Delta-like1 (*Dll1*), Jagged1 (*Jag1*) and Jagged 2 (*Jag2*), assessed by RT-PCR of total RNA isolated from CD4$^+$ T cells pretreated *in vitro* with GSI or DMSO and cultured in neutral conditions for 24 h. *Gapd* (bottom), loading control. Blank, no RNA added before RT-PCR; MWM, molecular size marker. Results are representative of two independent replicates for each time point.

we examined the initial 96 h of T helper cell differentiation at 24-hour intervals in polarization assays of GSI- and DMSO-pretreated CD4$^+$ cells. A single pretreatment with GSI did not affect proliferation during the first 96 h (**Fig. 1e**). Flow cytometry of polarized CD4$^+$ cells stained with 5-carboxyfluorescein diacetate succinamidyl ester (CFSE), whose fluorescence intensity is diminished by half with each cell division, showed similar CFSE expression (**Fig. 1e**) as well as percent proliferating cells (**Fig. 1f**) GSI- and DMSO-treated cultures at all time points. Thus, the notable differences in IFN-γ production found in GSI-pretreated polarization assays (**Fig. 2a**) could not be attributed to differences in proliferation in GSI- and DMSO-treated cultures.

GSI pretreatment differentially affects protein expression

We next analyzed cytokine expression at 24-hour intervals during the early stages of polarization. Pretreatment with GSI did not seem to alter IL-4 production; however, in contrast to DMSO controls, IFN-γ secretion was abrogated as early as 48 h after GSI pretreatment of T_H1-polarized cultures and remained low throughout the culture period (**Fig. 2a**). In contrast, treatment of developing CD4$^+$ T_H1 and T_H2 cells with GSI after 48 h in culture did not affect IFN-γ production (**Fig. 2b**). These data confirm that the first 24–48 h of T helper cell differentiation represent a critical time period during which blocking Notch activation inhibits T_H1 polarization without perturbing T_H2 cell fate choices.

Cytokines influence transcription through signals relayed by STAT molecules[26]. Phosphorylated STAT1 (phospho-STAT1) mediates IFN-γ receptor signaling[27], whereas phospho-STAT4 signals downstream of the IL-12 receptor[28,29], which is itself transcriptionally regulated by T-bet in T_H1 cells[13]. In similar way, phospho-STAT6 transduces signals through the IL-4 receptor in T_H2 cells[30]. We assessed expression of phospho-STAT1, phospho-STAT4 and phospho-STAT6 in polarization assays of GSI- and DMSO-pretreated CD4$^+$ cells during the first 96 h of culture. GSI pretreatment effectively prevented phosphorylation of STAT4 within 24 h, whereas phosphorylation of STAT6 was reduced but not totally abrogated (**Fig. 2c**). We did not detect phospho-STAT1 expression at any time point, regardless of pretreatment or polarizing conditions (data not shown), although it is possible that temporal expression of phospho-STAT1 is outside the time points we examined.

After T cell activation, Notch1 is upregulated[7] and further upregulates its own expression[31]. Thus, inhibition of γ-secretase prevents the generation of endogenous intracellular Notch (Notch^{IC}) as well as total Notch expression. Again using Notch1 protein expression as an indicator of GSI efficacy, we found Notch1 was upregulated in DMSO-pretreated CD4$^+$ cells in all culture conditions at 24 h and remained detectable in T_H1-polarized cultures throughout the 96-hour period examined (**Fig. 2c**). We detected Notch1^{IC} at 24 and 48 h in T_H1-polarized, DMSO-pretreated CD4$^+$ cells. In contrast, we detected no Notch1 or Notch1^{IC} in GSI-pretreated cultures regardless of polarizing conditions. Thus, by monitoring expression and cleavage of Notch1 protein, we demonstrated that GSI effectively inhibits CD4$^+$ T_H1 differentiation by modulating Notch protein expression as well as STAT4 phosphorylation. Phosphorylation of STAT6 seemed less sensitive to GSI pretreatment, consistent with the observation that T_H2 differentiation and IL-4 production remain intact in the absence of Notch activation.

Signaling through Notch receptors is initiated by ligand binding. Using RT-PCR, we assessed the presence of Notch ligands on CD4$^+$ cells pretreated with DMSO or GSI and cultured for 24 h in neutral

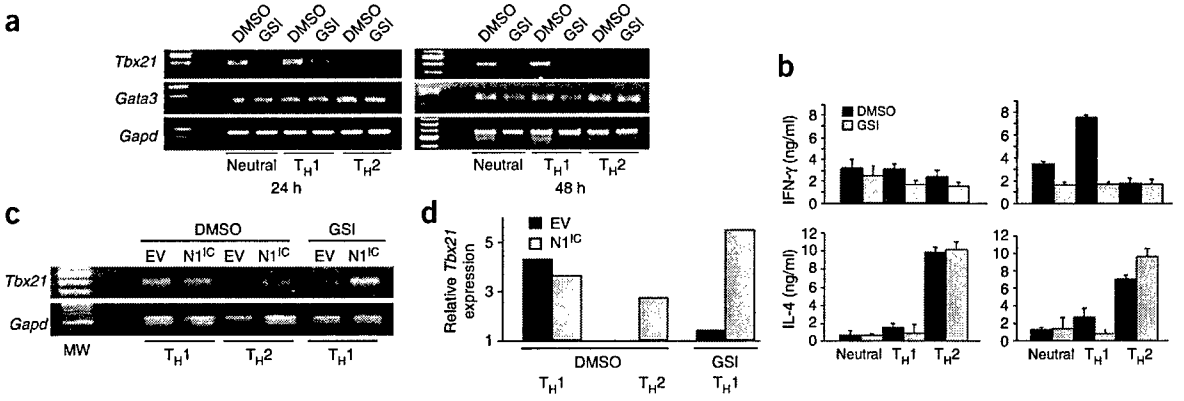

Figure 3 *Tbx21* mRNA expression is abrogated by 48 h in the absence of Notch signaling and *Tbx21* mRNA is re-expressed after expression of activated Notch1. (**a**) Expression of *Tbx21* and *Gata3* transcripts, assessed by RT-PCR of total RNA isolated from CD4$^+$ T cells pretreated *in vitro* with GSI or DMSO and cultured in polarizing conditions for 24 h (left) or 48 h (right). Results are representative of two independent replicates. (**b**) ELISA of IFN-γ and IL-4 secretion in supernatants collected after 24 h (left) or 48 h (right) of the culture in **a**, before RNA extraction. Results are the mean of triplicate wells ± s.d. and are representative of two independent replicates. (**c**) *Tbx21* expression. CD4$^+$ T cells were pretreated *in vitro* with GSI or DMSO and were cultured in polarizing conditions for 48 h, then were retrovirally infected with bicistronic human CD8–empty vector only (EV) or with a bicistronic human CD8–N1^{IC} construct (N1^{IC}); total RNA extracted 48 h later was analyzed by RT-PCR. (**d**) *Tbx21* expression in **c**, normalized to *Gapd* expression. Results are representative of two independent retroviral infections. MW, molecular weight markers.

conditions. We detected transcripts encoding the Notch ligands Jagged 1, Jagged 2 and Delta-like 1 in both DMSO- and GSI-treated cells, thus confirming that our *in vitro* polarization assay is a complete system with which to study CD4$^+$ T cell–intrinsic effects of Notch signaling during T helper cell differentiation (**Fig. 2d**).

To determine whether GSI inhibits T_H1 polarization through effects on CD44, another cleavage substrate of γ-secretase[32], we evaluated CD44 expression on DMSO- and GSI-pretreated CD4$^+$ cells. Regardless of pretreatment or polarizing conditions (**Supplementary Methods** online), CD44 expression remained equivalently high at 96 h. Furthermore, the ability of CD44 to bind its cognate ligand hyaluronic acid was not impaired in either T_H1- or T_H2-polarized cells pretreated with GSI, even though IFN-γ secretion was abrogated in GSI-pretreated T_H1-polarized cultures (**Supplementary Fig. 1** online). These data indicate that although GSI pretreatment of *in vitro*–polarized CD4$^+$ cells abrogates IFN-γ production, these effects may be independent of its effects, if any, on CD44 signaling. Along with the results from *in vitro* polarization of Notch1AS CD4$^+$ cells (**Fig. 1a**), these data provide additional supporting evidence that GSI prevents T_H1 polarization by inhibiting Notch activation and not through 'promiscuous' effects on CD44.

Notch activation correlates with *Tbx21* expression

Early attenuation of responses after GSI pretreatment suggested that its use might instill heritable alterations to genetic programs driving T_H1 polarization. T helper cell differentiation is complex and is subject to multiple levels of regulation. Expression of the transcription factor T-bet is indispensable for T_H1 commitment and is considered a 'signature' of T_H1 cells[11]. *Tbx21* induction in CD4$^+$ cells has been correlated with exposure to the Notch ligand fusion protein Delta-1–Fc[9]. Although that observation suggested involvement of Notch signaling in *Tbx21* expression, direct regulation of *Tbx21* by Notch has not yet been demonstrated. As early as 24 h after pretreatment of CD4$^+$ cells with GSI, the abundance of *Tbx21* transcript in developing T_H1 cells was comparable to that of DMSO-treated T_H2 cells (**Fig. 3a**). By 48 h, *Tbx21* expression was extinguished altogether in GSI-pretreated T_H1 cells and in DMSO-treated T_H2 cells and correlated closely with IFN-γ production in these cultures (**Fig. 3a,b**). Within

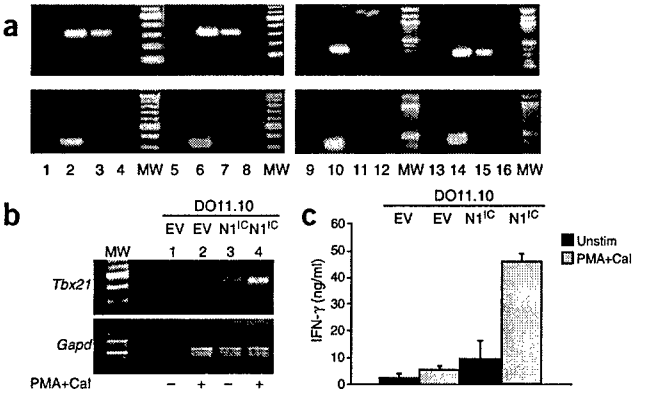

Figure 4 CSL binds constitutively to putative consensus sites in the *Tbx21* promoter and forms a complex with activated Notch1. (**a**) Chromatin immunoprecipitation of DO11.10 T cell hybridomas stably transduced with empty vector (lanes 1–4 and 9–12) or N1^{IC} (lanes 5–8 and 13–16). Anti-CSL (left) or anti-Notch1 (right) was used to precipitate CSL bound to DNA. DNA in complex was amplified by PCR with primers specific for *Tbx21* promoter sequences: primer set 1, top; primer set 2, bottom. Lanes 1, 5, 9 and 13, beads only; lanes 2, 6, 10 and 14, total chromatin input; lanes 3, 7, 11 and 15, immunoprecipitation with specific antibody; lanes 4, 8,12 and 16, immunoprecipitation with isotype control antibody. Results are representative of at least two independent assays. MW, molecular weight marker. (**b**) *Tbx21* expression, assessed by RT-PCR of total RNA isolated from DO11.10 T cell hybridomas stably transduced with empty vector (EV; lanes 1 and 2) or N1^{IC} (lanes 3 and 4). Cells were left unstimulated (lanes 1 and 3) or were stimulated with phorbol myristate acetate and calcium ionophore (PMA+Cal; lanes 2 and 4). *Gapd* (bottom), loading control. Results are representative of two independent experiments. (**c**) ELISA of IFN-γ expression in supernatants collected from DO11.10 T cell hybridomas cultured as described in **b**. Results are the mean of triplicate wells ± s.d. and are representative of two independent experiments.

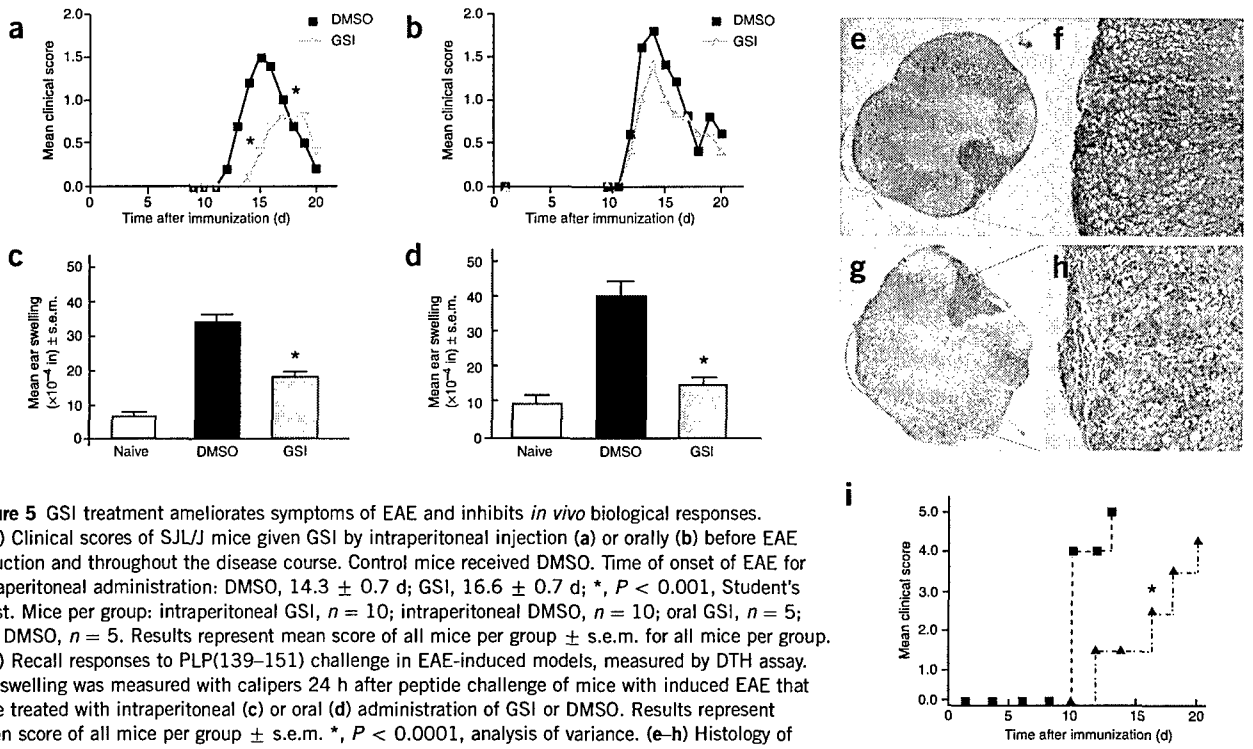

Figure 5 GSI treatment ameliorates symptoms of EAE and inhibits *in vivo* biological responses. (**a**,**b**) Clinical scores of SJL/J mice given GSI by intraperitoneal injection (**a**) or orally (**b**) before EAE induction and throughout the disease course. Control mice received DMSO. Time of onset of EAE for intraperitoneal administration: DMSO, 14.3 ± 0.7 d; GSI, 16.6 ± 0.7 d; *, $P < 0.001$, Student's *t*-test. Mice per group: intraperitoneal GSI, $n = 10$; intraperitoneal DMSO, $n = 10$; oral GSI, $n = 5$; oral DMSO, $n = 5$. Results represent mean score of all mice per group ± s.e.m. for all mice per group. (**c**,**d**) Recall responses to PLP(139–151) challenge in EAE-induced models, measured by DTH assay. Ear swelling was measured with calipers 24 h after peptide challenge of mice with induced EAE that were treated with intraperitoneal (**c**) or oral (**d**) administration of GSI or DMSO. Results represent mean score of all mice per group ± s.e.m. *, $P < 0.0001$, analysis of variance. (**e**–**h**) Histology of EAE-induced mice given oral DMSO or oral GSI for 6 weeks. After mice were killed, the presence of inflammatory infiltrates and areas of demyelination was evaluated in the spinal cords of one representative GSI-treated mouse (clinical score = 0; **e**,**f**) and one representative control mouse (clinical score = 4; **g**,**h**). (**i**) Clinical symptom scores in mice with induced active EAE. Control mice were killed when EAE score of 5 (moribund) was achieved and GSI-treated mice were killed 20 d after immunization. Mean clinical scores: DMSO (boxes), 4.6; GSI (triangles), 2.9; *, $P < 0.05$, Student's *t*-test; $n = 5$ for each group.

48 h of retroviral infection with a construct encoding activated Notch1 ($N1^{IC}$; **Supplementary Fig. 2** online), *Tbx21* expression was restored both in DMSO-pretreated T_H2 cells and GSI-pretreated T_H1 cells (**Fig. 3c,d**). There was increased IFN-γ secretion in supernatants of GSI-treated T_H1 cells showing $Notch1^{IC}$-induced re-expression of *Tbx21* (data not shown). These data confirm that Notch protein activation is an essential early event in T_H1 polarization and suggest that although functional redundancy among Notch proteins may exist, signaling through $Notch1^{IC}$ is sufficient to induce *Tbx21* expression.

Notch1 can directly regulate *Tbx21* transcription

Analysis of the *Tbx21* promoter remains incomplete, although STAT1 binding sites are present and positively regulate its transcription[13]. We examined approximately 1 kilobase of genomic DNA upstream of the mouse *Tbx21* start site and identified multiple putative binding sites for CSL, a transcription factor important in Notch-mediated signaling (**Supplementary Fig. 3** online). In the absence of activated Notch, CSL forms complexes with the transcriptional corepressors SMRT and SKIP to repress transcription from CSL binding sites[33]. When Notch signaling is initiated, however, $Notch^{IC}$ binds to the CSL complex, displacing the SMRT-SKIP corepressors, and recruits the coactivator Mastermind-like 1, among others, to convert CSL to a transcriptional activator[34]. To analyze *Tbx21* regulation by Notch1, we stably expressed amino acids 1,759–2,556 of $N1^{IC}$ or empty vector in the DO11.10 T cell hybridoma (called 'DO11.10-$N1^{IC}$' and 'DO11.10-EV', respectively). We did chromatin immunoprecipitation assays[35] using antibody to CSL (anti-CSL) or anti-Notch1 to precipitate proteins crosslinked to DNA. After releasing proteins, we used PCR to amplify two separate regions containing 'candidate' CSL binding motifs upstream of the *Tbx21* start site (**Supplementary Fig. 3** online). Immunoprecipitation with anti-CSL showed CSL bound to putative consensus sites both in DO11.10-EV and DO11.10-$N1^{IC}$ cells, suggesting it may bind constitutively to these sites (**Fig. 4a**, top left). Consistent with the function of CSL as a transcriptional repressor, *Tbx21* expression was barely detectable in DO11.10-EV cells (**Fig. 4b**, lanes 1 and 2). However, chromatin immunoprecipitation analysis using anti-Notch1 showed that Notch1 was detected in complex with CSL at these sites only in DO11.10-$N1^{IC}$ cells (**Fig. 4a**, top right). In agreement with the idea that $N1^{IC}$ can bind CSL and convert it to an activator, DO11.10-$N1^{IC}$ cells had more *Tbx21* expression than did

Table 1 GSI treatment prevents the development of relapsing EAE

			Clinical disease scores[b]				
Treatment	Incidence (%)	Time of onset[a]	1	2	3	4	5
GSI	2 of 9 (22)*	22.0 ± 6 d*	1	1	0	0	0
DMSO	8 of 10 (80)	16.6 ± 3 d	2	1	1	4	0

SJL/J mice were given oral GSI for 1 week before the induction of EAE and continuing for 6 weeks. [a]Data represent mean ± s.e.m. [b]Data represent number of mice attaining each clinical disease score. *, $P < 0.05$, GSI versus DMSO (Student's *t*-test). Mice per group: GSI, $n = 9$; DMSO, $n = 10$.

DO11.10-EV cells (**Fig. 4b**, lanes 3 and 4). Furthermore, DO11.10-$N1^{IC}$ cells secreted more IFN-γ, demonstrating a biological effect of $N1^{IC}$-mediated *Tbx21* induction (**Fig. 4c**). To assess the physiological relevance of CSL-$N1^{IC}$ interaction at these candidate CSL binding sites, we designed primers to amplify a second, nearby region in the *Tbx21* promoter that also contained putative CSL binding motifs (**Supplementary Fig. 3** online). Immunoprecipitation with anti-CSL did not detect CSL bound to these sites; thus, this second region was not amplified by PCR (**Fig. 4a**, bottom left). Notably, there was also no amplification of this region after immunoprecipitation with anti-Notch1 (**Fig. 4a**, bottom right), suggesting that in the absence of CSL binding, Notch1 is not recruited independently to these sites. The observation that $N1^{IC}$ associates with CSL only at specific CSL binding sites strongly suggests physiological relevance of this interaction. These data demonstrate that $N1^{IC}$ can form a complex with its nuclear binding partner CSL at candidate CSL binding sites in the *Tbx21* promoter of DO11.10-$N1^{IC}$ cells to directly and positively regulate *Tbx21* transcription and concomitant IFN-γ production. These data provide a T cell–intrinsic mechanism for Notch1-mediated regulation of $CD4^+$ T_H1 cell differentiation.

GSI ameliorates symptoms of EAE

Tight regulation of T_H1 and T_H2 responses is critical, as aberrant T_H1 conditions perpetuate destructive inflammation characteristic of autoimmune diseases such as multiple sclerosis, Crohn disease and rheumatoid arthritis[36–38], whereas a dysregulated T_H2 milieu can promote atopy and asthma[39]. We used the mouse EAE model, a classical T_H1-mediated model of multiple sclerosis, to determine what effects the blocking of Notch signaling *in vivo* with GSI has on disease onset and progression.

We treated SJL/J mice with GSI beginning 1 d (oral administration) or 3 d (intraperitoneal injection) before inducing EAE with amino acids 139–151 of proteolipid peptide (PLP(139–151)) and continued the GSI treatment throughout the disease course. We monitored mice for 20 d, then measured *in vivo* T_H1-mediated recall responses to PLP(139–151) challenge using a delayed-type hypersensitivity (DTH) assay. Mice treated intraperitoneally with GSI had a significant delay in the onset of disease compared with that of DMSO-treated control mice ($P < 0.001$; mean time of onset, 14.3 ± 0.7 d versus 16.6 ± 0.7 d for DMSO versus GSI; **Fig. 5a**). Both GSI-treated groups showed substantial reduction in clinical symptoms compared with that of DMSO-treated mice, regardless of administration or length of pretreatment before disease induction (**Fig. 5a,b**). Additionally, GSI-treated mice challenged *in vivo* with PLP(139–151) had a significantly reduced recall response compared with that of DMSO-treated control mice ($P < 0.0001$; **Fig. 5c,d**), further demonstrating the attenuation of T_H1-mediated responses. When we stimulated splenocytes from GSI-treated mice *ex vivo* with PLP(139–151), we noted decreased proliferation and reduction of T_H1-associated cytokines, including IFN-γ, compared with that of splenocytes from control mice (**Supplementary Fig. 4** online).

In a study of extended duration, we administered DMSO or GSI orally beginning 1 week before the induction of disease and continuing for 6 weeks. This treatment regimen also significantly reduced both the incidence ($P < 0.05$) and the severity ($P < 0.05$) of relapsing EAE (**Table 1**). Furthermore, when we examined the spinal cords of mice from each treatment group, there was a notable paucity of inflammatory lesions in tissues of mice treated with GSI (**Fig. 5e,f**) compared with that of control mice (**Fig. 5g,h**). Notably, we found no mortality or morbidity due to the inhibitor in the GSI-treated mice. Finally, when we induced a more severe EAE by coupling PLP (139–151) injection with administration of pertussis toxin, oral administration of GSI again delayed onset and substantially reduced the severity of disease compared with that of controls (mean clinical score, 4.6 versus 2.9 for DMSO versus GSI; $P < 0.05$; **Fig. 5i**). Attenuated *in vivo* DTH reactions together with diminished IFN-γ production after *ex vivo* peptide challenge suggest the inhibitory action of GSI administered *in vivo* successfully targets developing T_H1 cells. These data suggest treatment with GSI effectively ameliorates clinical symptoms of EAE in a mouse T_H1-mediated model of multiple sclerosis.

DISCUSSION

Studies using STAT1-deficient transgenic mice have indicated the existence of an IFN-γ receptor–STAT1–independent pathway for initiating *Tbx21* transcription. Although STAT1-deficient mice do not mount T_H1 responses sufficient to clear infection with *Toxoplasma gondii*, *Tbx21* transcript are still detected early during infection[15]. In other studies, abrogation of T-bet signaling by introduction of *Tbx21* small interfering RNA[16] or deletion of *Tbx21* (ref. 17) has been shown to protect from EAE, whereas STAT1 deficiency does not[17], again suggesting STAT1-independent regulation of T_H1 responses. Our data showing induction of *Tbx21* in developing $CD4^+$ T_H2 cells after retroviral infection with $N1^{IC}$ also provide evidence of an IFN-γ receptor–STAT1–independent pathway for *Tbx21* initiation, as these T_H2-polarized cultures contained anti-IFN-γ and thus prevented signaling through the IFN-γ receptor–STAT1 axis.

Also, the first 24–48 h of T helper cell differentiation seem to represent a critical 'window' during which Notch activation may be essential for the adoption of a T_H1 cell fate by $CD4^+$ cells. $CD4^+$ cells induce *Tbx21* expression when incubated with a Delta-1–Fc fusion protein[9]. Those experiments[9] did not distinguish which Notch family member is responsible for *Tbx21* induction or whether its regulation was direct or indirect. However, that observation agrees with our data demonstrating direct positive regulation of *Tbx21* by Notch in complex with CSL and showing that $N1^{IC}$ is sufficient to mediate this process. Although the location of regulatory sequences is often not conserved among species, candidate CSL binding sites are present within a 1-kilobase region upstream of the transcriptional start site in the human *TBX21* promoter region (data not shown). Thus, we propose a working model whereby CSL may bind constitutively to specific sites in the *Tbx21* promoter region to repress *Tbx21* transcription in the absence of activated Notch. After its activation, Notch binding in complex with CSL may convert CSL to a transcriptional activator, possibly through the recruitment of additional coactivators. A CSL-deficient mouse strain has been described that 'preferentially' adopts a T_H1 phenotype[40]. In agreement with our model, loss of CSL from putative binding sites may derepress the *Tbx21* promoter, possibly making it accessible to positive regulation by additional transcription factors.

Genetic studies have identified Notch and the β-amyloid precursor protein as dominant cleavage targets for the presenilin-containing γ-secretase complex[41]. Notch and amyloid precursor protein may compete as substrates for processing by γ-secretase[42]. It is reasonable to assume that in the immune system, Notch proteins represent a principal target of γ-secretase and that GSI works mainly to inhibit Notch activation. However, additional substrates of γ-secretase have been identified, and the adhesion molecule CD44 represents another target of interest in immune cells[32]. We did not evaluate CD44 signaling in our *in vivo* EAE model; however, our *in vitro* data suggest the contribution of CD44 to T_H1 polarization is minimal. Consistent with that conclusion, studies of the T_H1-mediated response to

challenge with *Mycobacterium tuberculosis* in CD44-deficient transgenic mice have shown that although pulmonary neutrophil influx increases in infected mice, no defect is noted in the trafficking of lymphocytes to the lungs or in the generation of T_H1-mediated protective immunity[43]. Our *in vitro* studies have demonstrated a distinct cell-intrinsic effect of GSI on $CD4^+$ cells; however, we cannot rule out the possibility of as-yet-undefined effects of GSI on additional substrates or cell types that may have contributed to its ability to attenuate T_H1 responses in our *in vivo* EAE studies. Experiments to evaluate possible additional mechanisms of GSI action are needed.

There is no consensus regarding the contribution that Notch may make in directing T helper cell differentiation. Involvement of Delta-1-mediated signaling in T helper cell differentiation has been described. However, whereas one study suggested it promotes T_H1-mediated clearance of *L. major* in a susceptible host[9], another purported it to be immunoprotective in a cardiac allograft model mediated by $CD8^+$ T cells[44]. Similarly, there are contradictory reports as to how Notch1 may influence T helper cell differentiation. One published report suggested no overt function for Notch1 in T_H2 differentiation[21], whereas another concluded Notch1 is critical in driving T_H2 differentiation, even in the absence of STAT6 (ref. 10).

Those conflicting data may result from the use of disparate $N1^{IC}$ constructs as well as different animal models. We have compared two very similar $N1^{IC}$ constructs, differing in their N-terminal sequence by only 11 amino acids. We found that transduction with one induced production of the transcription factor NF-κB and of IFN-γ, whereas introduction of the other had no effect (data not shown). Thus, for this study we used a human $N1^{IC}$ construct (consisting of amino acids 1,759–2,550) that closely resembles the endogenously generated, biologically relevant form of human $Notch1^{IC}$ (amino acids 1,744–2,556) in both its size and its downstream signaling capabilities, as measured by induction of NF-κB[20]. Other studies have used $N1^{IC}$ constructs containing the entire transmembrane domain and extending for approximately 36 amino acids into the extracellular domain (amino acids 1,701–2,556)[10]. When studying the effects of active Notch, it is difficult to evaluate the biological relevance of constructs containing extraneous sequences not normally present in endogenously generated $Notch^{IC}$. The first CSL binding site is in close proximity to the N terminus of cleaved Notch and, physiologically, it is unmasked only after γ-secretase cleavage. We would argue that in lieu of 'active' $N1^{IC}$, use of a construct containing extracellular and transmembrane sequences but without a leader peptide that allows it to be efficiently inserted into the membrane and activated by γ-secretase complicates data interpretation and makes comparison with expression of a constitutively active, intracellular construct difficult. We believe data from our *in vivo* and *in vitro* GSI studies as well as from our Notch1AS transgenic mice provide convincing evidence that blocking Notch activation prevents polarization toward a T_H1 phenotype. Furthermore, our retroviral infection experiments strongly complement those data and demonstrate that $N1^{IC}$ is sufficient to direct T_H1 differentiation and *Tbx21* expression in $CD4^+$ cells. Additionally, our data do not refute earlier work suggesting Notch may be involved in T_H2 differentiation[10]. Our data do suggest that in the absence of Notch signaling, there may be Notch-independent means of driving a T_H2 response, whereas there seem to be no Notch-independent means of inducing a T_H1 response. The direct consequence of our findings is that pharmacological suppression of Notch signaling in humans may result in selective inhibition of T_H1 differentiation while sparing T_H2 differentiation and it could therefore be used to manipulate the immune response in this direction when this is therapeutically desirable.

Another issue deserving further investigation is the possibility of redundant effects among the Notch proteins. GSI treatment entirely abrogates Notch signaling by preventing the cleavage of all four Notch receptors[45]. Our Notch1AS mouse data suggest that downregulation of Notch1 can substantially reduce IFN-γ production, and our 'rescue' experiments indicate that expression of $N1^{IC}$ is sufficient to reverse the effects of GSI. However, as all four Notch proteins are capable of binding CSL[45], it is possible that other Notch proteins also participate in T-bet regulation, either physiologically or as a compensatory effect when Notch1 is completely lost, as in gene-targeted cells.

Effective modulation of T_H1-mediated autoimmunity represents a considerable clinical challenge. An emerging paradigm suggests that inhibition of T-bet expression is an effective means of achieving this end[16,17]. Here we have provided strong evidence that GSI-mediated inhibition of Notch signaling confers $CD4^+$ T cell–intrinsic alterations, including abrogation of *Tbx21* induction, which attenuate biological responses and mitigate the paralysis and demyelination characteristic of EAE. A phase I clinical trial using GSI for the treatment of Alzheimer disease has been completed[46]. As early indications suggest that GSIs are well tolerated, our data would indicate potential therapeutic value for GSIs in treating the early relapsing-remitting phase of multiple sclerosis. Additional studies will show whether GSIs would be equally effective in treating other T_H1-mediated autoimmune diseases.

METHODS

EAE induction and GSI treatment. Mice were housed in animal care facilities at Northwestern University (Chicago, Illinois) or at the University of Massachusetts Amherst (Amherst, Massachusetts) and were cared for in compliance with institutional guidelines. The GSI administered *in vivo*, LY-411,575 (a mixture of four diasteriomers of a small molecule inhibitor of γ-secretase), was synthesized as described[47] and was administered orally (10 mg/kg/d dissolved in DMSO, resuspended in 50 μl strawberry KoolAid) or intraperitoneally (5 mg/kg/d, dissolved in DMSO) to 6-week-old female SJL/J mice beginning 1 d (oral) or 3 d (intraperitoneal) before EAE induction and continuing throughout disease course. Control mice received DMSO orally in KoolAid or DMSO intraperitoneally, as appropriate. Relapsing EAE was induced with 50 μg PLP(139–151) (HSLGKWLGHPDKF; Peptides International) per mouse, emulsified in complete Freund's adjuvant (4 mg/ml of *M. tuberculosis* H37RA; Difco) and distributed in 100-μl subcutaneous injections in the hind flanks. Active EAE was induced with 100 μg PLP(139–151) emulsified in complete Freund's adjuvant, plus 200 ng pertussis toxin administered intraperitoneally on day of induction and 48 h later. GSI (10 mg/kg/d) or DMSO was administered orally beginning 1 week before induction and throughout the disease course. Clinical scores were assigned as follows: 0, no abnormality; 1, limp tail or foot; 2, limp tail and hind limb weakness; 3, partial hind limb paralysis; 4, complete hind limb paralysis; and 5, moribund. For the DTH assay, mice were challenged with 10 μg of priming peptide, and the response was measured 24 h later. For histology, spinal cord sections were fixed in 4% paraformaldehyde and were embedded in paraffin, and sections were stained with periodic acid Schiff for the evaluation of pathology.

***In vitro* cell assays.** All antibodies and recombinant cytokines were purchased from BD Pharmingen unless indicated otherwise. For proliferation assays and LiquidChip cytokine analysis, pooled splenocytes from GSI- or DMSO-treated mice were stimulated for 96 h with various concentrations of PLP(139–151). Wells were pulsed with ^{3}H[thymidine] for the final 24 h of culture. Supernatants were collected and analyzed at 36 h for IFN-γ and IL-4 secretion using a LiquidChip kit (Beadlyte Mouse Multicytokine Detection System I; UpState Biotechnologies) according to the manufacturer's directions. For all *in vitro* polarization assays, the IMag magnetic bead system (mouse anti-CD4 DM particles, for direct magnetic separation; BD Pharmingen) was used to isolate naive $CD4^+$ T cells (more than 95% purity). For full polarization, 2.25×10^6 cells/ml were pretreated *in vitro* at 37 °C for 15 min with 0.1% DMSO or with GSI (50 μM zIL-CHO (a small peptide inhibitor of γ-secretase) in DMSO)

before being added to 12-well plates precoated with 1 μg/ml each of anti-CD3 plus anti-CD28. Cultures were pulsed 24 h later with 200 U/ml of recombinant human IL-2, were expanded on day 8 and lifted, and were restimulated with plate-bound anti-CD3 plus anti-CD28 on day 19, and supernatants were collected on day 20 for ELISA. The following combinations of antibodies and cytokines were added at the time of plating to induce polarization: T_H1, 10 μg/ml of anti-IL-4 plus 1 ng/ml of IL-12; T_H2, 10 μg/ml of anti-IFN-γ plus 10 ng/ml of IL-4; neutral, no polarizing antibodies or cytokines. For 96-hour polarization assays, $CD4^+$ T cells were isolated and treated as described above, but supernatants were collected at various time points without restimulation. Supernatants were analyzed in triplicate by standard ELISA for the secretion of IFN-γ and IL-4 with paired capture and detection antibodies. For CFSE analysis, $CD4^+$ T cells were labeled with 3 μM CFSE (Molecular Probes) before GSI or DMSO pretreatment and were polarized as described above. Fluorescence was measured with a FACSCalibur and was analyzed with CellQuest software (BD Immunocytometry Systems). For immunoblot analysis, 30 μg of protein from whole-cell lysates was resolved by SDS-PAGE, transferred to nitrocellulose membranes, blocked with 5% nonfat dry milk in 0.5% Tween in PBS, probed overnight with primary antibody, washed, probed with horseradish peroxidase (HRP)-conjugated secondary antibody and developed with enhanced chemiluminescence (ECL) Western Blotting Detection Reagents (Amersham Biosciences). Blots were sequentially stripped with Restore Western Blot Stripping Buffer (Pierce), following the manufacturer's instructions, and were reprobed as above. Antibodies included anti-Notch1 (rabbit C-20; Santa Cruz Biotechnology), anti–cleaved Notch1 (Val1744; Cell Signaling Technology), anti-phospho-STAT4 (Zymed), anti-phospho-STAT6 (Cell Signaling Technology) and anti-phospho-STAT1 (Tyr 701; Santa Cruz Biotechnology).

RT-PCR and retrovirus infection. For RT-PCR, total RNA was isolated from $CD4^+$ T cells polarized as described above using RNA-BEE (Tel-Test), following the manufacturer's directions. Reverse-transcriptase methods were used to generate cDNA, and transcripts of *Tbx21* and the gene encoding the zinc finger transcription factor GATA-3 (*Gata3*) were amplified by PCR. Transcripts of glyceraldehyde phosphodehydrogenase (*Gapd*) were amplified as a loading control. Primers were as follows: *Tbx21* forward, 5′-TGAAGCCCACACTCC TACCC-3′, and reverse, 5′-GCGGCATTTTCTAGTTGGG-3′; *Gata3*, forward, 5′-TCTCACTCTCGAGGCAGCATGA-3′, and reverse, 5′-GGTACCAATCTC GCCGCCACAG-3′; and *Gapd* forward, 5′-AATTCAACGGCACAGTCAAAG CCGAGAATG-3′, and reverse, 5′-GCGGCACGTCAGATCCACGCAGGAC-3′. Primers for Delta-like 1, Jagged 1 and Jagged 2 have been described[48]. For retrovirus infections, $CD4^+$ T cells were polarized for 48 h as described, then were subjected to one round of infection by replacement of 200 μl of culture supernatant with 200 μl of retroviral supernatants from Phoenix-Eco packaging cells transfected with the bicistronic pMX vector, containing an internal riobosomal entry site allowing expression of two proteins from a single promoter: pMX human CD8–EV (empty vector) or pMX human CD8-$N1^{IC}$ ($N1^{IC}$ (activated human Notch1), amino acids 1,759–2,556). Cells were cultured an additional 48 h in polarizing conditions, then RNA was isolated and RT-PCR was done using the primers described above. Infection efficiency was monitored by expression of human CD8 (as an indicator of $N1^{IC}$ expression, which is transcribed from the same promoter), using anti-human CD8–phycoerythrin and analysis with a FACSCalibur plus CellQuest software (BD Immunocytometry Systems).

Chromatin immunoprecipitation. The Chromatin Immunoprecipitation (ChIP) Assay Kit (17-295; Upstate Cell Signaling Solutions) was used for these analyses, but salmon sperm DNA–protein G agarose (Upstate Cell Signaling Solutions) was substituted for the beads provided. DO11.10 cells stably expressing bicistronic pMX human CD8–EV or a pMX human CD8-$N1^{IC}$ construct were treated with formaldehyde to crosslink protein to DNA, then were immunoprecipitated with anti-CSL (anti-RBP-Jκ (an antibody that recognizes CSL), clone K0043; Institute of Immunology) or anti-Notch1 (C-20; Santa Cruz Biotechnology). Isotype controls were as follows: for anti-RBP-Jκ, purified rat monoclonal immunoglobulin G1 (IgG1; clone 43414.11; R&D Systems); for Notch1, normal rabbit IgG (control IgG, sc-207; Santa Cruz Biotechnology). After 'de-crosslinking' and sonication, two regions of the *Tbx21* promoter containing putative CSL binding sites were amplified by PCR. Primer set 1 (327 base pairs (bp)) was forward, 5′-CACAGCCCC TACCCCCAATACGAA-3′, and reverse, 5′-CCCCCAGCCCCGAGGATGATG-3′ (−259 bp to −984 bp); primer set 2 (340 bp) was forward, 5′-CTGGGCA TACAGGAGGCAGCAACAAAT-3′, and reverse, 5′-GTCCCCTCACC CCG CCACCTTG-3′ (−235 bp to −577 bp). PCR conditions were as follows: 95 °C for 5 min, 95 °C for 1 min, 58 °C for 45 s and 72 °C for 1 min (35 cycles) and 72 °C for 5 min. For IFN-γ production, stably transfected DO11.10-EV and DO11.10-$N1^{IC}$ cells were left unstimulated or were stimulated for 5 h with 80 nM phorbol myristate acetate and 0.5 μM calcium ionophore, then supernatants were collected and IFN-γ was measured by ELISA.

Note: Supplementary information is available on the Nature Immunology website.

ACKNOWLEDGMENTS

The authors thank members of the Osborne Lab for discussions and R.A. Goldsby for critical reading of the manuscript. Supported by a Ruth L. Kirschstein National Research Service Award (L.M.M.).

COMPETING INTERESTS STATEMENT

The authors declare that they have no competing financial interests.

Received 5 January; accepted 13 April 2005
Published online at http://www.nature.com/natureimmunology/

1. Baron, M. An overview of the Notch signaling pathway. *Semin. Cell Dev. Biol.* **14**, 113–119 (2003).
2. De Strooper, B. *et al.* A presenilin-1-dependent γ-secretase-like protease mediates release of Notch intracellular domain. *Nature* **398**, 518–522 (1999).
3. Struhl, G. & Adachi, A. Nuclear access and action of notch *in vivo*. *Cell* **93**, 649–660 (1998).
4. Kopan, R. & Ilagan, M.X. γ-secretase: proteasome of the membrane? *Nat. Rev. Mol. Cell Biol.* **5**, 499–504 (2004).
5. Radtke, F., Wilson, A., Mancini, S.J.C. & MacDonald, R. Notch regulation of lymphocyte development and function. *Nat. Immunol.* **5**, 247–253 (2004).
6. Adler, S.H. *et al.* Notch signaling augments T cell responsiveness by enhancing CD25 expression. *J. Immunol.* **171**, 2896–2903 (2003).
7. Palaga, T., Miele, L., Golde, T.E. & Osborne, B.A. TCR-mediated Notch signaling regulates proliferation and IFN-γ production in peripheral T cells. *J. Immunol.* **171**, 3019–3024 (2003).
8. Murphy, K.M. & Reiner, S.L. The lineage decisions of helper T cells. *Nat. Rev. Immunol.* **2**, 933–944 (2002).
9. Maekawa, Y. *et al.* Delta1-Notch3 interactions bias the functional differentiation of activated $CD4^+$ T cells. *Immunity* **19**, 549–559 (2003).
10. Amsen, D. *et al.* Instruction of distinct CD4 T helper cell fates by different notch ligands on antigen-presenting cells. *Cell* **117**, 515–526 (2004).
11. Szabo, S. *et al.* A novel transcription factor, t-bet, directs Th1 lineage commitment. *Cell* **100**, 655–669 (2000).
12. Szabo, S. *et al.* Distinct effects of T-bet in Th1 lineage commitment and IFN-γ production in CD4 and CD8 T cells. *Science* **295**, 338–342 (2002).
13. Afkarian, M. *et al.* T-bet is a STAT1-induced regulator of IL-12R expression in naïve $CD4^+$ T cells. *Nat. Immunol.* **3**, 549–557 (2001).
14. Mullen, A.C. *et al.* Role of T-bet in commitment of T_H1 cells before IL-12-dependent selection. *Science* **292**, 1907–1910 (2001).
15. Gavrilescu, L.C., Butcher, B.A., Del Rio, L., Taylor, G.A. & Denkers, E.Y. STAT1 is essential for antimicrobial effector function but dispensable for γ interferon production during *Toxoplasma gondii* infection. *Infect. Immun.* **72**, 1257–1264 (2004).
16. Lovett-Racke, A.E. *et al.* Silencing t-bet defines a critical role in the differentiation of autoreactive T lymphocytes. *Immunity* **21**, 719–731 (2004).
17. Bettelli, E. *et al.* Loss of t-bet but not STAT1 prevents the development of experimental autoimmune encephalomyelitis. *J. Exp. Med.* **200**, 79–87 (2004).
18. Dal Canto, M.C., Melvold, R.V., Kim, B.S. & Miller, S.D. Two models of multiple sclerosis: experimental allergic encephalomyelitis (EAE) and Theiler's murine encephalomyelitis virus (TMEV) infection. A pathological and immunological comparison. *Microsc. Res. Tech.* **32**, 215–229 (1995).
19. Szabo, S.J., Dighe, A.S., Gubler, U. & Murphy, K.M. Regulation of the interleukin (IL)-12R beta 2 subunit expression in developing T helper 1 (Th1) and Th2 cells. *J. Exp. Med.* **185**, 817–824 (1997).
20. Cheng, P. *et al.* Notch-1 regulates NF-κB activity in hemopoietic progenitor cells. *J. Immunol.* **167**, 4458–4467 (2001).
21. Tacchini-Cottier, F., Allenbach, C., Otten, L.A. & Radtke, F. Notch1 expression is not required for $CD4^+$ T helper differentiation. *Eur. J. Immunol.* **34**, 1588–1596 (2004).
22. Bird, J.J. *et al.* Helper T cell differentiation is controlled by the cell cycle. *Immunity* **9**, 229–237 (1998).
23. Agarwal, S. & Rao, A. Modulation of chromatin structure regulates cytokine gene expression during T cell differentiation. *Immunity* **9**, 765–775 (1998).
24. Mullen, A.C. *et al.* Cell cycle controlling the silencing and functioning of mammalian activators. *Curr. Biol.* **11**, 1695–1699 (2001).

25. Seki, N. *et al.* IL-4-induced GATA-3 expression is a time-restricted instruction switch for Th2 cell differentiation. *J. Immunol.* **172**, 6158–6166 (2004).
26. Shuai, K. & Liu, B. Regulation of JAK-STAT signaling in the immune system. *Nat. Rev. Immunol.* **3**, 900–911 (2003).
27. Sekimoto, T., Nakajima, K., Tachibana, T., Hirano, T. & Yoneda, Y. Interferon-γ-dependent nuclear import of Stat1 is mediated by the GTPase activity of Ran/TC4. *J. Biol. Chem.* **271**, 31017–31020 (1996).
28. Thierfelder, W.E. *et al.* Requirement for Stat4 in interleukin-12-mediated responses of natural killer and T cells. *Nature* **382**, 171–174 (1996).
29. Kaplan, M.H., Sun, Y.L., Hoey, T. & Grusby, M.J. Impaired IL-12 responses and enhanced development of Th2 cells in Stat4-deficient mice. *Nature* **382**, 174–177 (1996).
30. Takeda, K. *et al.* Essential role of Stat6 in IL-4 signaling. *Nature* **380**, 627–630 (1996).
31. Deftos, M.L., He, Y.-W., Ojala, E.W. & Bevan, M.J. Correlating Notch signaling with thymocyte maturation. *Immunity* **9**, 777–786 (1998).
32. Lammich, S. *et al.* Presenilin-dependent intramembrane proteolysis of CD44 leads to the liberation of its intracellular domain and the secretion of an Aβ-like peptide. *J. Biol. Chem.* **277**, 44754–44759 (2002).
33. Zhou, S. & Hayward, D. Nuclear localization of CBF1 is regulated by interactions with the SMRT corepressor complex. *Mol. Cell. Biol.* **21**, 6222–6232 (2001).
34. Nam, Y., Weng, A.P., Aster, J.C. & Blacklow, S.C. Structural requirements for assembly of the CSL-intracellular Notch1-Mastermind-like1 transcriptional activation complex. *J. Biol. Chem.* **278**, 21232–21239 (2003).
35. Weinmann, A.S. Novel ChIP-based strategies to uncover transcription factor target genes in the immune system. *Nat. Rev. Immunol.* **4**, 381–386 (2004).
36. Barth, H. *et al.* Analysis of immunoregulatory T-helper cell subsets in patients with multiple sclerosis: relapsing-progressive course correlates with enhanced Th1, relapsing-remitting course with enhanced Th0 reactivity. *J. Neuroimmunol.* **133**, 175–183 (2002).
37. Parronchi, P. *et al.* Type 1 T-helper cell predominance and interleukin-12 expression in the gut of patients with Crohn's disease. *Am. J. Pathol.* **150**, 823–832 (1997).
38. Hartung, A.D. *et al.* Th-2 mediated atopic disease protection in Th1-mediated rheumatoid arthritis. *Clin. Exp. Rheumatol.* **21**, 481–484 (2003).
39. Larche, M., Robinson, D.S. & Kay, A.B. The role of T lymphocytes in the pathogenesis of asthma. *J. Allergy Clin. Immunol.* **111**, 450–463 (2003).
40. Tanigaki, K. *et al.* Regulation of αβ/γδ T cell lineage commitment and peripheral T cell responses by Notch/RBP-J signaling. *Immunity* **20**, 611–622 (2004).
41. Zhang, Z. *et al.* Presenilins are required for γ-secretase cleavage of β-APP and transmembrane cleavage of Notch-1. *Nat. Cell Biol.* **2**, 463–465 (2000).
42. Berezovska, O. *et al.* Notch1 and amyloid precursor protein are competitive substrates for presenilin1-dependent gamma-secretase cleavage. *J. Biol. Chem.* **276**, 30018–30023 (2001).
43. Kipnis, A., Basaraba, R.J., Turner, J. & Orme, I.M. Increased neutrophil influx but no impairment of protective immunity to tuberclosis in mice lacking the CD44 molecule. *J. Leukoc. Biol.* **74**, 992–997 (2003).
44. Wong, K.K. *et al.* Notch ligation by Delta1 inhibits peripheral immune responses to transplantation antigens by a $CD8^+$ cell-dependent mechanism. *J. Clin. Invest.* **112**, 1741–1750 (2003).
45. Mizutani, T., Taniguchi, Y., Aoki, T., Hashimoto, N. & Honjo, T. Conservation of the biochemical mechanisms of signal transduction among mammalian Notch family members. *Proc. Natl. Acad. Sci. USA* **98**, 9026–9031 (2001).
46. Siemers, E. *et al.* Effect of LY450139, a functional γ-secretase inhibitor, on plasma and cerebrospinal fluid concentrations of A-β and cognitive functioning in patients with mild to moderate Alzheimer's disease. *Neurology* **62**, A174 Abstract S17.001 (2004).
47. Lanz, T.A., Hosley, J.D., Adams, W.J. & Merchant, K.M. Studies of Aβ pharmacodynamics in the brain, cerebrospinal fluid, and plasma in young (plaque-free) Tg2576 mice using the gamma-secretase inhibitor N2-[(2S)-2-(3,5-difluorophenyl)-2-hydroxyethanoyl]-N1-[(7S)-5-methyl-6-oxo-6,7-dihydro-5H-dibenzo[b,d]azepin-7-yl]-L-alaninamide (LY-411575). *J. Pharmacol. Exp. Ther.* **309**, 49–55 (2004).
48. Anderson, G., Pongracz, J., Parnell, S. & Jenkinson, E.J. Notch ligand-bearing thymic epithelial cells initiate and sustain Notch signaling in thymocytes independently of T cell receptor signaling. *Eur. J. Immunol.* **31**, 3349–3354 (2001).

Oncogene (2005), 1–12

www.nature.com/onc

ORIGINAL PAPER

Gamma secretase inhibitor blocks Notch activation and induces apoptosis in Kaposi's sarcoma tumor cells

Christine L Curry[1,2], Laura L Reed[1], Todd E Golde[3], Lucio Miele[1], Brian J Nickoloff[1,2] and Kimberly E Foreman*[,1,2]

[1]Department of Pathology and Oncology Institute, Cardinal Bernardin Cancer Center, Loyola University Medical Center, Maywood, IL, USA; [2]Department of Microbiology and Immunology, Loyola University Medical Center, Maywood, IL, USA; [3]Department of Neuroscience, Mayo Clinic, Jacksonville, FL, USA

Kaposi's sarcoma (KS) is a common neoplasm in HIV-1-infected individuals causing significant morbidity and mortality. Despite recent advances, the pathogenesis of this potentially life-threatening neoplasm remains unclear, and there is currently no cure for KS. Notch proteins are known to play a fundamental role in cell fate decisions including proliferation, differentiation, and apoptosis. It is, therefore, not surprising that Notch proteins have been implicated in tumorigenesis and appear to function as either oncogenes or tumor suppressor proteins depending on cellular context. In this report, we demonstrate elevated levels of activated Notch-1, -2, and -4 in KS tumor cells *in vivo* and *in vitro* compared to endothelial cells, the precursor of the KS cell. Notch activation was confirmed through luciferase reporter assays and localization of Hes (Hairy/Enhancer of Split)-1 and Hey (Hairy/Enhancer of Split related with YRPW)1 (primary targets of the Notch pathway) in KS cell nuclei. Studies using γ-secretase inhibitors (GSI and LY-411,575), which block Notch activation, resulted in apoptosis in primary and immortalized KS cells. Similar studies injecting GSI into established KS cell tumors on mice demonstrated growth inhibition or tumor regression that was characterized by apoptosis in treated, but not control tumors. The results indicate that KS cells overexpress activated Notch and interruption of Notch signaling inhibits KS cell growth. Thus, targeting Notch signaling may be of therapeutic value in KS patients.

Oncogene advance online publication, 6 June 2005; doi:10.1038/sj.onc.1208783

Keywords: Kaposi's sarcoma; Notch; γ-secretase; apoptosis; growth arrest; KSHV

Introduction

Notch proteins belong to a family of four evolutionarily conserved transmembrane receptors that play a fundamental role in cell fate decisions including cell proliferation, differentiation, and apoptosis. In mammalian cells, there are four Notch receptors (termed Notch-1, -2, -3, and -4) and five ligands (termed Jagged-1, -2, and Delta-like (Dll)-1, -3, and -4). Although similar, the receptors show differences in structure that are likely responsible for their different expression patterns and unique functions. Notch signaling is initiated by receptor–ligand interactions between neighboring cells resulting in two successive proteolytic cleavages by TACE (TNF-α-converting enzyme) and the γ-secretase/presenilin complex. This processing results in the release of the intracellular domain (N^{IC}, the functionally active form of Notch), which translocates to the nucleus and binds CBF-1 (also termed CSL or RBP-Jκ), a DNA-binding protein. In the absence of N^{IC}, CBF-1 mediates gene repression by binding with the histone-deacetylase complex SMRT/sin3/HDAC-1; however, binding of N^{IC} to CBF-1 displaces the repressor complex and recruits nuclear coactivators such as MAML1 and histone acetyltransferases converting CBF-1 into a transcriptional activator. CBF-1/Notch interactions result in the expression of various target genes including Hes (Hairy/Enhancer of Split), Hey (Hairy/Enhancer of Split related with YRPW (also known as HesR, HRT, HERP, CHF, and gridlock)), NF-κB, and PPAR families of transcription factors, and cell cycle regulators such as $p21^{CIP1/WAF1}$ and cyclin D (Rangarajan *et al.*, 2001; Nickoloff *et al.*, 2002; Iso *et al.*, 2003).

The Hes (including Hes-1) and Hey (including Hey1 and Hey2) family members are transcription factors that are direct downstream targets of Notch activation. Both families share common domains including a basic helix–loop–helix (bHLH) domain, an orange domain, and a tetrapeptide motif, and they function to repress expression of tissue-specific transcriptional activators and ultimately prevent cell differentiation. Interestingly, these proteins have distinct repression mechanisms with Hes interacting with TLE/Groucho through the tetrapeptide motif and Hey engaging the mSin3 complex through the

*Correspondence: KE Foreman, Department of Pathology and Oncology Institute, Cardinal Bernardin Cancer Center-Room 302, Loyola University Medical Center, 2160 South First Avenue, Maywood, IL 60153-5385, USA; E-mail: kforema@lumc.edu
Received 29 October 2004; revised 19 April 2005; accepted 19 April 2005

bHLH domain (Iso *et al.*, 2001). Hes and Hey proteins not only form homodimers, but in cells that express both proteins, Hes and Hey form heterodimers that may extend their individual repression activity.

Given the complexity of the Notch signaling pathway, it is understandably difficult to predict the outcome of Notch activation. Not only are there multiple Notch receptors and ligands (each with a unique expression pattern), but the large number of target genes and potential crosstalk between Notch and other signaling cascades further complicate the system. This is well illustrated by studies showing that N^{IC}-1 functions differently depending on the cell context in which it is expressed. In mesenchymally derived cells, N^{IC}-1 overexpression has been implicated in tumorigenesis, while in keratinocytes, N^{IC}-1 appears to promote differentiation and possibly function as a tumor suppressor (Artavanis-Tsakonas *et al.*, 1999; Mumm and Kopan, 2000; Nicolas *et al.*, 2003).

Kaposi's sarcoma (KS), the most common neoplasm in AIDS patients, is a virally induced neoplasm that causes significant morbidity and mortality worldwide. Although the KS-associated herpesvirus (KSHV; also known as human herpesvirus 8, HHV-8) has been identified as the likely etiologic agent responsible for KS, it is currently unknown how KSHV infection leads to KS from a pathophysiological perspective. To date, Notch expression has not been studied in KS; however, endothelial cells (ECs), the precursor of KS cells, are known to express Notch-1, -2, and -4 as well as the ligands Jagged-1, -2, and Dll-1, -4 (Uyttendaele *et al.*, 1996; Luo *et al.*, 1997; Leimeister *et al.*, 2000; Shutter *et al.*, 2000; Tsai *et al.*, 2000; Villa *et al.*, 2001). In addition, Notch signaling has been shown to be essential for normal vascular development, and targeted disruption of Notch-1, Notch-1/Notch-4, Jagged-1 or Dll-1 in ECs results in the *in utero* demise of the embryo due to vascular defects and hemorrhage (Hrabe de Angelis *et al.*, 1997; Xue *et al.*, 1999; Huppert *et al.*, 2000).

In an attempt to better understand KS pathogenesis, we investigated the expression and activation of Notch proteins in KS and examined the effect of two pharmacologically unique γ-secretase inhibitors (a tripeptide aldehyde inhibitor (GSI) and a peptidomimetic inhibitor (LY-411,575)) on KS cell survival (Shimazaki *et al.*, 2001; Lanz *et al.*, 2004; Wong *et al.*, 2004). The results demonstrated elevated levels of both transmembrane and activated Notch-1, -2, and -4 in KS tumor cells *in vitro* and *in vivo* compared to normal ECs. Notch transcriptional activity was confirmed using luciferase reporter assays. Finally, GSI and LY-411,575 treatment resulted in apoptosis of KS cells *in vitro*. GSI also induced apoptosis and tumor regression or stabilization in nude mice bearing tumors of immortalized KS cells. These results suggest that Notch activation may be involved in KS pathogenesis, with important implications for the development of new therapeutic approaches for this neoplasm.

Results

KS tumor cells express activated Notch pathway proteins in vivo

Immunostaining of fresh frozen, cutaneous KS tissue sections (patch ($n=5$) or plaque ($n=4$) stage lesions) revealed expression of Notch-1, -2, and -4 in KS tumor cells in all specimens (Figure 1). Positive staining (ranging from moderate to intense) was localized in both the cytoplasm and nuclear/perinuclear region of the cells, with the latter finding being indicative of Notch activation. To further examine Notch activation, immunostaining was performed for the Notch target proteins, Hes-1 and Hey1. Positive staining for Hes-1 and Hey1 (ranging from modest to intense) was detected in both the cytoplasm and nucleus of the tumor cells in seven of nine lesions (Figure 1). Intense Hes-1-positive staining was also seen in an additional paraffin-embedded tissue specimen from a nodular stage KS lesion (data not shown). Finally, the Notch ligand, Jagged-1, was also identified on the KS tumor cells in the same seven KS lesions that expressed Hes-1 and Hey1 (Figure 1). Interestingly, both of the negative KS lesions were early, patch stage lesions, while all of the plaque stage lesions were positive for Hes-1, Hey1, and Jagged-1 as well as the only late-stage tumor nodule examined. Although definitive conclusions cannot be drawn without analysis of additional samples, the results suggest that Notch activation increases with tumor stage in KS. Immunostaining also demonstrated that the ECs within the KS lesions were frequently positive for the Notch pathway proteins, which was not unexpected in these angiogenic lesions. However, normal human skin showed little to no positive signal in the dermis for activated Notch-1, Notch-2, Hes-1, Hey1, or Jagged-1, although epidermal keratinocytes demonstrated varying levels of positivity providing an internal positive control (Figure 1 and data not shown).

KS tumor cells express activated Notch proteins in vitro

To confirm and extend these results, expression of Notch pathway proteins was examined in KS tumor cells grown in culture. Western blot analysis revealed constitutive activation of Notch-1 in primary KS tumor cells and the immortalized KS cell line, SLK, compared to normal ECs (Figure 2a). ECs expressed predominantly the transmembrane form of Notch-1, while the KS tumor cells expressed primarily the activated, N^{IC}-1 forms of the protein. SLK cells also expressed N^{IC}-1, although the levels were lower than in the primary KS isolates. Similarly, both primary KS tumor cells and SLK cells expressed higher levels of Notch-2 than ECs (Figure 2a). Densitometry revealed a 15.0- and 20.5-fold increase, on average, in transmembrane and activated Notch-2, respectively, in primary KS tumor cells, while SLK cells showed an average increase of 3.8- and 8.5-fold in transmembrane and activated Notch-2, respectively. A modest increase in N^{IC}-4 was observed with an

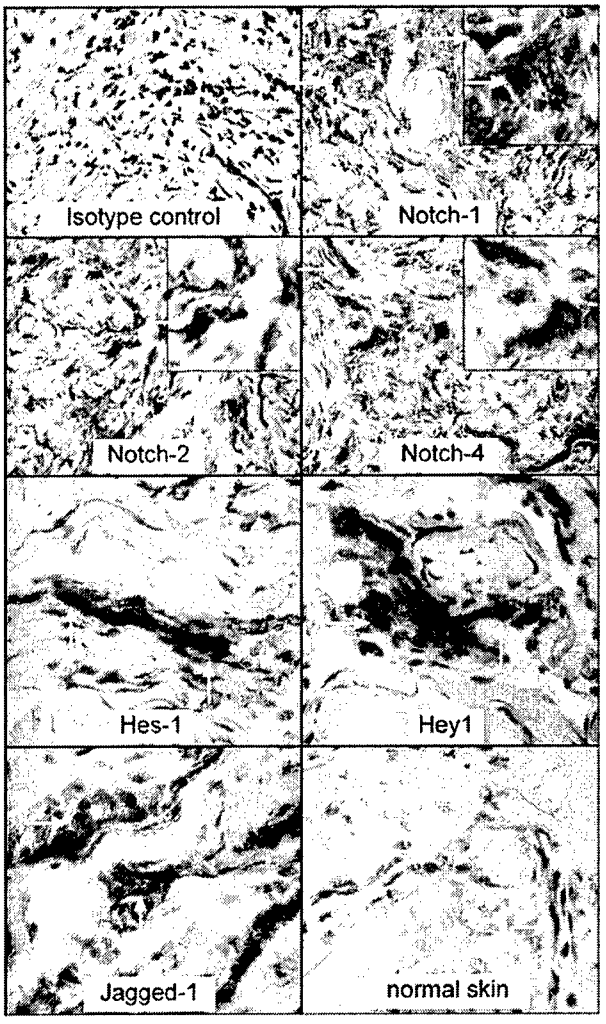

Figure 1 Immunoperoxidase staining for Notch receptors, ligand, and target proteins in KS lesional tissue. KS tumor cells expressed both cytoplasmic and nuclear Notch-1, -2, and -4, a finding indicative of Notch activation. Positive nuclear staining is highlighted in the inset figures within these panels. The tumor cells also expressed cytoplasmic and nuclear Hes-1 and Hey1, two direct downstream targets of Notch activation, and Jagged-1, a Notch ligand. As expected, normal ECs were frequently positive for the Notch pathway proteins in these angiogenic lesions. However, ECs in normal human skin showed little to no positive staining for Notch-1, -2, Hes-1, Hey1, or Jagged-1 (Notch-2 immunostaining is shown as an example). Panels in this figure are from plaque stage KS lesions with the exception of the normal human skin. The red reaction product signifies positive detection of the specified antigen, and staining performed with an isotype control antibody revealed no positive signal. Arrows highlight examples of positive cells

average increase of 2.0-fold in primary KS cells, and 2.4-fold in SLK cells compared to ECs. The increase in N^{IC}-4 was accompanied by a decrease in transmembrane Notch-4 in these cells (Figure 2a).

To further examine *in vitro* expression of Notch proteins, ECs, primary KS, and SLK cells were cultured on LabTek chamber slides. Immunostaining revealed diffuse, cytoplasmic positive staining for Notch-1, Notch-4, and Hes-1 in ECs with little detectable Notch-2 and Hey1 (Figure 2b). Occasionally, ECs with nuclear/perinuclear Notch, Hes-1, or Hey1 were noted indicating the presence of activated Notch. This finding was not unexpected in these subconfluent cultures. In contrast, primary KS cells and SLK cells showed intense cytoplasmic staining for Notch-1 and Notch-4 as well as nuclear/perinuclear localization (Figure 2b). Similarly, Notch-2 and Hey1 were identified in the nuclear/perinuclear area of the KS cells; however, overall cytoplasmic positivity was less intense. Notch-2 levels appeared even more modest in SLK cells; however, the expression was concentrated in the perinuclear region (Figure 2b). Notch activation was also indicated in the primary KS tumor cells by nuclear and cytoplasmic expression of Hes-1 and Hey1. Interestingly, Hes-1 appeared to be localized to the nucleoli of the KS cells. Hey1 expression was also localized to the nucleus in SLK cells; however, Hes-1 was predominantly cytoplasmic (Figure 2b).

Activated Notch in KS tumor cells is functional

As Notch activation promotes transcription of Hes-1, Hey1, and Hey2, luciferase reporter constructs driven by the promoters of these genes were used to confirm functional activity of Notch in KS cells (Jarriault *et al.*, 1995; Maier and Gessler, 2000; Iso *et al.*, 2002). Cells transfected with empty vectors (pGL2 or pLuc) showed low baseline luciferase levels (Figure 3). ECs transfected with HesA/B, Hey1, or Hey2 constructs showed detectable luciferase activity, but primary KS tumor cells showed significantly more activity (87-, 98-, and 130-fold increase compared to ECs, respectively; $P<0.05$; Figure 3). SLK cells also showed significant luciferase activity with the Hey1 and Hey2 constructs (69-fold, 143-fold increase compared to ECs, respectively; $P<0.05$; Figure 3); however, there was no difference between SLK cells with the HesA/B construct and the empty vector control. These results indicate that activated Notch is functionally active in both primary and immortalized KS tumor cells.

Notch inhibition results in apoptosis in cultured KS tumor cells

GSI, a pharmacologic agent known to block effectively Notch activation, was used to evaluate the effect of Notch inhibition on KS tumor cells. Initial studies confirmed GSI significantly reduced Notch-1, -2, and -4 activation in ECs and/or SLK cells under our experimental conditions, although Notch activation was retained for a longer time period in the SLK cells (Figure 4a and data not shown). The different time course of GSI activity may be related to changes in the half-life of N^{IC}, which has been shown to be extended in transformed cells (Weijzen *et al.*, 2002). GSI treatment also significantly blocked luciferase activity in primary KS cells transfected with the HesA/B, Hey1 or Hey2 reporter constructs (HesA/B: 68% decrease; Hey1: 89%

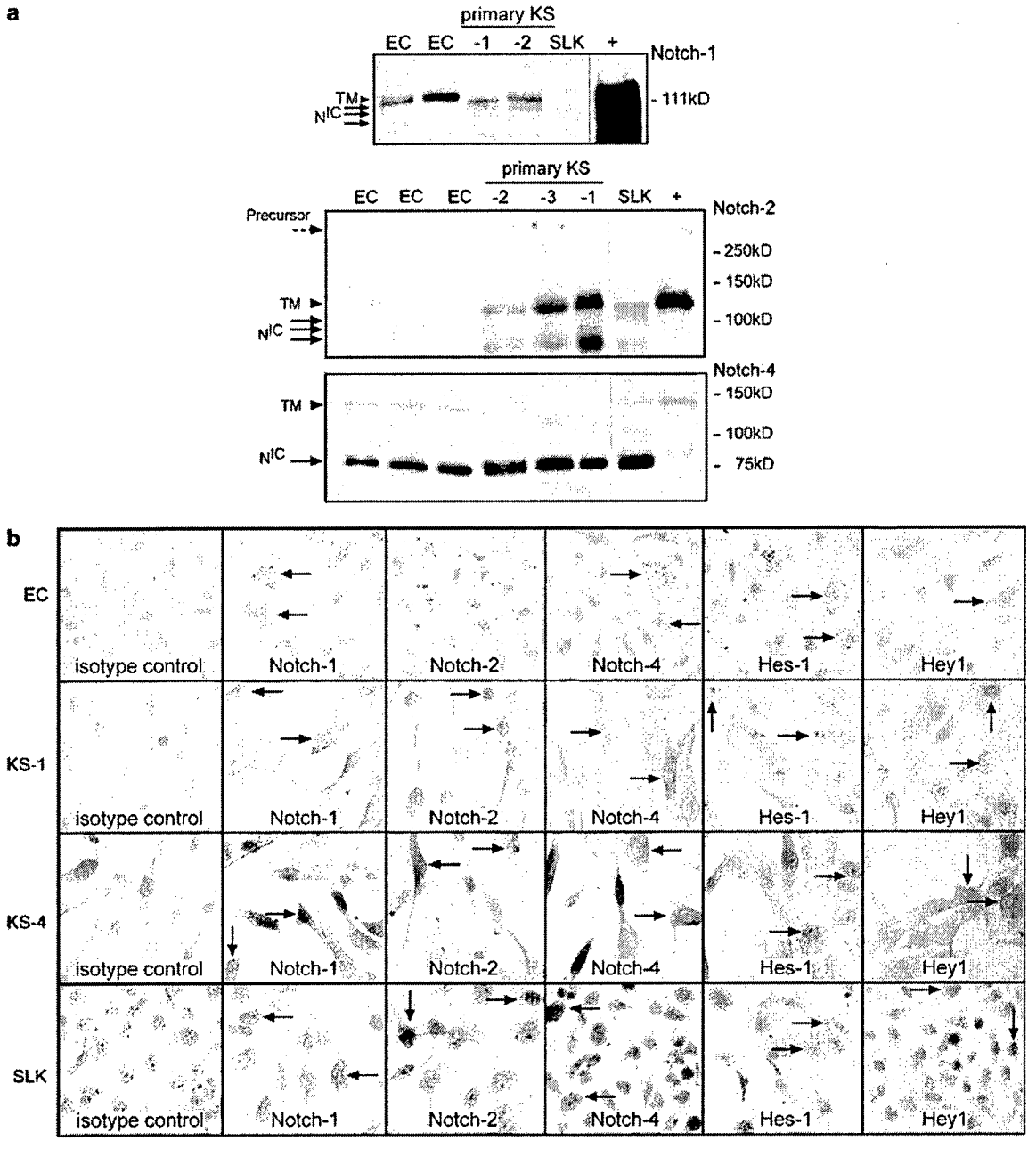

Figure 2 (**a**) Western blot analysis for Notch expression in two or three EC isolates, two or three primary KS tumor cells isolates, and the immortalized KS cell line, SLK cells. Normal ECs express primarily transmembrane Notch-1 and -2 (TM, arrowheads, approximately 120 kDa) and moderate levels of activated N^{IC}-4 (arrow, approximately 75 kDa). In contrast, primary KS and SLK cells express predominantly N^{IC}-1 and N^{IC}-2, as indicated by 1–3 bands (arrows) at 90–111 kDa. Previous studies have identified activated Notch as either a single band or a series of bands at approximately 110 kDa (Cheng *et al.*, 2001; Jang *et al.*, 2004). It has been hypothesized that the bands represent a TACE cleavage intermediate and N^{IC}, although these bands may represent degradation products. For primary KS cells, there was a 15-fold increase in transmembrane Notch-2 and a 20.5-fold increase in N^{IC}-2, on average, compared to EC. SLK cells showed an average increase of 3.8- and 8.5-fold in transmembrane Notch-2 and N^{IC}-2, respectively. The tumor cells also expressed higher levels of N^{IC}-4 (KS cells: 2.0-fold increase; SLK cells: 2.4-fold increase). The + sign indicates protein from a metastatic melanoma cell line, WM239, added as a positive control. (**b**) Immunostaining for Notch in ECs, SLK, and primary KS tumor cells cultured on LabTek chamber slides. ECs demonstrated diffuse, cytoplasmic positive staining for Notch-1, Notch-4, and Hes-1 with little detectable Notch-2 and Hey1. In contrast, SLK and primary KS cells showed intense cytoplasmic staining as well as nuclear/perinuclear localization of Notch-1 and Notch-4. Notch-2 was also identified in the nuclear/perinuclear area of KS and SLK cells, but overall positivity was less intense. Hes-1 and Hey1 were detected in the nucleus and cytoplasm of KS tumor cells. Hey1 was also expressed in the nuclei of SLK cells, but Hes-1 appeared to be primarily cytoplasmic. Arrows highlight examples of positive cells. Magnification: × 400

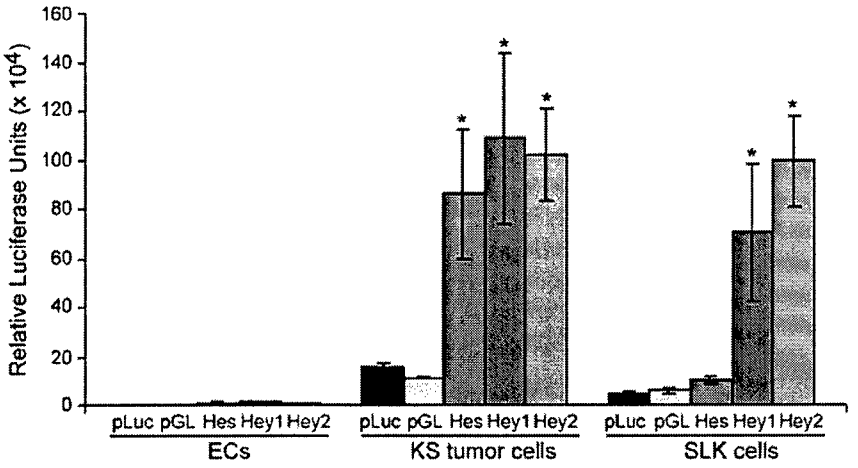

Figure 3 Luciferase activity in ECs, primary KS, and SLK cells transfected with HesA/B, Hey1, Hey2, or empty luciferase reporter constructs (pGL2, pLuc) as a control. The results showed significantly higher luciferase activity in primary KS tumor cells transfected with the HesA/B (87-fold), Hey1 (98-fold), and Hey2 (130-fold) constructs compared to ECs transfected with the same construct. Similarly, SLK cells showed significantly more luciferase activity with the Hey1 (69-fold) and Hey2 (143-fold) constructs compared to ECs; however, there was no significant difference between SLK cells with the HesA/B construct and the control vector. The figure represents combined data from a minimum of three experiments performed in triplicate. Data from the KS-1 primary KS tumor cell isolate are shown; however, similar results were also seen with the KS-5 cell isolate. Luciferase values were normalized for transfection efficiency. $*P<0.05$

decrease; Hey2: 90% decrease; $P<0.05$; Figure 4b). Reductions in luciferase were also seen at earlier time points and continued to decrease until the last time point evaluated (data not shown). ECs, primary KS, and SLK cells were treated with GSI for 24 or 48 h and examined for growth arrest and/or apoptosis using DNA/propidium iodide (DNA/PI) staining. While normal confluent ECs (mimicking EC lining the vasculature) were relatively resistant to the effects of GSI (average apoptosis: $11.9\pm1.2\%$; Figure 4c), primary KS tumor cells underwent apoptosis (average: $35.8\pm4.8\%$) after treatment with GSI (Figure 4c). Proliferating ECs, which express modest levels of activated Notch, were not as resistant to GSI and underwent apoptosis as expected (approximately 27% apoptotic; data not shown). Interesting, SLK cells first underwent G_2/M growth arrest (average: $50.5\pm3.7\%$) when treated with GSI for 48 h; however, apoptosis could be induced if the cells were treated with a second dose of GSI or if they were analysed at 96 h post-treatment (average: $97.8\pm1.3\%$; Figure 4c). Annexin V staining was used to confirm the results (data not shown).

To confirm that GSI induced growth arrest and/or apoptosis primarily through Notch inhibition, ECs and SLK cells were transduced with a retroviral vector expressing N^{IC}-1, -2, or -4. After demonstrating expression of activated Notch via Western blot and luciferase assays (data not shown), the cells were treated with GSI or DMSO as a control and cell proliferation measured. The effect of GSI on proliferating ECs or SLK cells was abrogated by expression of any of the N^{IC} proteins (Figure 4d and data not shown). Compared to SLK cells transduced with the empty retroviral vector, expression of N^{IC}-1, -2, or -4 in SLK cells resulted in a 2.7-, 3.1-, and 2.3-fold increase in proliferation, respectively, following GSI treatment (Figure 4d). Similar results were seen in proliferating EC cultures and in studies evaluating DNA/PI staining for both cell types (data not shown).

Although GSI is a potent inhibitor of γ-secretase activity, the aldehyde group on this peptide is able to covalently inhibit certain serine proteases. Therefore, similar experiments were performed with LY-411,575, a noncovalent peptidomimetic inhibitor of γ-secretase. LY-411,575 has been shown to block γ-secretase activity, but no compounds in its class are known to inhibit calpain or other serine proteases. Initial studies confirmed LY-411,575 blocks Notch activation using the luciferase reporter constructs driven by the HesA/B, Hey1 and Hey2 promoters. LY-411,575 did not decrease HesA/B activity (1.1-fold decrease; Figure 5a), a result that may be related to the overall low HesA/B activity seen in SLK cells in general (Figure 3). However, this compound potently blocked Notch activation and significantly reduced luciferase activity with the Hey1 and Hey2 reporter constructs (Hey1: 5.5-fold decrease; Hey2: 13.6-fold decrease; $P<0.05$; Figure 5a). With respect to growth arrest/apoptosis, treatment of SLK cells with LY-411,575 induced G_2/M growth arrest (average: $44.2\pm1.8\%$) compared to control-treated cells ($23.8\pm0.9\%$; $P<0.05$), a result that is consistent with those using GSI (Figure 5b). LY-411,575, however, had only a modest effect on ECs inducing apoptosis in only $17.4\pm1.7\%$ of the cells (Figure 5b).

Notch inhibition induces apoptosis in immortalized KS tumor cells in vivo

To determine if GSI could also induce apoptosis in an *in vivo* model system, nude mice were injected with SLK cells intradermally, and palpable tumors formed in 4–6

days. The established tumors were then injected with GSI (48 μg/dose), DMSO, or left untreated as a control. The injections were repeated every other day for 1 week, at which time the animals were sacrificed, photographed, and the tumors processed for histologic analysis. The results showed significant inhibition of

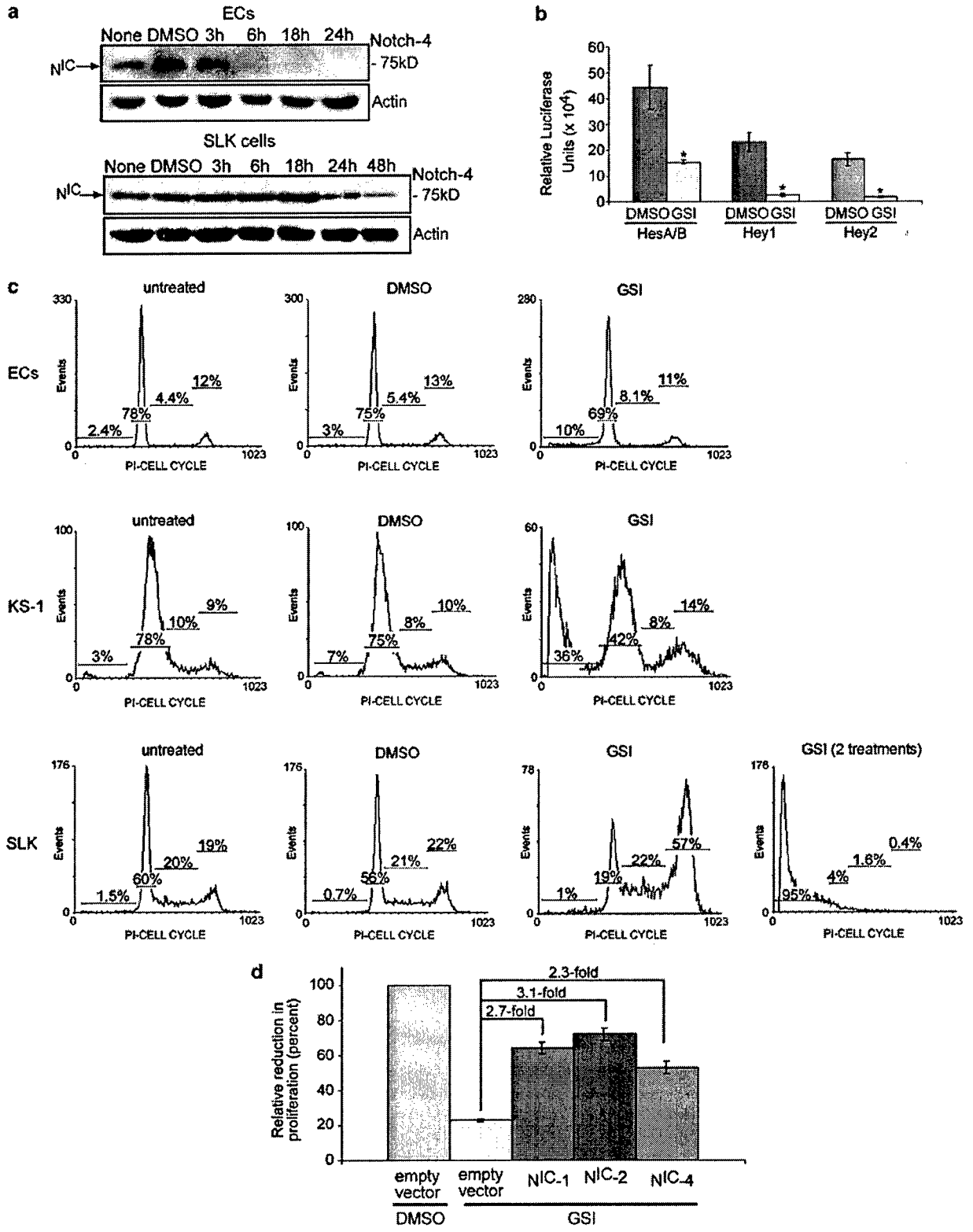

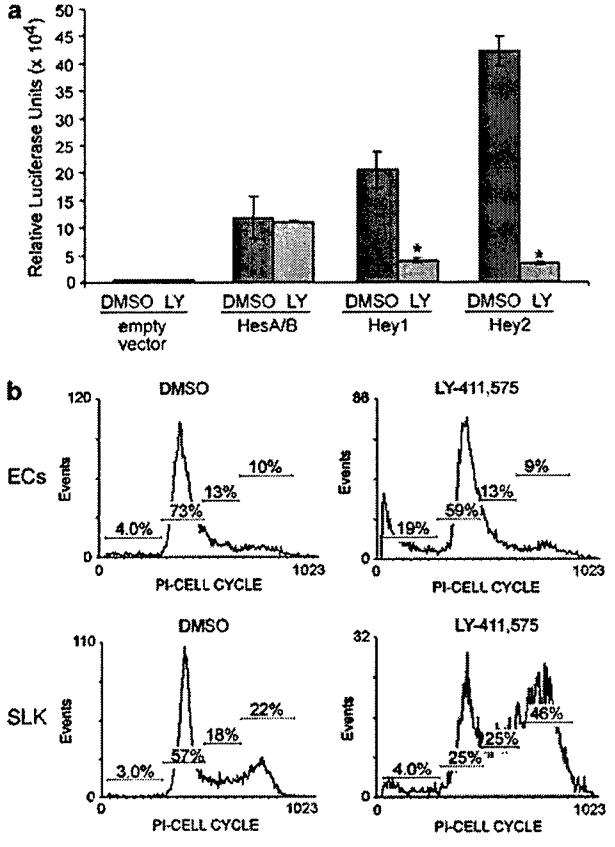

Figure 5 (**a**) Luciferase activity in SLK cells transfected with HesA/B, Hey1, Hey2, or the empty luciferase reporter constructs (pLuc) as a control. The cells were treated for 24 h with 500 μM LY-411,575 (prepared in DMSO) to block Notch activation or with the same dilution of DMSO as a control. The results showed significant reductions in luciferase activity in cells transfected with the Hey1 (5.5-fold) or Hey2 (13.6-fold) and treated with LY-411,575 compared to the control. However, there was little effect on HesA/B luciferase activity (1.1-fold decrease), which may be related to the overall poor Hes-1 response in these cells. Figure represent combined data from two experiments performed in duplicate. $^*P<0.05$. (**b**) LY-411,575 induces apoptosis in SLK cells *in vitro*. EC and SLK cells were treated with 500 μM Ly-411,575 for 24 h, and DNA/PI staining performed to evaluate apoptosis. The results showed SLK cells entered G_2/M growth arrest (average: 44.2$\pm$1.8%), while normal ECs showed only a modest apoptotic response to the treatment (17.4$\pm$1.7%). Representative data from three independent experiments are shown

tumor growth in the GSI-treated versus DMSO-treated and -untreated animals at days 4–7 (Figure 6a; $P<0.05$), while DMSO alone had no significant effect on tumor growth at any of the time points. Of the 13 GSI-treated tumors evaluated, two showed tumor regression, two showed stabilization, and the remaining nine tumors demonstrated significantly slower growth than DMSO-treated or -untreated lesions (data not shown). Histologic analysis indicated that GSI induced growth arrest and/or apoptosis in the SLK cells. Hematoxylin and eosin (H&E) staining revealed a large tumor in untreated animals containing actively dividing cells (Figure 6b). These cells were positive for Ki67, a marker of cell proliferation, while only an occasional cell was positive by TUNEL or activated caspase-3 staining, indicating low levels of apoptosis (7.6% of cells, on average, were activated caspase-3 positive). In contrast, the small GSI-treated tumor contained many cells with enlarged nuclei. These cells showed little evidence of proliferation as seen by the lack of Ki67 positivity, and many of the cells appeared to be apoptotic as indicated by positive TUNEL and activated caspase-3 activity (Figure 6b; 40% of cells, on average, were activated caspase-3 positive).

The results showed that two of 13 established SLK cell tumors on the mice regressed in response to GSI treatment. This result was not due to differences in the size of the tumors at treatment initiation (0.18 and 0.49 cm^3; tumors ranged from 0.15 to 0.72 cm^3), although GSI treatment tended to inhibit tumor growth better in smaller lesions (data not shown). This may be due to better penetration of the compound through the tumor during the intralesional injection. In addition, there was no evidence of systemic spread of the GSI in this experimental system, which may have hampered access of GSI to all of the tumor cells, resulting in the range of results from regression to stabilization to growth inhibition.

Discussion

The pathogenesis of KS is complex and not well understood. In particular, the molecular basis for KS

Figure 4 (**a**) Western blot analysis for N^{IC}-4 following GSI treatment. In normal ECs, 10 μM GSI dramatically reduced Notch-4 activation as early as 6 h after treatment. GSI also blocked Notch-4 activation in SLK cells; however, notable reductions in the 75 kDa N^{IC}-4 fragment did not occur until 24 h (1.52-fold decrease) and 48 h (4.0-fold decrease) after treatment. Similar results were seen in experiments examining Notch-1 and Notch-2 expression (data not shown). (**b**) Luciferase activity in KS tumor cells transfected with HesA/B, Hey1, or Hey2 reporter constructs and treated with GSI. GSI significantly blocked Notch activation as indicated by the decrease in luciferase activity after 24 h using all three reporter constructs (average decrease: HesA/B 68%, Hey1 89%, Hey2 90%). The results are shown as average data$\pm$s.e.m. from combined experiments. $^*P<0.05$. (**c**) GSI induces apoptosis in KS tumor cells *in vitro*. ECs, primary KS tumor cells, and SLK cells were treated with 10 μM GSI for 48 h, and DNA/PI staining performed to evaluate apoptosis. The results demonstrated significant apoptosis in KS tumor cells (average: 35.8$\pm$4.8), while confluent ECs showed only a modest response to the treatment (average: 11.9$\pm$1.2%). SLK cells, however, first underwent G_2/M growth arrest (average: 50.5$\pm$3.7%), but could be induced to undergo apoptosis when treated with a second dose of GSI or by analysing the cells at 96 h post-GSI treatment (average: 97.8$\pm$1.3%). (**d**) Activated Notch proteins rescue SLK cells from growth arrest. SLK cells transfected with an empty vector, N^{IC}-1, -2, or -4 were treated with 10 μM GSI for 24 h and proliferation measured by a WST-1 assay. Expression of the N^{IC} proteins protected the SLK cells from GSI-induced growth arrest when compared to GSI-treated SLK cells transduced with the empty retroviral vector (N^{IC}-1: 2.7-fold increase; N^{IC}-2: 3.1-fold increase; N^{IC}-4: 2.3-fold increase). Representative data from one of three independent experiments performed in triplicate are shown. The absorbance value of the DMSO-treated control was set to 100% and the relative reduction in proliferation calculated

tumor cell emergence, survival, and proliferation remains unclear despite active investigation. The current report demonstrates that KS cells both *in vitro* and *in vivo* express elevated levels of Notch receptors. In this context, Notch is constitutively activated as demonstrated by expression of Notch target proteins (Hes-1, Hey1) and induction of luciferase expression using reporter constructs driven by Notch-responsive promoters. Moreover, treatment of KS tumor cells with GSI or LY-411,575, two pharmacologically unique compounds that both block Notch activation, results in apoptosis in *in vitro* and/or *in vivo* model systems. Given that activated Notch plays a role in cell fate decisions and has been implicated in tumorigenesis, these novel findings may provide important clues to understanding KS pathogenesis and KS tumor cell proliferation.

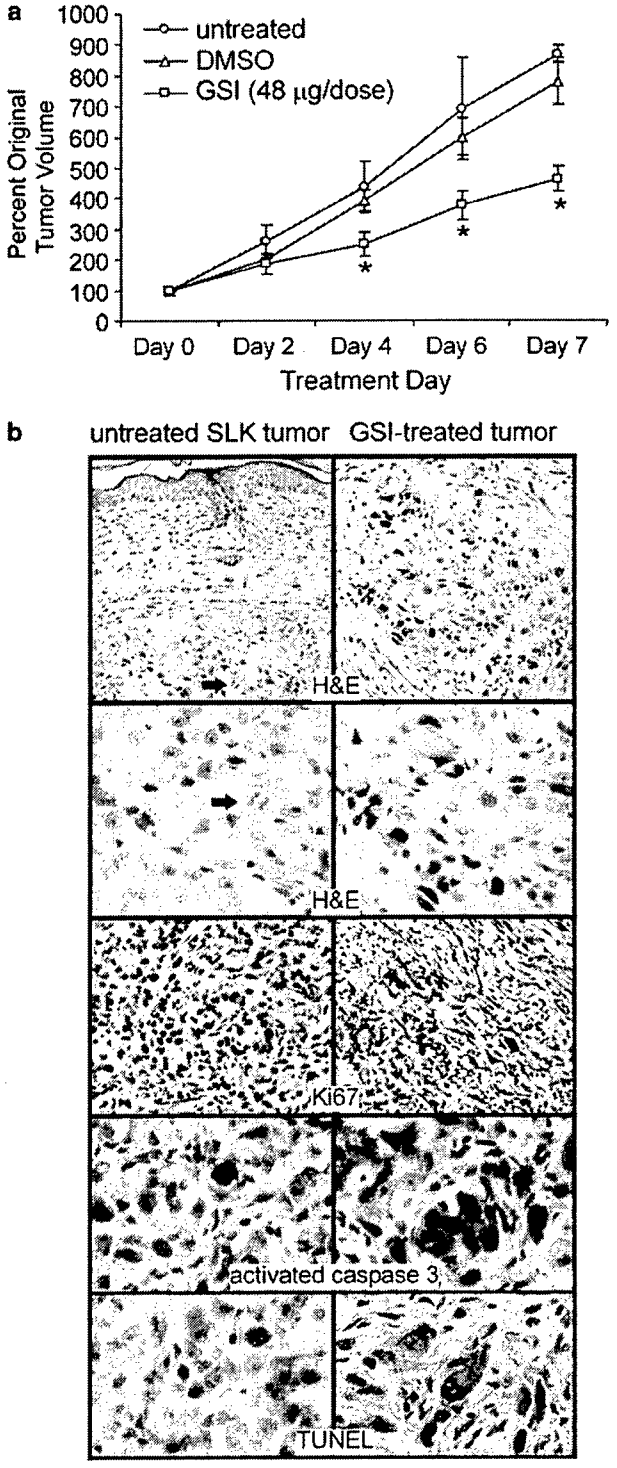

An oncogenic role for Notch was first identified by Sklar and colleagues in T-cell acute lymphoblastic leukemia (T-ALL) (Ellisen *et al.*, 1991). Early studies identified a (9 : 7) chromosomal translocation in 10% of T-ALL patients resulting in overexpression of N^{IC}-1 following fusion of the intracellular portion of Notch-1 to the T-cell receptor-β promoter/enhancer. More recently, studies have found as many as 50% of T-ALL patients have other mutations resulting in constitutive Notch-1 activation (Weng *et al.*, 2004). The activated forms of all four Notch receptors have been implicated in tumorigenesis in a variety of tumors including cervical, head and neck, lung, breast, and pancreatic carcinomas, mesotheliomas, malignant melanomas, and various hematologic malignancies (Gallahan *et al.*, 1996; Girard *et al.*, 1996; Pear *et al.*, 1996; Capobianco *et al.*, 1997; Soriano *et al.*, 2000; Jundt *et al.*, 2002). Interestingly, the Epstein–Barr virus (EBV) latency protein EBNA-2, which is required for EBV immortalization of B cells, mimics N^{IC} and binds to CBF-1 to recruit transcriptional coactivators and induce gene expression (Hayward, 2004). However, Notch, like other oncoproteins, is generally not tumorigenic when expressed alone, but instead requires coexpression of additional oncogenic alterations to promote transformation. Studies indicate that N^{IC}-1 can cooperate with c-Myc to induce lymphoid tumors and with ERBB2 to promote mammary tumors (Dievart *et al.*, 1999). N^{IC} can also cooperate with viral oncogenes. In cervical cancer, which is caused in part by human papilloma

Figure 6 (**a**) Graph of tumor measurements. Established SLK tumors were measured and then directly injected with GSI (48 μg/dose), DMSO, or left untreated as a control on days 0, 2, 4, and 6. The tumor volume at day 0 was set at 100%, and tumor volume at the subsequent time points was calculated and is presented as a percentage of the original tumor volume. GSI significantly inhibited tumor growth at days 4–7 compared to DMSO or untreated control tumors, while DMSO alone did not have a significant effect on the tumor. The following decreases in tumor volume were seen when comparing GSI to DMSO treatment: Day 2: 42.2%; day 4: 52.7%; day 6: 59.3%; day 7: 49.4%. Results are presented as an average ± s.e.m. for a minimum of 13 individual tumors. $^*P<0.05$. (**b**) Histologic analysis of nude mouse tumors. H&E staining of paraffin-embedded tissue demonstrates a large tumor in the untreated animals containing actively dividing cells (arrow shows a mitotic figure). Proliferation of these cells was confirmed by positive Ki67 staining and detection of only an occasional cell undergoing apoptosis (TUNEL and activated caspase-3 staining). In contrast, the small GSI-treated tumor contained many cells with enlarged nuclei. Many of these cells appear to undergo apoptosis as indicated by positive activated caspase-3 and TUNEL staining. In addition, the cells showed little evidence of proliferation as seen by the lack of Ki67 positivity

virus (HPV) infection, the HPV oncoproteins E6/E7 perform the critical functions of inactivating p53 and Rb, and activating telomerase. However, E6/E7 expression alone is insufficient to transform human epithelial cells, and Weijzen and co-workers recently demonstrated that N^{IC}-1 coexpression complements E6/E7 activity to fully transform cells (Lathion *et al.*, 2003; Weijzen *et al.*, 2003). These findings suggest that KSHV infection in KS may be important to constitutive Notch activation in KS tumor cells, and studies are in progress to determine if KSHV infection alters Notch expression and/or activation.

Our results showing GSI induces apoptosis in KS cells are consistent with a recent report demonstrating that GSIs indirectly activate caspase-3 in murine cells, and a study showing induction of apoptosis in melanoma cells (Alves *et al.*, 2004; Qin *et al.*, 2004). In that study, the investigators (including BJN and LM) found that malignant melanoma cells, which are notoriously resistant to apoptosis, can be effectively killed by GSI through the mitochondrial-based apoptotic pathway. The melanoma cells, but not normal melanocytes, induced expression of several proapoptotic proteins including NOXA, which appeared to mediate cell death. Our studies also showed induction of NOXA in GSI-treated SLK cells (unpublished data; CLC, LLR, KEF); however, we found that confluent, but not proliferating ECs were resistant to the effects of GSI. This may be related to the rate of proliferation in our experimental system where confluent ECs are contact inhibited and rarely divide. As ECs lining the normal vasculature *in vivo* are also growth arrested, these results suggest that GSI treatment would not have a detrimental effect on normal vessels. This conclusion is supported by our animal model data where the mice injected with GSI showed no evidence hemorrhage in or around the tumor. Interestingly, SLK cells initially entered a G_2/M growth arrest, and did not become apoptotic until 96 h post-treatment. It is possible that the cells initially enter mitotic catastrophe, a form of cell death resulting from aberrant mitosis or re-entry of tumor cells into the cell cycle after prolonged growth arrest (Roninson *et al.*, 2001). Further studies are needed to confirm or refute this theory.

Although studies have given insight into the apoptotic mechanisms involved in GSI-mediated cell death, it is still unclear how this compound induces apoptosis. γ-Secretases are known to mediate proteolysis of several transmembrane proteins in addition to Notch including the amyloid β-protein precursor, E-cadherin, and Erb-B4 (Esler *et al.*, 2000; Zhang *et al.*, 2000; Ni *et al.*, 2001; Marambaud *et al.*, 2002). We have demonstrated inhibition of Notch activation under our experimental conditions and transfection of proliferating ECs and SLK cells with activated Notch proteins rescued the cells from the effects of GSI. Although N^{IC} proteins were unable to completely restore cell proliferation, the results indicate that Notch inhibition by GSI was a key factor responsible for growth inhibition of the cells. In addition, a second compound (LY-411,575) that acts through a different mechanism to inhibit γ-secretase also blocked Notch activation in our studies and induced growth arrest in immortalized KS cells. We cannot, however, rule out that a portion of the involved mechanism is through a different signaling pathway. Experiments are in progress using RNA interference to block specifically individual Notch receptors and address this important question. Cancer cells, however, frequently express multiple Notch receptors, and in the case of KS tumor cells, activation of three different Notch receptors was found. Therefore, it may be necessary to simultaneously block multiple Notch receptors in order to kill tumor cells effectively.

In conclusion, this report demonstrates expression of activated Notch in KS tumor cells and shows that this Notch is functionally active. This novel finding adds to our understanding of KS pathogenesis and may be important in understanding the proliferation and enhanced survival of KS tumor cells. Furthermore, the induction of apoptosis in KS tumor cells by GSI and LY-411,575, two known Notch inhibitors, suggests that inactivation of Notch may be a therapeutic approach for treating patients suffering from this potentially life-threatening disease.

Materials and methods

Cell culture

Human dermal microvascular ECs were purchased from Cambrex (Walkersville, MD, USA) and cultured in EGM-2MV on plates coated with EC attachment factor (Cell Systems, Kirkland, WA, USA). KS tumor cells were isolated from primary lesions and characterized as described previously (Foreman *et al.*, 1996). The cells were plated on tissue culture dishes coated with EC attachment factor and were maintained in RPMI-1640 and 20% fetal bovine serum (FBS) supplemented with 10% Nutridoma HU (Roche Molecular Biochemicals, Indianapolis, IN, USA), 2 mmol/l L-glutamine, 100 U/ml penicillin, 100 μg/ml streptomycin, 50 μg/ml gentamicin, 50 μg/ml EC growth supplement (ICN Biochemicals, Aurora, OH, USA), and 16 U/ml heparin. SLK cells, a KSHV-negative immortalized KS cell line originally isolated from the oral mucosa of an HIV-negative patient, were maintained in RPMI-1640 containing 10% FBS, 2 mmol/l L-glutamine, 100 U/ml penicillin, 100 μg/ml streptomycin, and 50 μg/ml gentamicin (Herndier *et al.*, 1994).

Immunostaining

Formalin-fixed, paraffin-embedded tissue sections (5 μm thick) were dewaxed in xylene and ethanol, rehydrated, and briefly microwaved in 0.01 mol/l citrate buffer, pH 6.0, to optimize antigen retrieval. Alternatively, frozen sections or tissue culture cells grown on LabTek Slide Systems (Nalge Nunc International, Naperville, IL, USA) were fixed in ice-cold acetone. Sections were then immunostained to detect Notch receptors, ligands, or target proteins using a highly sensitive avidin–biotin immunoperoxidase technique (Vectastain ABC kit, Vector Laboratories, Burlingame, CA, USA) as described. Antibodies used in this study were purchased from Santa Cruz Biotechnology (Santa Cruz, CA, USA), unless otherwise noted, and include: Notch-1, Notch-2, Notch-4, Hes-1, Hey1 (HRT1), CD3 (Becton-Dickinson, San Jose, CA, USA), Ki67 (DakoCytomation, Carpinteria, CA, USA), and caspase-3

(R&D Systems, Minneapolis, MN, USA). For detection of apoptosis, TUNEL staining was performed using the ApoTag Peroxidase *In Situ* Apoptosis detection kit (Serologics Corporation, Norcross, GA, USA) following the manufacturer's instructions. Frozen KS tissue specimens were generously provided by the AIDS and Cancer Specimen Resource, sponsored by the National Cancer Institute, and evaluated by a dermatopathologist (BJN).

Western blot analysis

Whole-cell extracts were prepared by lysing cells in CHAPS buffer containing a mixture of protease inhibitors (Mini-Complete, Roche Molecular Biochemicals), incubating the cells for 20 min on ice and centrifuging to remove insoluble cellular debris (Tang *et al*., 2003). Protein concentration was determined using a Bradford Assay (Bio-Rad Laboratories, Hercules, CA, USA). Protein (50–100 μg) was loaded onto SDS–polyacrylamide gels, transferred to an Immobilon-P (polyvinylidene difluoride) membrane, and blocked with 5% powdered milk in TBST (50 mM Tris, pH 7.5, 150 mM NaCl, 0.01% Tween-20). The membrane was then incubated with primary antibodies diluted in 2.5% powdered milk in TBST, washed extensively, and incubated with HRP-conjugated species-specific secondary antibodies (Amersham Biosciences, Piscataway, NJ, USA). Proteins were visualized with ECL reagents (Amersham Biosciences) according to the manufacturer's instructions. Even loading of proteins was confirmed by Ponceau S staining and detection of the housekeeping protein, actin, on each blot. The antibodies against Notch1 (bTan20) and Notch2 (C651.6DbHN) developed by Dr S Artavanis-Tsakonas were obtained from the Developmental Studies Hybridoma Bank developed under the auspices of the NICHD and maintained by the University of Iowa (Iowa City, IA, USA). These antibodies recognize the least conserved portions of the intracellular domains of Notch-1 (nucleotides: 6658–7131) and Notch-2 (6508–6906) (Zagouras *et al*., 1995). Antibodies for all other Notch pathway proteins were purchased from Santa Cruz Biotechnologies and actin antibodies were obtained from ICN Biomedicals Inc. (Aurora, OH, USA). Differences in protein expression were determined by densitometry analysis using Scion Image Software (Scion Corporation, Frederick, MD, USA). Western blot experiments were repeated at least twice to confirm the results.

Plasmids and transfections

The Hey1 (also known as HesR1, HERP2, HRT1) luciferase reporter construct was the kind gift of Dr M Gessler (University of Wuerzburg, Wuerzburg, Germany). In this construct, approximately 3 kb of the presumed promoter region (−2839 to +87) of Hey1 was inserted in front of the luciferase gene in the promoterless vector pLuc. The Hey2 (also known as HesR2, HERP1, HRT2) luciferase reporter construct, containing 1 kb of the Hey2 promoter region inserted upstream of the luciferase gene in the pGL2 basic vector (Promega, Madison, WI, USA), was generously provided by Dr L Kedes (University of Southern California, Los Angeles, CA, USA). The Hes-1A/B luciferase reporter construct, containing the −194 to +160 promoter fragment of the Hes-1 gene inserted upstream of the luciferase gene in pGL2, was the gift of Dr S Siodia (University of Chicago, Chicago, IL, USA). Cells were transfected using Cytopure transfection reagent (Qbiogene, Carlsbad, CA, USA) following the manufacturer's instructions.

Luciferase assays

Cells from a transfected 60 mm dish were lifted with trypsin, washed, and resuspended in 150 μl of phosphate-buffered saline. Bright-N-Glo luciferase reagent (150 μl) (Promega) was added with thorough mixing following the manufacturer's instructions. The sample was incubated for 2 min at room temperature and the luciferase activity measured using an FB15 luminometer. The number of cells present in each sample was also counted to normalize the luciferase activity with the total number of cells (Lu *et al*., 2002). Owing to significant problems with promoter competition in these experiments, we were unable to cotransfect the cells with a vector to standardize transfection efficiency. As an alternative, we transfected control cells with a plasmid expressing green fluorescent protein (GFP) in each experiment. The percentage of transfected cells was determined by flow cytometry and the average value used to normalize the data for transfection efficiency (data not shown). Under these experimental conditions, we found that transfection efficiencies varied substantially between the different cell types, but reproducibility in replicate experiments within a particular cell type were acceptable. GFP positivity averaged 35.2 ± 4.2 for ECs, 9.1 ± 1.7 for KS tumor cells, and 19.0 ± 4.4 for SLK cells across a minimum of three independent experiments each performed in triplicate.

Inhibition of Notch activation

Cells were treated with increasing concentrations of various GSIs to inhibit Notch activation. As γ-secretase is involved in the activation of all four Notch receptors, GSIs are considered nonselective or pan-Notch inhibitors. Our preliminary studies demonstrated that GSI-I (Z-Leu-Leu-Nle-CHO (Nle = Norleucine); EMD Biosciences, San Diego, CA, USA) used at 5–10 μM was the most effective GSI under our experimental conditions. Direct evidence has been previously reported that GSI blocks Notch-1 and Notch-4 cleavage *in vitro*. The results were confirmed using a pharmacologically distinct γ-secretase inhibitor, LY-411,575, known to block Notch activation (Lanz *et al*., 2004; Wong *et al*., 2004).

Detection of apoptosis

DNA/PI staining was performed using standard methodologies. Briefly, 1×10^6 cells were permeabilized with 100% ethanol in the presence of 15% FBS. The cells were washed and then treated for 15 min at 37°C with 10 μg/ml RNAse. PI (5 μg/ml) was added, and the cells incubated for 1 h at 4°C prior to analysis by flow cytometry using a Coulter Epics MCL flow cytometer with 10 000 cells analysed per gated determination. The results were confirmed using the Immunotech Annexin V staining kit following the manufacturers' instructions. At least three independent experiments were performed showing similar results.

Proliferation assay

Cell proliferation was quantitated using a WST-1 assay, a highly sensitive, colorimetric alternative to ^{3}H-thymidine incorporation assays. Briefly, 4×10^4 cells/well were plated in a 96-well plate and allowed to proliferate overnight. The cells were then treated with GSI or DMSO as a control, and after 24 h, 10 μl of WST-1 reagent (Roche Applied Science) was added per well. After an additional 4 h incubation, the plate was shaken thoroughly for 1 min, and color development measured on a microplate reader at 450 nm.

Nude mouse model

Nude mice were injected with $2–3 \times 10^6$ SLK cells intradermally in the rear flank, and palpable tumors formed in 4–6 days. On the seventh day, the established tumors were directly injected with GSI (resuspended in DMSO and diluted in sterile saline; 48 μg/dose), DMSO (diluted in sterile saline), or were left untreated as a control. Injections continued every other day for a week and tumor dimensions were measured and recorded at each injection. Following treatment, the animals were killed and the tumors measured, photographed, and excised for histology and immunostaining. Unexpectedly, GSI injection resulted in a pain/distress response by the animals, which was completely alleviated by 0.1 mg/kg buprenorphine. Therefore, all animals were given buprenorphine 15 min prior to administering the GSI or DMSO control. Comparison of data with and without buprenorphine revealed no differences. All animal experiments were performed following institutional guidelines in accordance with the US Public Health Service *Policy on Humane Care and Use of Laboratory Animals*, and approval of the Loyola IACUC committee.

Acknowledgements

We thank Dr Abdul Fauq for assistance with LY-411,575, Drs Gessler, Kedes, and Siodia for luciferase reporter constructs driven by the Hes-1, Hey1, and Hey2 promoters, and Dr Brian Bonish for assistance with figures. We appreciate the generosity of the AIDS and Cancer Specimen Resource, sponsored by the National Cancer Institute, in providing frozen KS tissue specimens for immunostaining. We also thank the members of the Skin Cancer Research Program at the Cardinal Bernardin Cancer Center of Loyola University for helpful discussions. This work was supported by a grant from the National Institutes of Health CA108450 (KEF) and PO1 CA59327 (BJN).

References

Alves da Costa C, Ayral E, Hernandez JF, George-Hyslop P and Checler F. (2004). *J. Neurochem.*, **90,** 800–806.

Artavanis-Tsakonas S, Rand MD and Lake RJ. (1999). *Science*, **284,** 770–776.

Capobianco AJ, Zagouras P, Blaumueller CM, Artavanis-Tsakonas S and Bishop JM. (1997). *Mol. Cell. Biol.*, **17,** 6265–6273.

Cheng P, Zlobin A, Volgina V, Gottipati S, Osborne B, Simel EJ, Miele L and Gabrilovich DI. (2001). *J. Immunol.*, **167,** 4458–4467.

Dievart A, Beaulieu N and Jolicoeur P. (1999). *Oncogene*, **18,** 5973–5981.

Ellisen LW, Bird J, West DC, Soreng AL, Reynolds TC, Smith SD and Sklar J. (1991). *Cell*, **66,** 649–661.

Esler WP, Kimberly WT, Ostaszewski BL, Diehl TS, Moore CL, Tsai JY, Rahmati T, Xia W, Selkoe DJ and Wolfe MS. (2000). *Nat. Cell Biol.*, **2,** 428–434.

Foreman KE, Wrone-Smith T, Boise LH, Thompson CB, Polverini PJ, Simonian PL, Nunez G and Nickoloff BJ. (1996). *Am. J. Pathol.*, **149,** 795–803.

Gallahan D, Jhappan C, Robinson G, Hennighausen L, Sharp R, Kordon E, Callahan R, Merlino G and Smith GH. (1996). *Cancer Res.*, **56,** 1775–1785.

Girard L, Hanna Z, Beaulieu N, Hoemann CD and Jolicoeur P. (1996). *Genes Dev.*, **10,** 1930–1944.

Hayward SD. (2004). *Semin. Cancer Biol.*, **14,** 387–396.

Herndier BG, Werner A, Arnstein P, Abbey NW, Demartis F, Cohen RL, Shuman MA and Levy JA. (1994). *AIDS*, **8,** 575–581.

Hrabe de Angelis M, McIntyre J and Gossler A. (1997). *Nature*, **386,** 717–721.

Huppert SS, Le A, Schroeter EH, Mumm JS, Saxena MT, Milner MA and Kopan R. (2000). *Nature*, **405,** 966–970.

Iso T, Chung G, Hamamori Y and Kedes L. (2002). *J. Biol. Chem.*, **277,** 6598–6607.

Iso T, Kedes L and Hamamori Y. (2003). *J. Cell. Physiol.*, **194,** 237–255.

Iso T, Sartorelli V, Poizat C, Iezzi S, Wu HY, Chung G, Kedes L and Hamamori Y. (2001). *Mol. Cell. Biol.*, **21,** 6080–6089.

Jang MS, Miao H, Carlesso N, Shelly L, Zlobin A, Darack N, Qin JZ, Nickoloff BJ and Miele L. (2004). *J. Cell. Physiol.*, **199,** 418–433.

Jarriault S, Brou C, Logeat F, Schroeter EH, Kopan R and Israel A. (1995). *Nature*, **377,** 355–358.

Jundt F, Anagnostopoulos I, Forster R, Mathas S, Stein H and Dorken B. (2002). *Blood*, **99,** 3398–3403.

Lanz TA, Hosley JD, Adams WJ and Merchant KM. (2004). *J. Pharmacol. Exp. Ther.*, **309,** 49–55.

Lathion S, Schaper J, Beard P and Raj K. (2003). *Cancer Res.*, **63,** 8687–8694.

Leimeister C, Schumacher N, Steidl C and Gessler M. (2000). *Mech. Dev.*, **98,** 175–178.

Lu C, Gordon GM, Chandran B, Nickoloff BJ and Foreman KE. (2002). *Arch. Pathol. Lab. Med.*, **126,** 941–946.

Luo B, Aster JC, Hasserjian RP, Kuo F and Sklar J. (1997). *Mol. Cell. Biol.*, **17,** 6057–6067.

Maier MM and Gessler M. (2000). *Biochem. Biophys. Res. Commun.*, **275,** 652–660.

Marambaud P, Shioi J, Serban G, Georgakopoulos A, Sarner S, Nagy V, Baki L, Wen P, Efthimiopoulos S, Shao Z, Wisniewski T and Robakis NK. (2002). *EMBO J.*, **21,** 1948–1956.

Mumm JS and Kopan R. (2000). *Dev. Biol.*, **228,** 151–165.

Ni CY, Murphy MP, Golde TE and Carpenter G. (2001). *Science*, **294,** 2179–2181.

Nickoloff BJ, Qin JZ, Chaturvedi V, Denning MF, Bonish B and Miele L. (2002). *Cell Death Differ.*, **9,** 842–855.

Nicolas M, Wolfer A, Raj K, Kummer JA, Mill P, van Noort M, Hui CC, Clevers H, Dotto GP and Radtke F. (2003). *Nat. Genet.*, **33,** 416–421.

Pear WS, Aster JC, Scott ML, Hasserjian RP, Soffer B, Sklar J and Baltimore D. (1996). *J. Exp. Med.*, **183,** 2283–2291.

Qin JZ, Stennett L, Bacon P, Bodner B, Hendrix MJ, Seftor RE, Seftor EA, Margaryan NV, Pollock PM, Curtis A, Trent JM, Bennett F, Miele L and Nickoloff BJ. (2004). *Mol. Cancer Ther.*, **3,** 895–902.

Rangarajan A, Talora C, Okuyama R, Nicolas M, Mammucari C, Oh H, Aster JC, Krishna S, Metzger D, Chambon P, Miele L, Aguet M, Radtke F and Dotto GP. (2001). *EMBO J.*, **20,** 3427–3436.

Roninson IB, Broude EV and Chang BD. (2001). *Drug Resist. Update*, **4,** 303–313.

Shimazaki T, Shingo T and Weiss S. (2001). *J. Neurosci.*, **21,** 7642–7653.

Shutter JR, Scully S, Fan W, Richards WG, Kitajewski J, Deblandre GA, Kintner CR and Stark KL. (2000). *Genes Dev.*, **14,** 1313–1318.

Soriano JV, Uyttendaele H, Kitajewski J and Montesano R. (2000). *Int. J. Cancer*, **86,** 652–659.

Tang J, Gordon GM, Muller MG, Dahiya M and Foreman KE. (2003). *J. Virol.*, **77,** 5975–5984.

Tsai S, Fero J and Bartelmez S. (2000). *Blood*, **96,** 950–957.

Uyttendaele H, Marazzi G, Wu G, Yan Q, Sassoon D and Kitajewski J. (1996). *Development*, **122,** 2251–2259.

Villa N, Walker L, Lindsell CE, Gasson J, Iruela-Arispe ML and Weinmaster G. (2001). *Mech. Dev.*, **108,** 161–164.

Weijzen S, Rizzo P, Braid M, Vaishnav R, Jonkheer SM, Zlobin A, Osborne BA, Gottipati S, Aster JC, Hahn WC, Rudolf M, Siziopikou K, Kast WM and Miele L. (2002). *Nat. Med.*, **8,** 979–986.

Weijzen S, Zlobin A, Braid M, Miele L and Kast WM. (2003). *J. Cell. Physiol.*, **194,** 356–362.

Weng AP, Ferrando AA, Lee W, Morris JP, Silverman LB, Sanchez-Irizarry C, Blacklow SC, Look AT and Aster JC. (2004). *Science*, **306,** 269–271.

Wong GT, Manfra D, Poulet FM, Zhang Q, Josien H, Bara T, Engstrom L, Pinzon-Ortiz MC, Fine JS, Lee HJ, Zhang L, Higgins GA and Parker EM. (2004). *J. Biol. Chem*, **279,** 12876–12882.

Xue Y, Gao X, Lindsell CE, Norton CR, Chang B, Hicks C, Gendron-Maguire M, Rand EB, Weinmaster G and Gridley T. (1999). *Hum. Mol. Genet.*, **8,** 723–730.

Zagouras P, Stifani S, Blaumueller CM, Carcangiu ML and Artavanis-Tsakonas S. (1995). *Proc. Natl. Acad. Sci. USA*, **92,** 6414–6418.

Zhang Z, Nadeau P, Song W, Donoviel D, Yuan M, Bernstein A and Yankner BA. (2000). *Nat. Cell Biol.*, **2,** 463–465.